FEB 19 2003 25 S

STATION 3

ENGINEERING DATA TRANSMITTAL

1. EDT 634031

2. To: (Receiving Organization) S-112 Retrieval Projects	3. From: (Originating Organization) SST Project Engineering	4. Related EDT No.: N/A
5. Proj./Prog./Dept./Div.: S-112/SST Retrieval Proj/Projects	6. Design Authority/Design Agent/Cog. Engr.: P. W. Gibbons	7. Purchase Order No.: N/A
8. Originator Remarks: This document is being approved and released into the supporting document system for retrievability purposes.		9. Equip./Component No.: N/A
		10. System/Bldg./Facility: 241-S-112
		12. Major Assm. Dwg. No.: N/A
11. Receiver Remarks: For release.	11A. Design Baseline Document? (●) Yes ( ) No	13. Permit/Permit Application No.: N/A
		14. Required Response Date: 2/13/2003

15. DATA TRANSMITTED

(A) Item No.	(B) Document/Drawing No.	(C) Sheet No.	(D) Rev. No.	(E) Title or Description of Data Transmitted	(F) Approval Designator	(G) Reason for Transmittal	(H) Originator Disposition	(I) Receiver Disposition
1	RPP-10413	N/A	0	Tank S-112 Saltcake Waste Retrieval Demonstration Project Leak Detection, Monitoring and Mitigation Strategy	Q/E	2	1	1

16. KEY

Approval Designator (F)	Reason for Transmittal (G)	Disposition (H) & (I)
E, S, Q, D OR N/A (See WHC-CM-3-5, Sec. 12.7)	1. Approval 2. Release 3. Information 4. Review 5. Post-Review 6. Dist. (Receipt Acknow. Required)	1. Approved 2. Approved w/comment 3. Disapproved w/comment 4. Reviewed no/comment 5. Reviewed w/comment 6. Receipt acknowledged

17. SIGNATURE/DISTRIBUTION (See Approval Designator for required signatures)

(G) Reason	(H) Disp.	(J) Name	(K) Signature	(L) Date	(M) MSIN	(G) Reason	(H) Disp.	(J) Name	(K) Signature	(L) Date	(M) MSIN
2	1	Design Authority W.F. Zuroff	[signature]	2-11-03	S2-24	1	1	R.E. Bauer	[signature]	2/11/03	S7-65
		Design Agent				1	1	R.C. Wilson	[signature]	2/13/03	S7-65
2	1	Cog. Eng. C.E. Hanson	[signature]	2/11/03	S7-65	1	1	P.W. Gibbons	[signature]	2-10-03	S7-65
2		Cog. Mgr. W.T. Thompson	[signature]	2/11/03	S7-65						
2	1	QA J.F. Bores	[signature]	02/11/03	R2-87						
		Safety									
2	1	Env. M.L. Beffenbaugh	[signature]	2/11/03	R2-51						

18. [signature] J.L. Mitchem 2/10/03 Signature of EDT Originator / Date	19. N/A Authorized Representative for Receiving Organization / Date	20. [signature] FOR Rev Taken WARREN THOMPSON 2-19-03 Design Authority/ Cognizant Manager / Date	21. DOE APPROVAL (if required) Ctrl No. ____ ( ) Approved ( ) Approved w/comments ( ) Disapproved w/comments

DISTRIBUTION SHEET

To	From	Page 1 of 2
S-112 Retrieval Project	SST Projects Engineering	Date 2/10/2003
Project Title/Work Order		EDT No. EDT-634031
RPP-10413, Rev.0, "Tank S-112 Saltcake Waste Retrieval Demonstration Project Leak Detection, Monitoring and Mitigation Strategy"		ECN No. N/A

Name	MSIN	Text With All Attach.	Text Only	Attach./ Appendix Only	EDT/ECN Only
Babcock Services					
J. R. Biggs	S7-66	X			
CH2M HILL Hanford Group, Inc.					
D. G. Baide	S7-65	X			
W. B. Barton	R2-11	X			
R. E. Bauer	S7-65	X			
J. F. Bores	R2-87	X			
P. M. Branson	S7-65	X			
K. E. Carpenter	S7-65	X			
M. L. Deffenbaugh	R1-51	X			
G. W. McLellan	S7-65	X			
D. A. Reynolds	R2-11	X			
M. H. Sturges	S7-65	X			
W. T. Thompson	S7-65	X			
L. R. Webb (H)	R1-10		X		
R. C. Wilson	S7-65	X			
A. E. Young	S7-65		X		
W. R. Zuroff	S7-24	X	X		
COGEMA					
C. E. Hanson	S7-66	X			
NHC					
P. W. Gibbons (4 copies)	S7-65	X			
PNNL					
J. L. Huckaby	H6-60	X			
Office of River Protection					
A. J. Stevens	H6-60	X			
James F. Thompson Jr.	H6-60	X			

DISTRIBUTION SHEET

To	From	Page 2 of 2
S-112 Retrieval Project	SST Projects Engineering	Date 2/10/2003
Project Title/Work Order RPP-10413, Rev.0, "Tank S-112 Saltcake Waste Retrieval Demonstration Project Leak Detection, Monitoring and Mitigation Strategy"		EDT No. EDT-634031 ECN No.

Name	MSIN	Text With All Attach.	Text Only	Attach./ Appendix Only	EDT/ECN Only
Office of River Protection cont.					
R. M. Yasek	H6-60	X			
DOE Reading Room	H2-53	X			

A-6000-135 (10/97)

Tank S-112 Saltcake Waste Retrieval Demonstration Project Leak Detection, Monitoring and Mitigation Strategy

C.E. Hanson
CH2M HILL Hanford Group, Inc.
Richland, WA 99352
U.S. Department of Energy Contract DE-AC06-96RL13200

EDT/ECN: EDT-634031 UC:
Org Code: 7P300 Charge Code: 116707
B&R Code: Total Pages: 101

Key Words: Tank 241-S-112, Tank S-112, S-112, S Farm, Saltcake, Waste Retrieval, Waste, Retrieval, Demonstration, Project Leak Detection, Project, Leak Detection, Monitoring, Mitigation, Strategy

Abstract: N/A

2-19-2003

Release Approval Date Release Stamp

Approved For Public Release

TANK S-112 SALTCAKE WASTE RETRIEVAL DEMONSTRATION PROJECT LEAK DETECTION, MONITORING, AND MITIGATION STRATEGY

February 2003

Prepared By
CH2M HILL Hanford Group, Inc.
Richland, Washington

This page intentionally left blank.

EXECUTIVE SUMMARY

The purpose of this document is to describe the proactive and mitigative approach for management of potential leaks that will be implemented by the S-112 Saltcake Waste Retrieval Demonstration Project (S-112 Project) and the basis for its selection. The approach is based on preventing leakage, minimizing leak volumes if a leak should occur, and providing the best available leak detection and monitoring technologies. Tank S-112 is categorized as a nonleaking tank. However, given the age of the tank and the planned retrieval method there is a need to address leakage and deploy means to detect and monitor potential leakage events.

The leak detection and monitoring system along with the leak mitigation strategy described meets the functions and requirements and conditional approvals defined for this project. This is accomplished through a combination of innovative, first-of-a-kind operational improvements in retrieval strategy with best available leak detection and leak monitoring technology.

Leak mitigation is accomplished through design features and the operational strategy developed for the waste retrieval system. Mitigation includes actions that reduce the chance of a leak and the environmental impact of a leak, should one occur. Potential leaks are proactively and responsively prevented and/or minimized throughout the retrieval demonstration operations. A summary of the mitigative operational approach is as follows:

- Control in-tank liquid inventory during retrieval to less than previous nonleaking interstitial liquid level. Years of static level monitoring have shown the tank to have not leaked below this level.
- Retrieve waste from the center of the tank out to minimize liquid contact with the tank wall, the location of most historical single-shell tank leaks.
- Design the retrieval system and operational strategy to minimize "time at risk." By minimizing the time at risk potential leak volumes are limited in size. For a slow leak (less than 2 gal/hr) the leak volume would be more than an order of magnitude smaller than the detection limit of current leak detection equipment.
- Use the retrieval pump to minimize tank S-112 liquid inventory between retrieval campaigns (e.g., while waiting for cross-site transfers) to further reduce any leak driving head and exposure of the tank wall.
- Minimize potential leak volume by providing a (nominal 90 gal/min) pump, located as close to tank bottom as possible, to rapidly pump down liquids if a leak were to be detected.

Leak detection is accomplished through deployment of best available technology. A summary of the leak detection approach is as follows:

- Use existing drywells that surround tank S-112 to watch for potential leakage plumes. The drywells will be monitored for soil gamma levels (to indicate leakage of cesium-137 from the tank) and changes in soil moisture content. Existing truck-mounted gamma detectors will be used to perform soil gamma surveys before and after waste retrieval, and truck-mounted neutron moisture probes will be used to perform soil moisture surveys at intervals during waste retrieval operations.

- Use manually deployed neutron moisture probes to frequently monitor the moisture of the most likely plume depths (up to three times per week).

- Monitor the tank S-112 liquid level between retrieval campaigns and during significant interruptions to detect possible tank bottom leakage. Between retrieval campaigns the liquid will be pumped down and drainable liquid in the saltcake will drain to the center of the tank until hydraulic equilibrium is reached. It is expected that during the static test the liquid level will rise asymptotically toward an equilibrium level. Any drop in the liquid level during this time might indicate a leakage event.

- Augment primary leak detection systems with alternate methods to develop a "defense-in-depth" approach. This will be accomplished by monitoring process measurements and observations to assess tank S-112 and transfer system integrity.

Leak monitoring, the determination of the waste volume leaked (if any), is accomplished through collection and evaluation of data from the leak detection system. Gamma and neutron moisture detector surveys will be used to assess the magnitude, shape or direction of a leak plume, should one occur.

The S-112 Project assembled a multi-disciplinary project team composed of CH2M HILL Hanford Group, Inc. Process Control engineers, the Vadose Zone Program, S-112 Project technical support, the tank S-112 design architect/engineer, and Pacific Northwest National Laboratory to determine the best available leak detection technology to support the S-112 Project. Detailed analyses were performed to assess the expected performance capability of both in-tank mass balance and ex-tank drywell leak detection methods. These analyses included development of system equations, reduction of equations to measurable variables, determination of variable distributions, and performance and interpretation of Monte Carlo statistical analyses on the equations.

These analyses determined that in-tank mass balance methods have a performance uncertainty of at least 80,000 gallons. Although uncertainties are not additive, insight into the large uncertainty associated with material balance methods can be gained by considering the large uncertainties associated with the initial waste volume and mass. This is further compounded by uncertainties associated with the distribution of waste within the tank (i.e., heterogeneities in waste composition and physical properties) and waste behavior during retrieval. The analyses indicated that improvements in instrumentation will not substantially reduce the overall uncertainty associated with in-tank leak detection. Consequently, in-tank mass balance methods do not represent best available technology in Hanford saltcake tanks and will only be used to corroborate data gathered by the ex-tank surveys.

Ex-tank drywell methods were found to have uncertainties that varied with leak rate and the travel distance from a leak site to a drywell. Based on the conceptual model and leak parameters evaluated, a slow leak corresponding to historical Hanford tank leak rates (less than 2 gal/hr), drywell logging techniques have a 95th percentile volume of 300 gallons for the cases with a drywell located 10 feet from the leak site. The 95th percentile volume increases to 18,000 gallons if the drywell is located 45 feet from the leak site. The travel times associated with leaks from the side of the tank range from 1 to 70 days and the travel times from the center of the tank floor range from 4 days to 12 years depending on the leak rate. This means that a leak from the tank floor is unlikely to be consistently detected by drywells during waste retrieval operations. To monitor for high rate leaks near the center of the tank floor, periodic verification of static liquid level will be used. This combination of drywell monitoring and static liquid level monitoring covers the full range of potential leak cases.

Ex-tank resistivity technologies currently under development by CH2M HILL Hanford Group, Inc. will be considered for deployment at tank S-112 if it is deemed practical and schedules permit. If resistivity methods are deployed they would be operated in a test mode and would not be used as primary leak detection methods. These technologies were not considered for an integrated deployment with the tank S-112 waste retrieval as they are still under development for use at Hanford and are not yet available for operations.

This page intentionally left blank.

CONTENTS

APPENDICES

FIGURES

TABLES

LIST OF TERMS

Ecology	Washington State Department of Ecology
HFFACO	*Hanford Federal Facility Agreement and Consent Order*
LDMM	leak detection, monitoring, and mitigation
SST	single-shell tank

This page intentionally left blank.

1.0 INTRODUCTION

1.1 PURPOSE AND SCOPE

The purpose of this document is to describe the tank S-112 Saltcake Waste Retrieval Demonstration Project (S-112 Project) strategy for leak detection, monitoring, and mitigation (LDMM). The bases for the selected LDMM methodology are presented, as well as the bases for not including an in-tank material balance as a primary leak detection method. Specific topics addressed in this document include the following:

- S-112 Project response to identified requirements, expectations and conditions
- S-112 Project leak mitigation strategy
- S-112 Project leak detection and monitoring system
- Limitations of the S-112 Project leak management approach.

1.2 BACKGROUND

The mission of the River Protection Project includes the retrieval, immobilization, storage, and disposal of Hanford Site tank waste. In support of the River Protection Project mission, and to achieve compliance with federal and state hazardous waste requirements as enforced by the *Hanford Federal Facility Agreement and Consent Order* (HFFACO; Ecology et al. 1989), CH2M HILL Hanford Group, Inc. has identified several initiatives to implement the recently renegotiated HFFACO strategy defined in approved Change Number M-45-00-01A for near-term waste retrieval activities. The new strategy places an emphasis on scheduling waste retrieval from those single-shell tanks (SSTs) with a high volume of contaminants of concern (i.e., mobile, long-lived radionuclides that have a potential of reaching the groundwater and the Columbia River). The near-term waste retrieval strategy also focuses on the performance of key waste retrieval technology demonstrations in a variety of different waste forms and tank farm locations to establish a technical basis for future work. Specific HFFACO milestones have been established, consistent with this new strategy, for demonstrating SST waste retrieval technologies in tank S-112. These milestones reinforce the need to proceed with waste retrieval using available technologies.

The waste retrieval strategy for the S-112 Project focuses on the deployment of a modified sluicing waste retrieval technology to recover as much waste as technically practical. A process that controls liquid inventories during waste retrieval has been selected for this waste retrieval demonstration. The water used by the modified sluicing system acts as a solvent to dissolve and mobilize the soluble waste constituents and carry insoluble solids. The resulting slurry can then be pumped from tank S-112 to safe storage in a more reliable double-shell tank.

Goals established in HFFACO Milestone M-45-03C for the S-112 Project include the recovery and safe storage of approximately 550 curies of mobile, long-lived radioisotopes and 99% (not to exceed 360 ft^3 of residual waste per Milestone M-45-00) of the tank contents by volume based on the best-basis inventory of August 8, 2000 (BBI 2001). HFFACO Milestone M-45-03C requires completion of the full-scale saltcake waste retrieval technology demonstration at tank S-112 by September 30, 2005.

1.3 OVERVIEW

The leak detection and leak monitoring system was selected based upon best available technology. An analysis of in-tank mass balance leak detection methods are presented in Appendix A, and an analysis of ex-tank drywell monitoring methods is presented in Appendix B to support selection of the best available technology. The analyses illustrate that there are large uncertainties associated with material balance leak detection methods when all elements of the system are considered, and that there are limitations associated with both in-tank and ex-tank leak detection methods.

LDMM capabilities and actions have been legally agreed to by U.S. Department of Energy, Washington State Department of Ecology (Ecology), and U.S. Environmental Protection Agency in the HFFACO. LDMM definitions as accepted by the U.S. Department of Energy, Office of River Protection, and Ecology are as follows:

- **Leak Mitigation**: Technologies, waste retrieval methods, or systems that can reduce the potential for a leak to occur, the volume of a leak if it were to occur, actions taken to minimize leak volumes in the event a leak is detected during waste retrieval.
- **Leak Detection**: Technologies, methods, or systems used to detect a leak.
- **Leak Monitoring**: Technologies, methods, or systems used to quantify liquid waste release volumes from a SST if a release is detected during waste retrieval operations. Leak monitoring also includes assessment of leak monitoring data in an effort to estimate the rate and direction of movement through the soil.

Details regarding the specific functions and requirements were confirmed and agreed to in *Single-Shell Tank S-112 Full Scale Saltcake Waste Retrieval Technology Demonstration Functions and Requirements* (RPP-7825). RPP-7825 is a primary document prepared in response to HFFACO Milestone M-45-03-T03. Conditional approval of RPP-7825 has been received from Ecology (Dahl 2002).

2.0 LEAK DETECTION, LEAK MONITORING, AND LEAK MITIGATION REQUIREMENTS

This section gives the requirements that drive the S-112 Project LDMM approach, and how the proposed strategy responsibly meets those requirements. Requirements, expectations, and conditions are found in three sources:

1. The HFFACO identifies key programmatic expectations for the advancement of retrieval and leak detection technologies.

2. RPP-7825 identifies the state and federal regulations that apply to the tank S-112 LDMM program. These regulatory requirements are imposed on the design of the tank S-112 LDMM system via the requirement statements in Section 4.0 of RPP-7825.

3. The conditional approval (Dahl 2002) of the tank S-112 functions and requirements document (RPP-7825) by Ecology, which identifies additional conditions related to LDMM.

Table 2.1 identifies the specific LDMM-related requirements, expectations, and conditions for the S-112 Project. The source documents are also identified in the table, as well as the S-112 Project response action to fulfill the requirement or expectation. Cross references to sections within this document are provided for further detail.

Table 2.1. Tank S-112 Requirements (5 Sheets)

No.	Leak Mitigation, Leak Detection, or Leak Monitoring, or Related Requirement, Condition, or Expectation	Project Approach, Action, or Response	Source Document
1.	Seek to improve on past-practice sluicing in the areas of expected retrieval efficiency, leak loss potential, and suitability for use in potentially leaking tanks.	The tank S-112 waste retrieval system has been designed around the requirement that tank S-112 liquid inventory be kept to a practical minimum at all times. This will significantly reduce the likelihood of tank wall leaks and the potential volume of a leak, should one occur.	Ecology, EPA, and DOE, 1989, *Hanford Federal Facility Agreement and Consent Order*, as amended, Milestone M-45-03-C.
2.	The demonstration shall include installation and implementation of full-scale LDMM technologies.	The leak mitigation strategy along with the leak detection and monitoring strategy defined in Section 3.1 and the system described in Section 4.0 provide for full-scale leak mitigation coupled with leak detection and monitoring during waste retrieval operations.	Ecology, EPA, and DOE, 1989, *Hanford Federal Facility Agreement and Consent Order*, as amended, Milestone M-45-03-C.
3.	The system shall be designed to detect a cumulative leak loss during the retrieval campaign of 8,000 gallons or the system shall be designed using the BATEA to detect tank leaks during retrieval to ALARA.	The S-112 Project is deploying the system that represents the best available technology, gamma and neutron moisture detection surveys in the drywells near tank S-112 (see Section 3.0). This approach is augmented with in-tank methods to provide defense-in-depth leak detection and monitoring.	RPP-7825, Section 4.6.1, *Single-Shell Tank S-112 Full Scale Saltcake Waste Retrieval Technology Demonstration Functions And Requirements*, Rev. 1.
4.	The tank S-112 waste retrieval system shall have a probability of leak detection of greater than 95% and a probability of false alarm less than or equal to 5%.	The uncertainties associated with the planned leak detection and monitoring system are described in Section 5.0. The uncertainties associated with leak detection capability using both in-tank dynamic material balance and ex-tank drywell monitoring techniques are evaluated based on conceptual models and parameter distributions developed for both methods. 95th percentile leak volumes are presented for both methods. There is insufficient data to define a minimum detectable leak volumes tied to a probability of false alarm. In lieu of this, the project will use an investigative approach to leak detection that will be defined in the process control plan.	RPP-7825, Section 4.6.1, *Single-Shell Tank S-112 Full Scale Saltcake Waste Retrieval Technology Demonstration Functions And Requirements*, Rev. 1.

Table 2.1. Tank S-112 Requirements (5 Sheets)

No.	Leak Mitigation, Leak Detection, or Leak Monitoring, or Related Requirement, Condition, or Expectation	Project Approach, Action, or Response	Source Document
5.	The tank S-112 waste retrieval system shall quantify liquid waste release volumes from tank S-112 if a release is detected during waste retrieval operations. The data shall be collected, in the event of a leak, to help respond to the leak and to support a post-retrieval RPE, which will be used to address retrieval of the next S farm tank. Data collected will address estimates of the volume and composition of leaked material, as well as the residual waste in the tank.	The leak detection system will be used to quantify leak volumes from tank S-112 in the event that a leak is detected (see Section 3.0). Following detection of a leak, if one should occur, response actions will be taken and additional drywell monitoring performed to estimate the volume and characteristics of the waste released from the tank.	RPP-7825, Section 4.6.2, *Single-Shell Tank S-112 Full Scale Saltcake Waste Retrieval Technology Demonstration Functions And Requirements*, Rev. 1.
6.	The tank S-112 waste retrieval system shall minimize waste generation to the greatest extent practical, including water introduced into the tanks and solid waste.	Water is the only process chemical currently planned for addition during the tank S-112 retrieval. Process controls described in the process control plan (e.g., the ability to recycle pumped fluids) prevent excessive water usage.	RPP-7825, Section 4.8, *Single-Shell Tank S-112 Full Scale Saltcake Waste Retrieval Technology Demonstration Functions And Requirements*, Rev. 1.

Table 2.1. Tank S-112 Requirements (5 Sheets)

No.	Leak Mitigation, Leak Detection, or Leak Monitoring, or Related Requirement, Condition, or Expectation	Project Approach, Action, or Response	Source Document
7.	The integrated retrieval and leak detection and monitoring system shall be designed and operated to mitigate leak volumes ranging from 8,000 gallons to 40,000 gallons for the duration of the retrieval demonstration. The tank S-112 waste retrieval system shall mitigate leaks as the primary means of minimizing environmental impact caused by releases during retrieval of SST waste. If a leak occurs, the release shall be evaluated according to the RPE and the appropriate actions implemented (e.g., continue or discontinue retrieval). As the primary mitigation means, the retrieval pump shall be designed to allow continuous pumping for a sufficient amount of time (to be determined during design) to remove all pumpable liquids from tank S-112. An operational approach that minimizes the free liquid in the tank shall be employed for waste retrieval, ensuring that the interstitial liquid level remains below its starting level. The current interstitial liquid level is approximately 10.3 feet (124 inches). Mitigation activities will be consistent with the intent of HNF-SD-WM-AP-005, *SST Leak Emergency Pumping Guide*.	The operational strategy designed for the waste retrieval was developed to mitigate the potential for leaks. The addition of liquids will be controlled to maintain the interstitial liquid level at or below the pre-saltwell pumping level (see Section 3.1). Additionally, waste will be retrieved from the center out to minimize liquid contact with the tank walls. Based on evaluations of currently available leak detection and monitoring technologies, it was determined that the best available leak detection and monitoring technology for tank S-112 involves monitoring the existing drywells surrounding the tank for gamma radiation and moisture. With this technology the ability of the system to detect leaks from the center of the tank is unlikely in the time frame of this retrieval activity. Such leak will be detected by level monitoring of the liquid pool. Tank wall leaks would be detectable by drywell monitoring at lower volumes (see Sections 3.0 and 5.0).	RPP-7825, Section 4.9, *Single-Shell Tank S-112 Full Scale Saltcake Waste Retrieval Technology Demonstration Functions And Requirements*, Rev. 1.
8.	CA #1. Resolve all non-RPE-specific RCR comments.	The S-112 Project accepts this condition. This condition was met with the issuance of Revision 1 of RPP-7825.	Dahl, 2002, Letter from S. Dahl (Ecology) to J. Rasmussen (DOE/ORP), Re: Conditional Approval of the C-104 and S-112 Functions and Requirements (F&R) Documents, RPP-7807, Rev. 0 and RPP-7825, Rev. 0, Deliverables of HFFACO Milestone M-45-03-T04 and M-45-03-T03, July 2002.

Table 2.1. Tank S-112 Requirements (5 Sheets)

No.	Leak Mitigation, Leak Detection, or Leak Monitoring, or Related Requirement, Condition, or Expectation	Project Approach, Action, or Response	Source Document
9.	CA #2. (paraphrased) Ecology requires all RPE-related corrections, requested changes and additional information be incorporated into future RPE and SST closure documentation.	Ongoing discussions are being held between CH2M HILL, ORP, and Ecology on risk assessment methods and changes to the RPE methodology to be incorporated into future RPEs and SST closure documentation.	Dahl, 2002, Letter from S. Dahl (Ecology) to J. Rasmussen (DOE/ORP), Re: Conditional Approval of the C-104 and S-112 Functions and Requirements (F&R) Documents, RPP-7807, Rev. 0 and RPP-7825, Rev. 0, Deliverables of HFFACO Milestone M-45-03-T04 and M-45-03-T03, July 2002.
10.	CA #3. Ecology requires that ORP maintain design flexibility to incorporate at least one viable ex-tank LDMM technology for each retrieval. Ecology expects that ORP will continue to seek out and invest in technology to improve the capability to detect and mitigate leaks during retrieval.	ORP and CH2M HILL are continuing evaluation of new ex-tank LDM technologies. The results of recent demonstration tests are currently under evaluation. Current plans involve completing evaluation of the test results and developing cost and schedule estimates for deployment in a tank farm. Based on the evaluations and estimates a decision will be made regarding additional testing within a tank farm. These technologies are not sufficiently mature to rely on for leak detection in the absence of sufficient demonstration testing in the farms (see Section 3.0).	Dahl, 2002, Letter from S. Dahl (Ecology) to J. Rasmussen (DOE/ORP), Re: Conditional Approval of the C-104 and S-112 Functions and Requirements (F&R) Documents, RPP-7807, Rev. 0 and RPP-7825, Rev. 0, Deliverables of HFFACO Milestone M-45-03-T04 and M-45-03-T03, July 2002.
11.	CA #4. DOE will provide Ecology the latest information regarding the ex-tank technology(s) DOE chooses to incorporate into the tank S-112 design.	This report provides the latest information regarding ex-tank technologies and the planned LDMM approach for tank S-112 waste retrieval.	Dahl, 2002, Letter from S. Dahl (Ecology) to J. Rasmussen (DOE/ORP), Re: Conditional Approval of the C-104 and S-112 Functions and Requirements (F&R) Documents, RPP-7807, Rev. 0 and RPP-7825, Rev. 0, Deliverables of HFFACO Milestone M-45-03-T04 and M-45-03-T03, July 2002.

Table 2.1. Tank S-112 Requirements (5 Sheets)

No.	Leak Mitigation, Leak Detection, or Leak Monitoring, or Related Requirement, Condition, or Expectation	Project Approach, Action, or Response	Source Document
12.	CA #5. (Paraphrased) DOE should make reasonable efforts to prevent leaks of any kind. Ecology expects DOE will continue to develop and implement technology improvements. Leak detection should be based on the limits of BAT, not risk.	The S-112 Project accepts this condition and has developed a mitigative operational strategy that makes reasonable efforts for preventing the occurrence of a retrieval leak (see Section 3.1). DOE continues to fund programs to identify, develop, and implement technology improvements in the area LDMM.	Dahl, 2002, Letter from S. Dahl (Ecology) to J. Rasmussen (DOE/ORP), Re: Conditional Approval of the C-104 and S-112 Functions and F&Rs Documents, RPP-7807, Rev. 0 and RPP-7825, Rev. 0, Deliverables of HFFACO Milestone M-45-03-T04 and M-45-03-T03, July 2002.

ALARA = as low as reasonably achievable.
BAT = best available technology.
BATEA = best available technology economically achievable.
CA = Conditional Approval.
CH2M HILL = CH2M HILL Hanford Group, Inc.
DOE = U.S. Department of Energy.
Ecology = Washington State Department of Ecology.
F&R = function and requirement.
HFFACO = *Hanford Federal Facility Agreement and Consent Order.*
LDMM = leak detection, monitoring, and mitigation.
ORP = Office of River Protection.
RCR = review comment record.
RPE = retrieval performance evaluation.
SST = single-shell tank.

3.0 LEAK DETECTION, MONITORING, AND MITIGATION STRATEGY

The primary goal of the S-112 Project LDMM strategy is leak mitigation. The tank S-112 retrieval system and retrieval strategy have been designed to reduce the possibility of a leak and the potential environmental impact of a leak, should one occur. The leak detection strategy places emphasis on using the best available technology. Recent Office of River Protection investments in the development of new, more sensitive leak detection technologies for the Hanford tanks are promising (RPP-10604), but none of the new technologies are mature enough to form the basis of the tank S-112 leak detection strategy. The S-112 Project has evaluated existing in-tank and ex-tank options, and determined that tank wall leaks would be most quickly and reliably detected by monitoring the soil around the tank via existing drywells, and that leaks from the center of the tank floor would be most reliably detected using static liquid level tests at appropriate times during the retrieval. The S-112 Project strategy for leak monitoring is to use data from the leak detection systems to locate and quantify the leak. The following subsections provide further descriptions of the LDMM system and strategy, along with summaries of the analyses that have been conducted to select the LDMM baseline system.

3.1 LEAK MITIGATION

The leak mitigation strategy (i.e., reduction of leak loss potential) is twofold. The operational strategy involves taking actions to minimize leakage potential from the onset of retrieval and, if a leak is detected, involves responding to minimize the overall environmental impact.

The operational strategy to minimize the leak potential (initiation of a leak and leak volume) during retrieval in the absence of any indication of a leak involves the following:

- Control in-tank liquid inventory during retrieval to less than previous nonleaking interstitial liquid level. Years of static level monitoring have shown the tank to have not leaked below this level.

- Retrieve waste from the center of the tank out to minimize liquid contact with the tank wall, the location of most historical SST leaks (see Figure 3.1). In the center-out retrieval strategy, dissolved waste and released interstitial liquids drain quickly into a central pool, and can be rapidly pumped from the tank if a leak is detected.

- Design the retrieval system and operational strategy to minimize "time at risk." By minimizing the time at risk, potential leak volumes are limited in size. The relatively short retrieval duration (2 to 4 weeks) limits the overall leakage volume from a leak, should it go undetected. Table 3.1 provides leakage volumes as a function of leak rate and leak duration. A conservative leak rate based on historical data of 1.8 gal/hr is provided along with the highest historical leak rate of 100 gal/hr.

- Use the retrieval pump to minimize tank S-112 liquid inventory at the end of each retrieval campaign (e.g., while waiting for cross-site transfers) to further reduce any leak driving head and exposure of the tank wall.

- Minimize potential leak volume by providing a (nominal 90 gal/min) pump, with the inlet located as close to tank bottom as possible, to rapidly pump down liquids if a leak were to be detected.

Figure 3.1. Illustration of Leak Mitigative, Center-Out Retrieval Strategy

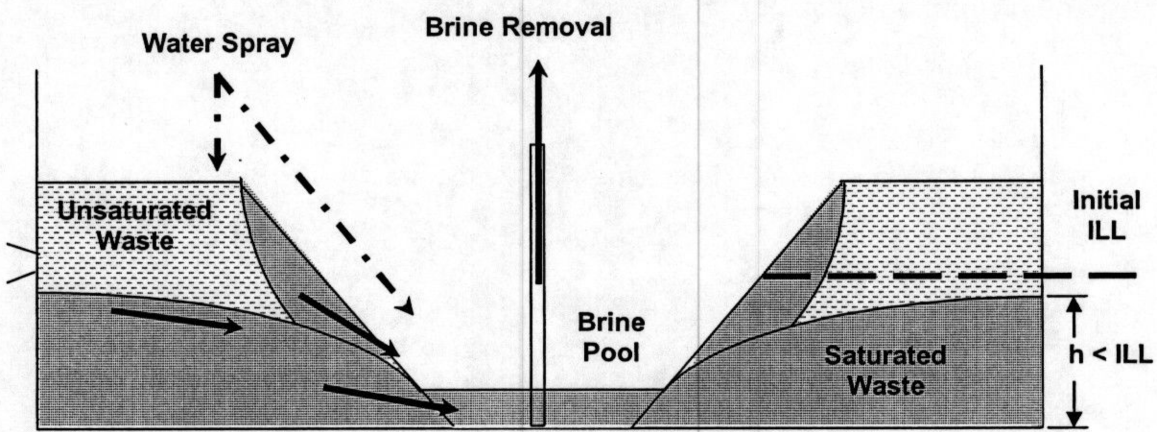

ILL = interstitial liquid level.

Table 3.1. Leakage Volumes

Leak Rate (gal/hr)	Duration (weeks)					
	1	2	3	4	8	12
0.5	84	168	252	336	672	1,008
1	168	336	504	672	1,344	2,016
1.8	302	604	907	1,209	2,419	3,628
5	840	1,680	2,520	3,360	6,720	10,080
10	1,680	3,360	5,040	6,720	13,440	20,160
50	8,400	16,800	25,200	33,600	67,200	100,800
100	16,800	33,600	50,400	67,200	134,400	201,600

In the event a leak is detected, sluicing operations will be stopped and the tank quickly pumped down to a minimum liquid level using the retrieval pump. Waste retrieval operations may resume after assessing tank conditions if warranted and further leakage can be mitigated. Details of the operational response to a leak will be defined in the process control plan.

3.2 LEAK DETECTION

The S-112 Project evaluated both in-tank and ex-tank methods that have been used historically for leak detection. The following subsections discuss the evaluations performed, the conclusions drawn, and the resulting S-112 Project leak detection strategy.

The tank S-112 waste retrieval functions and requirements identified a limited number of leak detection and monitoring technologies that have been proven in the tank farm environment

(RPP-7825). To be a suitable candidate for full-scale deployment, leak detection and monitoring technologies must be technically mature and capable of being deployed in the tank farm in a manner that supports waste retrieval schedule and operational performance and reliability requirements. The strategy described in RPP-7825 for leak detection and monitoring during tank S-112 waste retrieval activities involved using static and dynamic in-tank methods for primary leak detection coupled with ex-tank methods for secondary leak detection. At the time that RPP-7825 was written, this approach was thought to constitute the best available technology for leak detection and monitoring. Since issuance of RPP-7825, uncertainty analyses have been conducted on the in-tank dynamic and ex-tank drywell monitoring leak detection methods. The details of the uncertainty analyses are summarized in Section 5.0 and are presented in detail in Appendices A and B.

Based on evaluating the uncertainties associated with available leak detection and monitoring technologies, the strategy has been revised to rely on drywell monitoring techniques to detect leaks that originate on the sidewalls of the tank or near the tank edge and using static liquid level monitoring to detect leaks originating from the center portion of the tank floor. This will be supplemented with the observation of in-tank process control data as a defense-in-depth approach to monitor for catastrophic leaks.

3.2.1 In-Tank Leak Detection

In-tank leak detection methods include dynamic mass balance and static liquid level monitoring. SST retrieval activities have historically relied on material balance methods, and leak detection in quiescent SSTs has been based on level monitoring. This method as applied to tank C-106 is the basis of the 8,000-gallon leak detection requirement in RPP-7825. The dynamic mass balance method works well if the tank being retrieved and the receiver tank both have a free liquid surface over the entire diameter of the tank that can be accurately measured and used to estimate waste inventory in both tanks. As described in Section 5.0 and Appendix A, the uncertainties associated with dynamic mass balance are large and are not suited for leak detection and monitoring in tanks containing saltcake waste without a free liquid surface over the entire diameter like tank S-112. The static liquid level leak detection method is also expected to work well when there is a free liquid surface across the entire tank, and the transitory effects of water addition, salt dissolution, seepage, and pumping have subsided. However, the tank S-112 retrieval strategy, to reduce leak potential, will not allow a free liquid surface across the entire tank diameter until late in the retrieval process. Static liquid level methods will not work during operations because the liquid level is subject to oscillations associated with variable water application, drainage, pumping rates, etc. After liquid additions are stopped it is expected that a number of weeks will be required for the liquid level to equilibrate for a valid static level check to be performed using historical liquid level monitoring methods.

The S-112 Project plans to use a modified form of static leak detection to check for large leaks from the tank floor where drywell monitoring is least timely. In this case any decrease in liquid level would indicate a possible leak, but sensitivity will be low until equilibrium is reached.

3.2.1.1 In-Tank Static Level Observation

Volumetric methods measure the liquid surface in a static tank and convert the level data to volume data from the known tank parameters. Historically static level measurements were performed on a free-liquid surfaces that covered the waste and were available for level monitoring. In the case of tank S-112, interim stabilization has removed the surface liquid. While the tank S-112 retrieval strategy will create a center pool that can be accessed for level measurement it will not be available during sluicing, nor will it be stable enough for a static measurement of historical accuracy for several weeks due to plans to pump the liquid down between waste retrieval campaigns. The causes of this instability are listed in Section 5.0.

As drywell monitoring is not sensitive to leaks from the center of the tank, static level observation will be adapted to fill this need. Before level monitoring the liquid will be pumped down to approximately 12 inches in depth as part of the leak mitigation strategy. Following removal of liquid from the central pool, liquid from the surrounding waste will seep into the central pool over a period of time (see Figure 3.1). Under these conditions it is expected that the liquid level would slowly rise to an equilibrium level, any lowering of the liquid level (using the standard 0.5-inch criteria) will indicate a leak. Any leak will initially be masked by the level rise, but a large leak will become evident. Detection of small leaks will not be possible until the liquid level reaches equilibrium which could take several weeks. Static-level observations will be done near the end of scheduled down times associated with transferring waste out of the receiver tank as well as unscheduled delays to improve the chances of detecting a small leak.

3.2.1.2 In-Tank Dynamic Mass Balance

Mass balance observations using process control data involves monitoring the volumetric inventory balance using level instruments in the waste retrieval tank along with flow meters and inventory estimates to balance the flow in and out of the waste retrieval tank. This method provides a rough indication of gross leaks. The driving disadvantage of this method is that the minimum discernable leakage volumes are large, limiting this method to monitoring for catastrophic leaks.

Dynamic mass balance leak detection, not selected for use in tank S-112 based on performance uncertainty, is sensitive to a number of environmental and operational interferences. Limitations in the ability to accurately measure the physical and chemical conditions (e.g., uncondensed evaporation, dynamic changes in the waste properties, homogeneity, layering) significantly affect the accuracy of available dynamic leak detection technologies. These uncertainties will result in a dynamic leak detection system that will be required to decipher the discrepancies between what is added to tank S-112, how much is removed from the tank, and how much remains at any point during the waste retrieval. Uncertainties and their analyses are discussed further in Appendix A.

3.2.2 Ex-Tank Leak Detection

Available ex-tank leak detection methods involve indirect measurement of subsurface conditions in the drywells surrounding the tank. Drywell monitoring has been used extensively in the past for leak detection and monitoring. Drywell monitoring methods have inherent limitations and uncertainty depending on the proximity of a leak site to a drywell, interception of the leak plume with the drywell, leak rate, and soil properties.

There are 8 monitoring wells, ranging in depth from 100 to 145 feet below ground surface near tank S-112. Five of the wells are nominally within 5 to 10 feet of the tank (see Section 4.1).

The remaining three wells are near tanks S-109 and S-111. Two are within 15 feet of the tank and the third is about 25 feet away.

The baseline leak detection methodology involves deployment of the existing truck mounted geophysical logging systems using both gamma and moisture monitoring tools. This system will be deployed before waste retrieval operations begin and at the end of waste retrieval operations. Moisture monitoring will be done periodically during waste retrieval operations. An initial baseline will be established by deploying calibrated gamma and neutron moisture probes over the full depth of each drywell. During waste retrieval operations, the truck mounted systems will be supplemented by the use of manually deployed moisture gauges on a frequency to be established in the process control plan at depths corresponding to moist layers. Moist layers should be the first affected by a new leak plume and may decrease detection times. In the event of an unexplained increase in soil moisture content, additional monitoring with the truck-mounted system will be used to determine if there have been any changes in gamma-emitting radionuclide concentration surrounding the drywells.

The use of manually deployed moisture monitors represents an enhancement to the truck-mounted system by providing more frequent moisture measurements in areas of interest without having to continually deploy the trucks into the farm (Appendix B).

Water has utility as a leak indicator over other potential waste constituents for the following reasons:

- Neutron moisture monitors are sensitive to small changes in moisture content in soil surrounding drywells.
- Water will be added to the tanks during the planned waste retrieval demonstrations.
- Gamma-emitting radionuclides that remain in the tanks have decayed to the point where cesium-137 is the primary radionuclide remaining. Cesium-137 in dilute tank waste is only slightly mobile and its retardation may be sufficient to inhibit timely detection of changes to the area surrounding the drywells.
- Manually deployed neutron moisture monitors are readily available and can be deployed by waste retrieval personnel on a more frequent basis than truck mounted systems.
- Data from the neutron moisture monitors can be readily analyzed to determine if changes have taken place.
- Neutron moisture monitors are fully capable of detecting increases in soil moisture content as low as 2%.

Based on the results of the uncertainty analysis, it was determined that drywell monitoring is best suited to detecting leaks originating near the tank sidewall. Different potential leak locations of interest to drywell monitoring are illustrated in Figure 3.2. Figure 3.2 shows two potential leak locations, at or near the tank sidewall and near the center of the tank floor. As shown in the upper portion of the figure leaks on the order of 300 gallons can be detected for slow leaks that originate near the edge of the tank (A) within 10 feet of a drywell. Leaks on the order of

18,000 gallons originating near the center of the tank floor can be detected in a drywell (B) but not in the 4 week timeframe of waste retrieval activity. Based on the drywell configuration, portions of the tank wall could be up to 25 feet from a drywell resulting in a detectable leak on the order of 8,000 gallons. It should be noted that any tank leak may find a favorable path to a drywell.

Figure 3.2. Schematics of Potential Tank Leak Conditions During Retrieval

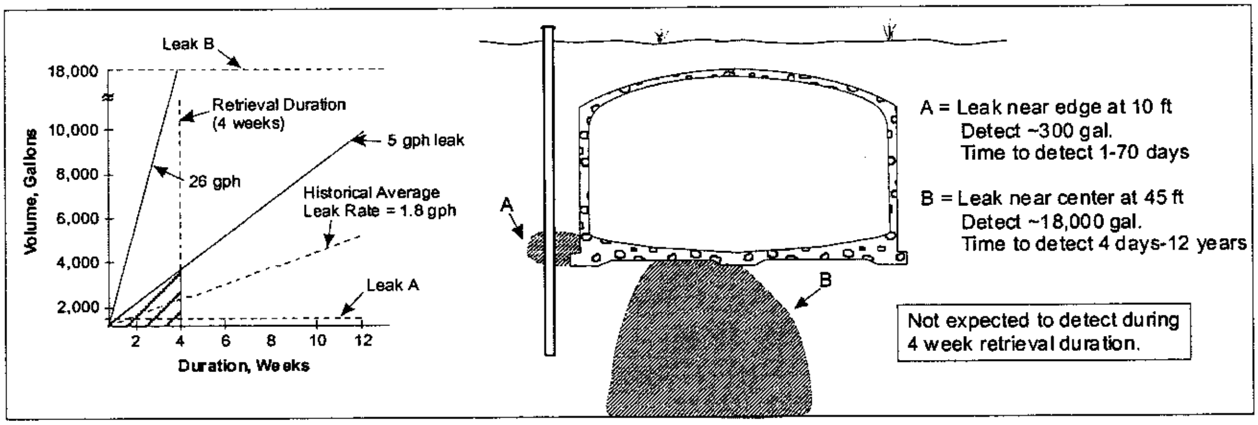

3.2.3 Summary of Leak Detection Strategy

The overall strategy for leak detection is as follows:

- Survey the existing drywells using both truck-mounted gamma and neutron moisture probes. The existing wells will be monitored before and after retrieval using the truck mounted logging system to establish a baseline. Additionally, monthly moisture scans will be performed depending on the retrieval duration. This will be supplemented by a manually deployed calibrated moisture neutron moisture detector deployed more frequently at depths corresponding to moist layers under the tank during retrieval to shorten the detection interval. In the event of an unexplained increase in soil moisture content, the truck-mounted logging systems using gamma and moisture logging tools will be deployed to monitor for changes in the baseline concentration of isotopes and moisture levels in the soil around the tank.

- Conduct static level monitoring during periods between retrieval campaigns for evidence of any leakage from the tank center floor. This is the location that is least likely to be detectable by drywell. This approach provides the opportunity to detect leaks and minimize the leak duration. It allows for static level monitoring at times when the waste retrieval system is shut down and the liquids have been pumped down.

- Observation and measurement of the receiver tank to assess transfer integrity. Static observation periods shall occur during double-shell tank cross-site transfer operations and during maintenance outages.

- Diligently observe process control data concerning mass balance (dynamic mass balance) for the possibility of a catastrophic release while waste is actively being retrieved as a defense-in-depth approach.

This approach represents deployment of the best available technology and meets the functions and requirements identified in RPP-7825 and conditional approvals defined for this project. This is accomplished through a combination of operational improvements in retrieval strategy with best available, leak detection and leak monitoring technology. The requirements identified in Section 2.0 serve to provide a basis for the strategy described in this section and the system description provided in Section 4.0.

3.3 LEAK MONITORING STRATEGY

If a leak is detected during waste retrieval operations, the leak will be monitored using the same drywell logging / static level measuring equipment to estimate the total volume or leak rate. Gamma surveys and neutron moisture detection will determine the extent of a contamination plume by understanding the changes and rate of change associated with measurements at the drywell locations. A leak volume estimate must be performed to quantify the environmental impact resulting from a leak (RPP-7825). The data collected through monitoring, in addition to being used to estimate leakage volumes, will be evaluated in an attempt to estimate the rate and direction of movement through the soil. Estimated leak volumes will be used to assess the potential need for corrective action, consideration of retrieval leakage criteria for future retrievals in the S tank farm, and characterization needs for tank farm closure.

This page intentionally left blank.

4.0 BASELINE SYSTEM DESCRIPTIONS

The waste retrieval and leak detection and monitoring systems summarized in this section represent the systems to be used in tank S-112. Potential uncertainties related to the leak detection and leak monitoring systems are summarized in Section 5.0.

4.1 TANK S-112 WASTE RETRIEVAL SYSTEM DESCRIPTION

The S-112 Project will utilize two separate systems to dissolve and mobilize waste and remove it from the tank:

- **Water distribution system**: Water is introduced to the tank through four water distribution devices. The water distribution system has three directable nozzles in the three outer risers. The fourth distribution device is a modified tank washer nozzle (oscillating spray nozzle) that will be located 6 feet off center. The stream of the fourth nozzle is not directable once installed, but will be used to carve out a well around the central pump to ensure flow away from the tank wall and toward the pump. The flow rate through the water distribution system can be varied and the flow monitored and recorded. The water is applied in a manner that will retrieve the waste from the "inside-out"; that is, the waste is first removed from the center of the tank to create a well or pit around the central pump (see Figure 4.1). This central well is gradually enlarged until the tank wall is reached. At this point, the remaining waste is undermined to fall away from the wall. Finally, the remaining heel is removed.

- **Waste solution removal system**: Waste is removed by a centrally located pump and pumped via a hose-in-hose transfer line to the SY tank farm. The pump has a capacity of approximately 90 gal/min to quickly pump down liquid inventory. Pump operation will be integrated with water addition to manage liquid level in the tank. The pump inlet is located as close to the tank bottom as possible to maximize retrieval recovery. The hose-in-hose transfer line utilizes leak detectors to ensure line integrity. The pumping system can, if necessary, recirculate waste back to the tank through a pipe routed through an open riser in the pump pit to reduce the total amount of water added by increasing contact time of the water with the waste.

Figure 4.1. Proposed Tank S-112 Saltcake Waste Retrieval System
(not to scale)

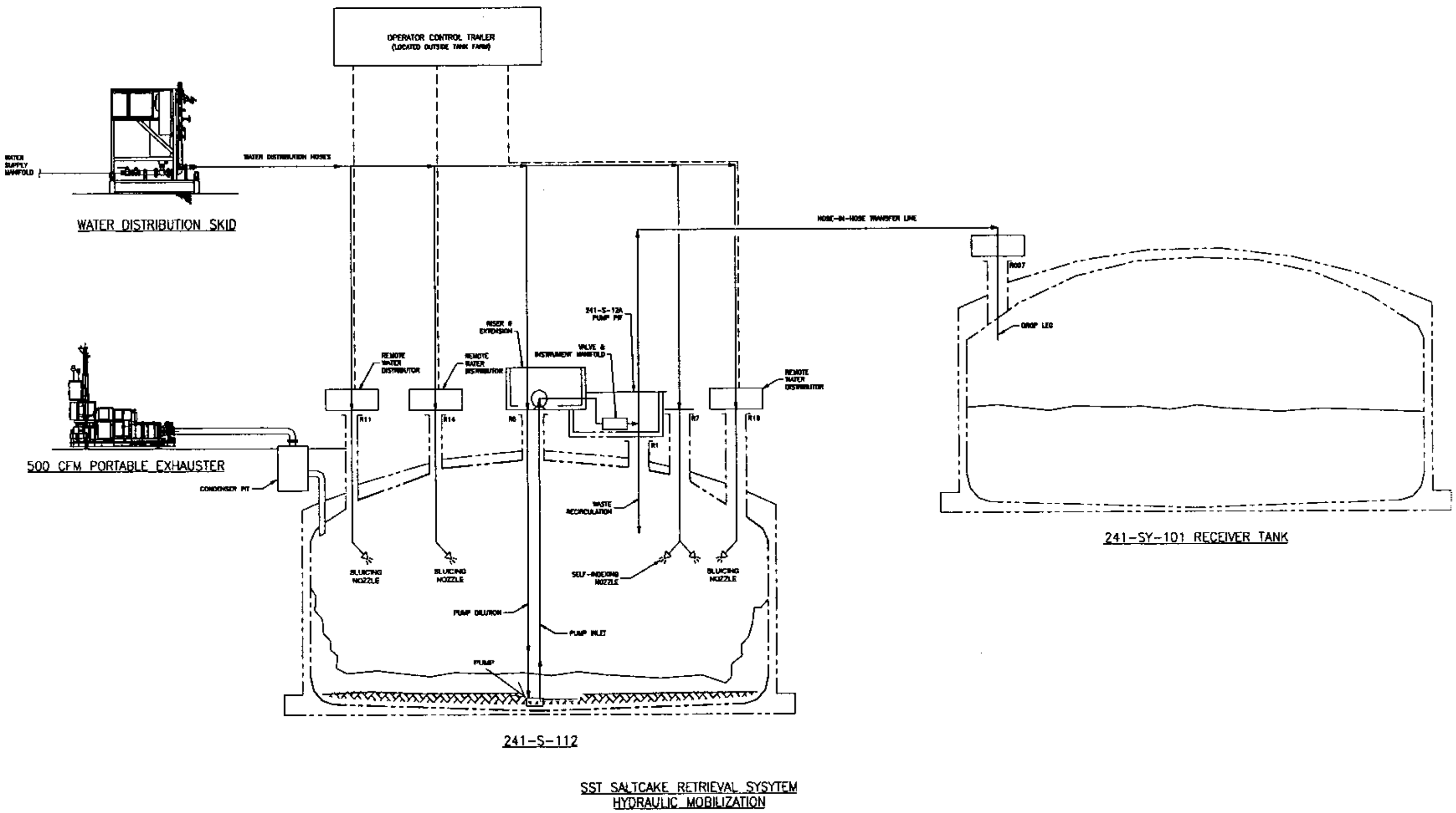

4.2 LEAK DETECTION AND LEAK MONITORING SYSTEM DESCRIPTION

The baseline method for leak detection and leak monitoring involves periodic gamma and neutron moisture surveys of the drywells surrounding the tank. This will be supplemented by static liquid level monitoring of a pumped down pool performed between waste retrieval campaigns or at other times when retrieval operations are shut down and there is sufficient time to perform the static test. Less accurate in-tank process control parameters will be observed throughout the waste retrieval campaign to supplement the ex-tank drywell and in-tank static level methods and provide a defense-in-depth approach to identify indications of potential "gross" leaks. The following sections describe the equipment used for these methods. Operational specifics of this equipment are deferred until the final process control plan is developed.

4.2.1 Primary Leak Detection and Leak Monitoring System Description

4.2.1.1 Ex-Tank Leak Detection

Eight existing drywells surrounding tank S-112 will be used for monitoring of fluid losses that may occur during waste retrieval operations (Figure 4.2). The 8 drywells that will be monitored are (in clockwise order around this tank) 40-09-06, 40-12-02, 40-11-09, 40-11-08, 40-12-04, 40-12-06, 40-12-07, and 40-12-09. Drywell 40-09-06 is associated with tank S-109 and drywells 40-11-08 and 40-11-09 are associated with tank S-111, but these are located sufficiently close to detect a plume coming from tank S-112. Five of the drywells are nominally within 10 feet of the tank. Additional drywells within the farm may be monitored to investigate whether observed changes at tank S-112 are localized or more widespread as would be expected from seasonal changes in precipitation. Existing truck-mounted logging systems will be used with gamma and neutron moisture probes. Neutron moisture probes are used to identify changes in water or moisture content surrounding a drywell. Manually deployed neutron moisture detectors will supplement the truck mounted systems.

4.2.1.2 Static Liquid Level Monitoring

A direct Enraf™[1] level-sensing instrument in a stilling well will be used in tank S-112. This instrumentation has a high degree of resolution and repeatability and is well suited for the volumetric method in tanks with a measurable air-liquid interface. Currently, the Enraf™ gauge is contacting solids and cannot be used for static testing until sufficient waste is retrieved from the tank to create a cone shaped well (or pool) in the center of the tank. A description of the Enraf™ gauges and their use in the current monitoring program is provided in RPP-9645. This document also describes the loss of resolution under varying waste conditions.

---

[1] Enraf™-Nonius Series 854 is a trademark of Enraf-Nonius, N.V. Verenigde Instrumentenfabrieken Enraf-Nonius CORPORATION NETHERLANDS Rontegenweg 1 Delft NETHERLANDS

Figure 4.2. S Tank Farm Plan View of Drywell Locations

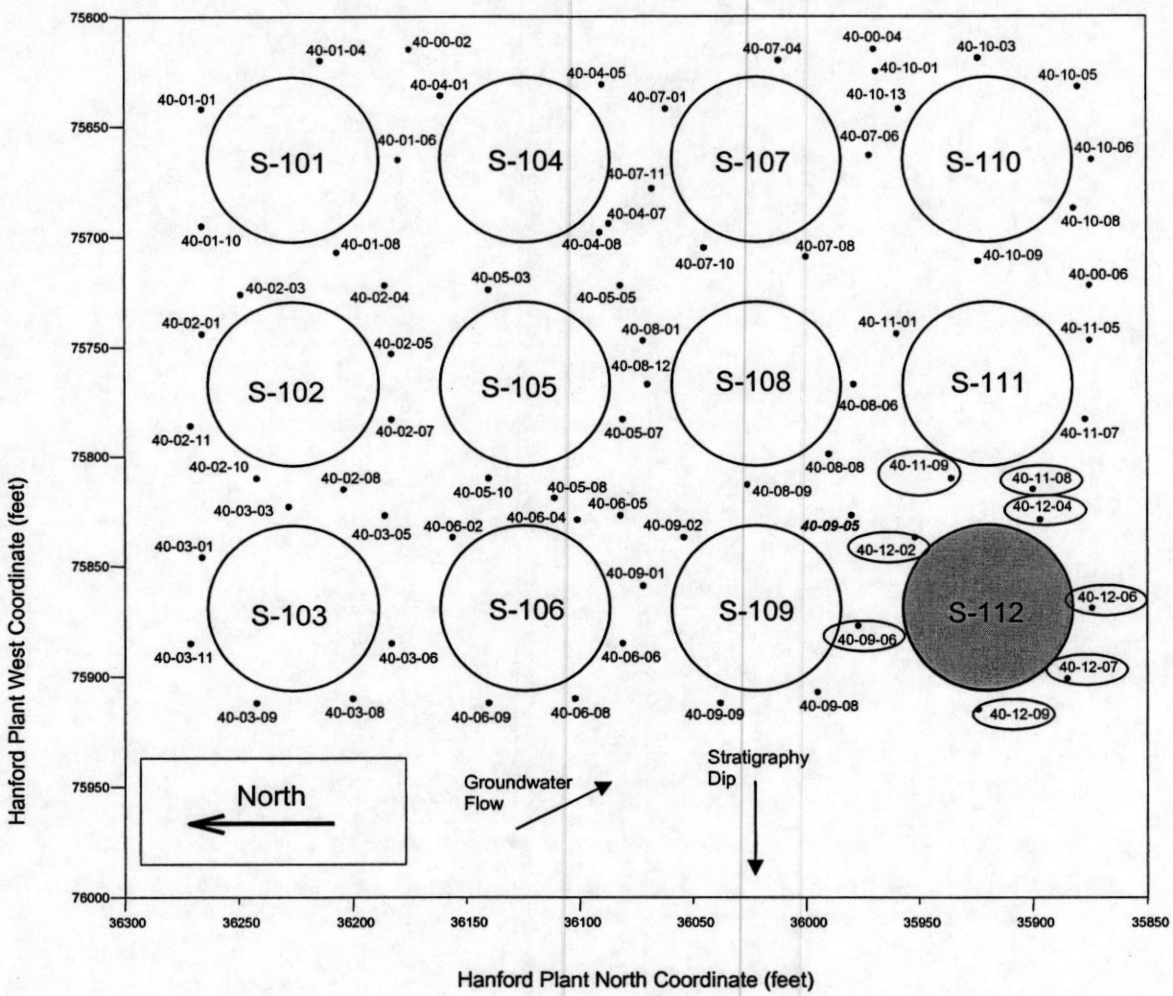

Legend
= Drywells used for baseline tank S-112 external leak detection.

4.2.1.3 Additional Data Collection

The S-112 Project recognizes that ex-tank monitoring has technical limitations associated with it despite representing best available technology. The project will attempt to improve confidence in data obtained by the primary leak detection equipment by routinely collecting corroborating data from in-tank measurements, video surveillance, and process control data as potential indicators of a catastrophic leak.

The volumes of water introduced to tank S-112 and the volumes of liquid transferred out of the tank during waste retrieval will be recorded as an aspect of routine process control. This is accomplished by the use of flow meters, level gauges, and measurements of changes in specific gravity of the solution being pumped from the tank. Because of the large uncertainty (greater than 70,000-gallons, Appendix A, Table A.6) in initial waste volume, mass balance monitoring will not be used as a primary leak detection method. This technique will provide potential indication of a catastrophic leak and will be used to provide defense in depth to the primary leak detection equipment. The advantage of this technology is that it can provide continuous real-time measurements, albeit of low quality. This method may be able to indicate a problem that causes immediate monitoring using the primary leak detection equipment.

4.2.2 Leak Detection in Transfer Lines and Pits

Liquid waste and slurries will be transferred from tank S-112 to tank SY-101 using temporary hose-in-hose over ground transfer lines and existing valve pits. Leak detectors located in the SY-101 drop leg, S-A valve pit, and S-12A pump pit will be monitored in the tank S-112 retrieval control trailer. The waste retrieval system will shut down if a leak is detected in the transfer system.

Leakage from the primary over ground transfer hose (inner hose) will be contained by the secondary confinement system (outer hose) and detected by one of the three leak detectors. The secondary confinement system has been designed to drain any fluid released from the primary hose to a common point for collection, detection, and removal. The hydraulics of the tank S-112 to tank SY-101 over ground transfer line cause any leakage to the secondary containment to drain towards either the S-A valve pit or the S-12A pump pit. Leak detection elements installed in the pits actuate an alarm and annunciator light in the control room if a leak is detected and shut down the retrieval pump.

4.2.3 Leak Detection in the Receiver Double-Shell Tank

A leak from the primary vessel of tank SY-101 is detected by either a conductivity probe leak detection system installed in the annulus or a continuous air monitor that detects airborne radionuclides entrained in the annulus ventilation exhaust stream. Detection of a leak into the annulus of the tank by either system activates an audible alarm and an annunciator panel light.

The tank annulus is designed to collect and direct waste that leaks from the primary tank to the annulus for detection and transfer. Slots cut in the insulating concrete that supports the tank at the bottom are designed to drain any leakage to the annulus floor. Conductivity probe assemblies and a radiation monitor leak detection system are installed on the annulus ventilation system to detect tank leaks.

This page intentionally left blank.

5.0 UNCERTAINTY ANALYSES

This section summarizes results of leak detection uncertainty analyses performed on proposed leak detection methods and technologies for the S-112 Project. The detailed analyses and interpretation of results are provided for in-tank dynamic mass balance and ex-tank drywell methods in Appendices A and B, respectively. The purpose of these analyses was to investigate the uncertainties associated with each method and support the selection and implementation of the best available leak detection technology. This section summarizes the results of these analyses.

5.1 UNCERTAINTY OF MASS BALANCE METHODS

The S-112 Project used an integrated, multi-disciplinary team to provide the bases and details of the mass balance uncertainty analysis. As presented in Appendix A, homogeneous waste regions for the center-out mining strategy were identified, and material balance equations for the waste retrieval process were developed. Three leak volume models were developed from material balance equations for the total liquid mass, total water mass, and total liquid and solid mass inventories. The majority of the model parameters have significant uncertainties. The leak volume models were therefore evaluated using Monte Carlo simulations. For this evaluation, the magnitude of the uncertainty (and not specific leak volumes) was evaluated. Regression analyses were also performed to identify the relative importance of parameters.

Parameter distributions were developed by the project team based on in-tank measurements, data reconciliation, Hanford tank farm data, chemical modeling, and instrumentation accuracy. Although individual parameter uncertainties are not additive, insight into the large uncertainty associated with in-tank methods can be gained by considering the large uncertainty in the initial waste mass. The initial condition uncertainty is a measure of how well the actual mass of the waste in the tank is known. This is composed of uncertainties associated with the physical properties of the tank such as waste volume, porosity, density, and retained gas volume. The initial condition uncertainty range is at least 70,000 gallons at the 95% confidence interval depending on the material balance methodology (Appendix A, Table A.6). This uncertainty is not easily reduced given the complex nature of the waste.

The 95% confidence interval uncertainty range for leak volumes in tank S-112 for each of the mass balance models is summarized in Table 5.1. As shown in the table the uncertainty range is a function of the amount of waste retrieved from the tank. The total liquid mass balance method outperformed the other methods presented with a 95% confidence interval uncertainty range of 82,000 gallons when 80% of the original waste has been retrieved, which is an order of magnitude greater than the risk-based 8,000-gallon leak detection requirement developed in RPP-7825. Generally the uncertainty increases throughout the waste retrieval process as the uncertainty with retrieval conditions increase. As shown in Table 5.1 the uncertainty with water mass balance is greater than liquid mass balance methods because of the uncertainty associated with the fraction of water in the liquid waste. The total mass balance has the largest uncertainty range because of the need to account for the solid mass and its associated uncertainty.

Table 5.1. 95% Confidence Interval Best Estimate Uncertainty Range in Leak Detection for Tank S-112

Equation	95% Confidence Interval Range (gallons)				
	Original Waste Retrieved (%)				
	10	20	40	60	80
Liquid mass balance	18,000	28,500	48,900	62,100	82,400
Water mass balance	18,000	29,700	52,200	66,400	90,800
Total mass balance	90,300	137,800	203,200	198,600	161,000

The results of the regression analysis showed that the ranking of parameters in terms of significance (the key contributors to the leak volume uncertainty) varied as a function of the amount of waste retrieved and by the type of mass balance. The results of the sensitivity analysis are presented in Appendix A, Section A3.3. In general, the parameters that have the greatest influence on the total mass balance uncertainty include the following:

- Waste volumes at initial and retrieval conditions
- Mass fraction of water in the bulk waste
- Bulk density of the waste
- Volume of water added
- Density of the brine produced by dissolution of soluble solids.

Improvements in the ability to measure waste volume using the tank volume measurement system (laser based surface mapping) were evaluated separately in the uncertainty analysis and only reduced the uncertainty range by 4%, which is not considered significant.

Acknowledgment of the uncertainty associated with initial conditions and the increase in uncertainty throughout the waste retrieval process makes the 8,000-gallon requirement identified in RPP-7825 for leak detection unachievable by mass balance methods. This requires the project to deploy a system that utilizes a combination of other technologies aimed at detecting different types of leaks (leak location and leak rates) to represent best available technology.

5.2 UNCERTAINTY OF IN-TANK STATIC LEVEL MONITORING

A detailed uncertainty analysis of static liquid level monitoring methods was not conducted. However, a qualitative assessment of in-tank conditions that may impact static level observations include the following:

- Evaporation from the central pool.
- Gas accumulation or release from the central pool.
- Liquids not yet at hydraulic equilibrium with the solids.
- Undissolved waste sloughing/falling into the pool.

After the liquids are pumped down it may take weeks for the liquid level to fully equilibrate. However, it is expected that the liquid level will asymptotically approach the equilibrium level and deviations from this anticipated trend can be used as a potential indication of a leak. If there is a drop in the liquid level during this period of time, with the ventilation secured, it would be an indication of a leak. Until the liquid level reaches equilibrium the accuracy of static level monitoring will be reduced.

5.3 UNCERTAINTY OF EX-TANK DRYWELL MONITORING METHODS

The S-112 Project utilized expertise from the Tank Farms Vadose Zone Project to evaluate uncertainties associated with drywell logging methods. Determinations were made of best-case and worst-case scenarios to bound potential performance. A calculational method was used to describe leak volumes, volumes of soil contaminated, and changes in moisture content due to a leak. This was followed by a Monte Carlo analysis to assess the uncertainty range for leak detection using ex-tank drywell logging. Details on the ex-tank drywell monitoring leak detection evaluation are provided in Appendix B.

For slow leak rates ranging from 0.03 gal/hr to 1.44 gal/hr, the travel time and associated leak volumes for a leak originating near a drywell are small. The theoretical leak volume and associated time required to reach a drywell from the center of the tank floor to a drywell (modeled as a 45-foot distance) are larger. Detection of a slow leak from the center of the tank floor with a drywell is unrealistic as the time required for sufficient liquid to leak from the tank and migrate to the drywell is significantly longer than the planned waste retrieval duration. Summary statistics for travel time and total volume leaked under slow leak conditions are shown in Table 5.2. The mean values for travel times are 12 days for the 10-foot distance and 2.0 years for the 45-foot distance. The corresponding mean values for volume leaked are 100 gallons and 6,200 gallons. The 5th and 95th percentile values are also listed in Table 5.2. Approximately 90% of the results fall between these two extremes.

Table 5.2. Summary Statistical Results for Ex-Tank Leak Detection Response Time (for leaks less than 1.5 gal/hr)

Parameter	10-foot Distance (f = 0.75)	45-foot Distance (f = 0.50)
Mean travel time	12 d	710 d (2.0 y)
Median travel time	4.8 d	290 d (0.80 y)
5th percentile time	1.0 d	59 d
95th percentile time	43 d	2,600 d (7.1 y)
Mean volume leaked	100 gal	6,200 gal
Median volume leaked	73 gal	4,400 gal
5th percentile volume	20 gal	1,200 gal
95th percentile volume	300 gal	18,000 gal

Notes: The mean value is the sum of the times or volumes divided by the number of trials. The median value is the time or volume is the 50th percentile in the cumulative distribution (i.e., half the results lie below the median value). The 5th and 95th percentiles show the range of times or volumes that encompass 90% of the calculated results.

Additional uncertainty analyses were performed to evaluate a larger range in potential leak rates. Historical leak rates were reviewed and a range in-tank leak rates from 0.03 to 102 gal/hr. To account for the higher probability of a slow leak compared to a fast leak a lognormal distribution was assigned to the leak rate parameter (referred to as the lognormal leak rate model). For this leak range the 95th percentile volume at both the 10-foot and 45-ft distance increased over those shown in Table 5.2. The summary statistics for the larger leak rate range are provided in Table 5.3. It is interesting to note the frequency charts in Appendix B (Figures B1.6 and B1.7) for the lognormal leak rate model are highly skewed toward the low end, indicating that in all likelihood a leak, if one should occur, would show up sooner and have leaked a smaller volume than indicated by the 95th percentile values. It should be noted that leaks have been recorded that did not follow this model and leaked larger volumes than shown in Table 5.3.

Table 5.3. Summary Statistical Results for Ex-Tank Leak Detection Response Time (for large leaks)

Parameter	10-foot Distance (f = 0.75)	45-foot Distance (f = 0.50)
Mean travel time	20 d	1,200 d (3.3 y)
Median travel time	2.2 d	130 d
5th percentile time	0.07 d	4.1 d
95th percentile time	72 d	4,400 d (12 y)
Mean volume leaked	100 gal	6,200 gal
Median volume leaked	73 gal	4,400 gal
5th percentile volume	20 gal	1,200 gal
95th percentile volume	300 gal	18,000 gal

Notes: The mean value is the sum of the times or volumes divided by the number of trials. The median value is the time or volume is the 50th percentile in the cumulative distribution (i.e., half the results lie below the median value). The 5th and 95th percentiles show the range of times or volumes that encompass 90% of the calculated results.

This page intentionally left blank.

6.0 REFERENCES

BBI, 2001, *Tank Waste Information Network System (TWINS),* May 22, 2001 [Best Basis Inventory Calculation Detail for Tank S-112], http://twins.pnl.gov:8001/twins.htm.

Dahl, 2002, Letter from S. Dahl (Ecology) to J. Rasmussen (DOE/ORP), Re: Conditional Approval of the C-104 and S-112 Functions and Requirements (F&R) Documents, RPP-7807, Rev. 0 and RPP-7825, Rev. 0, Deliverables of HFFACO Milestone M-45-03-T04 and M-45-03-T03, July 2002.

Ecology, EPA, and DOE, 1989, *Hanford Federal Facility Agreement and Consent Order*, as amended, Washington State Department of Ecology, U.S. Environmental Protection Agency, and U.S. Department of Energy, Olympia, Washington.

HNF-SD-WM-AP-005, 1999, *SST Emergency Pumping Guide,* Rev. 8., D. D. Wiggins, CH2M HILL Hanford Group, Inc., Richland, Washington.

RPP-7825, 2001, *Single-Shell Tank S-112 Full Scale Saltcake Waste Retrieval Technology Demonstration Functions And Requirements*, Rev. 0, CH2M HILL Hanford Group, Inc., Richland, Washington.

RPP-9645, 2002, *Single-Shell Tank System Surveillance and Monitoring Program*, Rev. 0, CH2M HILL Hanford Group, Inc., Richland, Washington.

RPP-10604, 2002, *Ex-Tank LDM Technology Assessment and Down-Select Report*, Rev. 0, CH2M HILL Hanford Group, Inc., Richland, Washington.

This page intentionally left blank.

APPENDIX A
MASS BALANCE EQUATIONS AND EXAMPLE UNCERTAINTY ANALYSIS IN TANK S-112 FOR LEAK DETECTION DURING SALTCAKE DISSOLUTION

This page intentionally left blank.

CONTENTS

FIGURES

TABLES

APPENDIX A
MASS BALANCE EQUATIONS AND EXAMPLE UNCERTAINTY ANALYSIS IN TANK S-112 FOR LEAK DETECTION DURING SALTCAKE DISSOLUTION

A1.0 INTRODUCTION

One of the techniques used for leak detection in single-shell-tanks (SSTs) during retrieval is to calculate a mass balance based on initial and final inventories and inflows and outflows. Mass balances can detect leaks on the order of 10,000 gallons if both the retrieved and receiver tanks have a uniform liquid surface to measure the waste inventory accurately (Adams 1999). A means to accurately measure the density of the fluid being transferred is also required (Stewart et al. 1997, Cuta et al. 2000, Onishi et al. 2001). Retrieval of SSTs using the saltcake dissolution method is designed to minimize the liquid inventory and will not provide a free liquid surface (Crass 2001). Thus in the saltcake dissolution method there is a large inherent uncertainty in the waste inventory until most of the waste has been retrieved. Also, the dissolution process introduces uncertainties such as in the relation of brine produced to water added.

The combined effects of these uncertainties tend to make leak detection in SSTs during retrieval much less sensitive than in past operations or in typical transfers between double-shell-tanks. This appendix presents mass balance equations for assessing the potential leak volume during saltcake dissolution and evaluates the uncertainty of the methodology. Three separate leak volume equations are developed based on the total liquid mass, total water mass, and total liquid and solid mass inventory in a tank. The models are exercised on a retrieval process in Tank S-112. As the model parameters have significant uncertainties, a Monte Carlo simulation approach is used. The model parameters that have the most significant impact on the simulations are identified using a stepwise forward regression analysis, and the effect the inclusion of the tank volume measurement system (TVMS) is investigated.

The analysis determined the magnitude of the uncertainty based on best estimate waste parameters and showed that the uncertainties associated with the leak volume are quite large (best result is > 80,000 gallons 95% confidence interval uncertainty range at 80% original waste retrieval). This uncertainty range, however, is relatively small (9% of the transfer volume) compared to the total transfer volume. This leak volume uncertainty range is improved by approximately 4% with the inclusion of the TVMS.

The mass balance equations are derived in Section A2.0. In Section A3.0, the input parameter uncertainties and uncertainty analysis results are presented. Conclusions are included in Section A4.0, and cited references are listed in Section A5.0.

A2.0 MASS BALANCES

The mass balance on the total mass content in a SST during retrieval may be expressed in a rudimentary form as

$$\dot{M}_{WASTE} = \dot{M}_{SOLVENT} - \dot{M}_{TRANSFER} - \dot{M}_{LEAK} \quad (A.1)$$

where $\dot{M}$ is the change in mass with time or mass flow rate. The subscripts waste, solvent, transfer, and leak denote their respective mass flows.

SST waste is comprised of a combination of solids, liquids and gas heterogeneously distributed throughout the tank. The waste is typically configured as liquid-over-sediment, saturated sediment, or unsaturated and saturated sediment. The waste characteristics (solid and gas volume fraction, solid density, rheology, etc.) may vary considerably within these regions as well as between regions. The heterogeneities are caused by a multitude of factors including initial waste feed, long-term storage effects (settling and compaction, temperature changes and gradients, evaporation, etc.), saltwell pumping, and retrieval activities.

If we consider an actual or assumed homogeneous (spatially constant waste characteristics) waste region, the mass in this region is the sum of the solid and liquid content. The solid and liquid volumes in region i are given by

$$V_{Si} = \phi_{Si} V_i \quad (A.2)$$

and

$$V_{Li} = (1 - \phi_{Si}) \psi_i V_i \quad (A.3)$$

respectively where ϕ_S is the solid volume fraction, and ψ is the saturation (volume fraction of pore space [non-solid volume] that is occupied by liquid). The change in the total mass in region i is therefore

$$\dot{M}_i = \frac{d}{dt} V_i \left[\phi_{Si} \rho_{Si} + (1 - \phi_{Si}) \psi_i \rho_{Li} \right] \quad (A.4)$$

where ρ_S is the dry solid density and ρ_L is the liquid density. The change in the total tank mass with time is then simply

$$\dot{M}_{WASTE} = \frac{d}{dt} \sum_{i=1}^{n} V_i \left[\phi_{Si} \rho_{Si} + (1 - \phi_{Si}) \psi_i \rho_{Li} \right] \quad (A.5)$$

where n is the number of actual or assumed homogeneous waste regions.

The mass flow rates for the solvent, transfer, and leak may also be expressed in terms of a volumetric flow rate Q and density ρ.

Saltcake dissolution process planning has emphasized leak prevention. This involves minimizing the liquid inventory at all times and keeping liquid away from the tank wall as long as possible. This has led to a "center out" retrieval strategy where the waste is dissolved first near the tank center forming a roughly funnel-shaped central cavity that expands toward the wall as the retrieval progresses. The waste in an SST after saltwell pumping will typically consist of three main regions; a central liquid pool, a layer of liquid saturated waste, and a layer of unsaturated waste. Interstitial liquid exists in both the saturated and unsaturated layers. Other potential sub-regions include regions of sludge or insoluble waste, a layer of insolubles collected at the bottom of the pool, regions recently drained by saltwell pumping, and regions re-saturated by waste retrieval activities. In practice, identification of region boundaries and differentiation of material properties between similar waste regions (saturated and sludge, and unsaturated and recently drained for example) will be difficult at best. We will therefore focus on the three main waste regions (assumed homogeneous, see Section A2.1) for this analysis, with the sludge and insolubles at the bottom of the pool included with the saturated waste, and the recently drained and re-saturated zones included in the unsaturated region.

A sketch of the liquid flows and inventories during center-out saltcake dissolution with three homogeneous waste regions is shown in Figure A.1. The solvent water at rate Q_W is added to the unsaturated waste dissolving soluble solids to reduce the waste volume at rate ΔV_U and creating brine (including the water added) at the rate Q_B. The interstitial liquid liberated from the volume dissolved, plus the brine created in the process, saturates previously unsaturated waste. Brine can also infiltrate the unsaturated waste from the pool at rate Q_I or drain into the pool from saturated waste at rate Q_D. Brine is also transferred out of the pool at Q_T and can leak out of the tank from the saturated waste at a rate Q_{LEAK}.

Figure A.1. Waste Configuration during Saltcake Dissolution

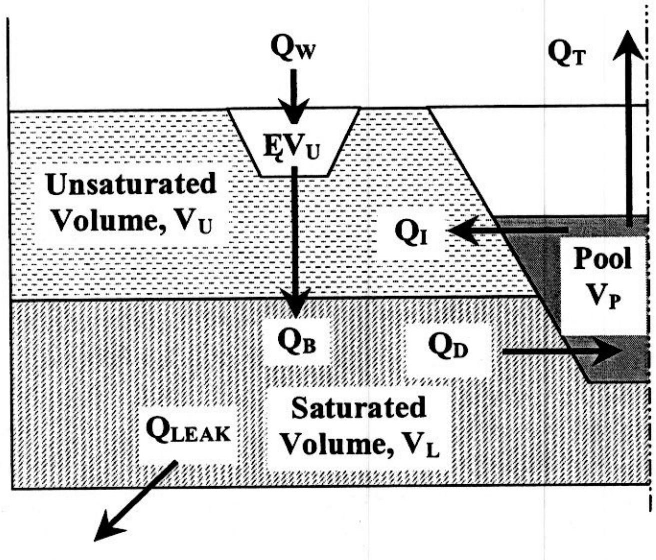

The mass balances on the liquid contained in the central pool and in the two waste layers are derived separately and added together to form the total liquid mass balance. A mass balance for the water in the tank is developed concurrently. Section A2.1 lists the assumptions involved in the derivation for the mass balances, and Section A2.2 lists the nomenclature for the parameters. Section A2.3 covers the mass balance in the central pool, Section A2.4 discusses the unsaturated waste outside the pool and Section A2.5 treats the saturated waste. The individual mass balances are combined into the overall leak detection equations in Sections A2.6 and A2.7. In Section A2.8, a mass balance on the total solid and liquid inventory is presented.

A2.1 ASSUMPTIONS

The assumptions made in deriving this simplified mass balance are many and sweeping. The net effect is to reduce measurement uncertainty in the result at the expense of increasing the modeling uncertainty. Adding detailed models to remove the assumptions would probably increase measurement uncertainty while possibly decreasing the modeling uncertainty. It is not clear whether adding to the model would provide a net improvement in leak detection ability.

- The dissolution process occurs instantaneously, creates a mixture of dissolved solids and solvent water at saturation in the dominant species, liberates interstitial liquid stored in the dissolved waste, and leaves insoluble solids behind.
- Volume is conserved when fluids are mixed.
- Solid volume fraction, dry solid density, and interstitial liquid density are equivalent for saturated and unsaturated waste.
- Insoluble solids pack to the same volume fraction as the waste prior to dissolution.
- All solvent water added dissolves soluble solids.
- The liquid in the pool is assumed to be always saturated with dissolved solids so that no dissolution occurs in the pool.
- Infiltration of brine from the pool fills unsaturated waste and creates saturated waste.
- Dissolution can occur only in unsaturated waste so draining rate determines the dissolution rate once all initially unsaturated waste is dissolved.
- The central pool includes only liquid. Insoluble sediments on pool bottom is included in the waste.

The spatial and temporal variability of the waste parameters of Equation (A.5) for the specific waste regions during retrieval are discussed below.

- **Clear Pool**

  Liquid density: Varies with time as dissolution products and efficiencies change. Varies mainly vertically due to density gradients, unless pool is very shallow and broad.

- **Unsaturated Region**

  Solid volume fraction: Constant, but varies significantly with radius (measured – greater at outer radii), unknown vertically but expected to be lower toward surface.

Saturation: Constant. Expected to vary spatially, probably affected mostly by particle size.

Interstitial liquid density: Constant. Could vary spatially, but variation is expected to be small.

Dry solid density: Calculable from measured composition. Constant and can theoretically vary spatially, but expected variation is small.

- **Saturated Region**

  Similar to unsaturated zone, constant over the time scale of retrieval, but significant spatial variation as defined by core samples. Description of waste properties same as for unsaturated zone.

The variations and the assumptions made for those parameters that vary in time and/or space are summarized in Table A.1. The bases for the assumptions are denoted in the table by the following:

1. Process modeling & experiments.
2. Unavailable/unattainable data.
3. Variation is small.

Table A.1. Waste Parameter Variability

Parameter Name	Varies with Time? *Assumption*	Assumption Basis	Varies in Space? *Assumption*	Assumption Basis
Pool Liquid Density	Yes *Yes*	1	Yes *No*	2, 3
Solid Volume Fraction	No *No*	-	Yes *No*	2
Saturation	No *No*	-	Yes *No*	2
Interstitial Liquid Density	No *No*	-	Yes *No*	2
Dry Solid Density	No *No*	-	Yes *No*	2, 3

A2.2 NOMENCLATURE

ϕ_S Volume fraction of waste occupied by solids

ψ_{LU} Volume fraction of pore space (non-solid volume) in unsaturated waste that is occupied by liquid

ψ_{LS}	Volume fraction of pore space (non-solid volume) in saturated waste that is occupied by liquid. Less than 100% due to retained gas.
ρ_{IL}	Density of original interstitial liquid in both saturated and unsaturated waste
ρ_P	Density of brine in the central pool
ρ_B	Density of brine produced by dissolution of soluble solids, including water added
ρ_H	Density of solvent water added
ρ_S	Density of dry solids
ρ_T	Density of bulk degassed waste
w_{IL}	Mass fraction of water in the interstitial liquid
w_P	Mass fraction of water in the liquid in the central pool
w_B	Mass fraction of water in the brine produced by dissolution of soluble solids
w_T	Mass fraction of water in the bulk waste
ϕ_H	Volume fraction of water in the liquid
α	Volume fraction of gas in the saturated waste
m	Slope of the linear function describing the mass fraction of water in the liquid as a function of the liquid density
Q_W	Volume flow rate of water added
Q_D	Volumetric flow rate at which saturated brine drains into pool
Q_I	Volumetric flow rate at which saturated brine from pool infiltrates unsaturated waste
V_{QW}	Total volume of water added over a given time period
ΔV_U	Net rate of unsaturated waste volume reduction by dissolution
Q_B	Rate at which brine volume is created by dissolution only, including added water
Q_{LEAK}	Volumetric leak flow rate
V_{LEAK}	Total volume of brine leaked over a given time period
V_{LEAKW}	Total volume of brine leaked over a given time period as determined from water balance

V_{LEAKT}	Total volume of brine leaked over a given time period as determined from total tank mass balance
Q_T	Volumetric flow rate at which brine is pumped from the pool
V_T	Total volume of brine pumped out of the pool over a given time period
F_B	Volume of brine produced directly by dissolution per unit volume of water added
V_P	Volume of central liquid pool, excluding settled insolubles on the bottom
V_W	Volume of liquid-saturated and unsaturated waste outside the pool, including the settled insolubles on the bottom of the pool
V_L	Volume of liquid saturated waste outside the central pool including settled insolubles on the bottom of the pool
V_U	Volume of unsaturated waste

A2.3 MASS BALANCE IN THE CENTRAL LIQUID POOL

Referring to Figure A.1 and applying Eq. (A.1) to the liquid pool, the change in the volume of liquid in the pool depends on the rates of draining of brine from the saturated waste, brine infiltration into the unsaturated waste and brine transferred out of the pool by pumping. We assume that no solvent water enters the pool directly. Evaporation, which would be minimal in low-temperature concentrated brine, and thermal expansion are ignored. The mass balance of Eq. (A.1) with Eq. (A.4) on the liquid in the central pool is expressed as

$$\frac{d}{dt}\left(\rho_P V_P\right) = \rho_{IL} Q_D - \rho_P Q_I - \rho_P Q_T \qquad \text{(A.6)}$$

The mass of water in a given mass of liquid is the product of the mass of the liquid and the mass fraction of water in that liquid. The mass balance on the water in the central pool is therefore

$$\frac{d}{dt}\left(\rho_P V_P w_P\right) = \rho_{IL} Q_D w_{IL} - \rho_P Q_I w_P - \rho_P Q_T w_P \qquad \text{(A.7)}$$

A2.4 MASS BALANCE IN THE UNSATURATED WASTE

The amount of liquid stored in the unsaturated zone is determined from the bulk waste volume in this region as given by Eq. (A.3). Since there is no direct measurement relating directly to the unsaturated waste volume, it is computed as the difference between the total waste volume, V_W, and the saturated waste volume, V_L, as

$$V_U = V_W - V_L \qquad \text{(A.8)}$$

The rate of change in the mass of interstitial liquid in the unsaturated waste is equal to the rate of brine infiltrating from the pool less the rate of interstitial liquid lost by dissolution (Eq. [A.1] applied to the unsaturated waste). The mass of interstitial liquid lost by dissolution is simply the mass of interstitial liquid in the dissolved volume ΔV_U. The brine created by dissolution along with the liberated interstitial liquid is assumed to join the saturated waste. Using Eqs. (A.1), (A.4) and (A.8) the mass balance on the liquid in the unsaturated waste is expressed as

$$\frac{d}{dt}\left[\rho_{IL}(1-\phi_S)\psi_{LU}(V_W - V_L)\right] = \rho_P Q_I - \rho_{IL}(1-\phi_S)\psi_{LU}\Delta V_U \qquad (A.9)$$

The mass balance for the water in the unsaturated waste is likewise given by

$$\frac{d}{dt}\left[\rho_{IL}(1-\phi_S)\psi_{LU}(V_W - V_L)w_{IL}\right] = \rho_P Q_I w_P - \rho_{IL}(1-\phi_S)\psi_{LU}\Delta V_U w_{IL} \qquad (A.10)$$

A2.5 MASS BALANCE IN THE SATURATED WASTE

The volume of liquid stored in the saturated zone is again determined from Eq. (A.3). From Eq. (A.1) applied to the saturated waste, the rate of change in the mass of interstitial liquid in the saturated waste outside the pool is equal to the rate of brine created by dissolution plus the corresponding flow of liberated interstitial liquid from the unsaturated zone less the rate of brine drainage into the pool and the rate of interstitial liquid lost by leakage. The rate, Q_B, at which brine is produced by dissolving soluble solids in unsaturated waste including the flow rate, Q_W, of added water can be expressed by

$$Q_B = Q_W F_B \qquad (A.11)$$

where F_B is the volume of brine produced per unit volume of water added during dissolution. Using Eqs. (A.1), (A.4) and (A.11), the mass balance for the liquid in the saturated waste is expressed as

$$\frac{d}{dt}\left[\rho_{IL}(1-\phi_S)\psi_{LS}V_L\right] = \rho_B Q_W F_B + \rho_{IL}(1-\phi_S)\psi_{LU}\Delta V_U - \rho_{IL}(Q_D + Q_{LEAK}) \qquad (A.12)$$

The mass balance on the water in the saturated region is determined similarly as

$$\begin{aligned}&\frac{d}{dt}\left[\rho_{IL}(1-\phi_S)\psi_{LS}V_L w_{IL}\right] \\ &= \rho_H Q_W + \rho_{IL}(1-\phi_S)\psi_{LU}\Delta V_U w_{IL} - \rho_{IL}(Q_D + Q_{LEAK})w_{IL}\end{aligned} \qquad (A.13)$$

Note that the volume of brine produced per unit volume of water added during dissolution (F_B) is not required in Eq. (A.13).

A2.6 LEAK RATE EQUATIONS

The rate of change for the entire liquid or water inventories in the tank can be determined by combining Eqs. (A.6), (A.9) and (A.12), and Eqs. (A.7), (A..10) and (A.13) yielding

$$\frac{d}{dt}(\rho_P V_P) + \rho_{IL}(1-\phi_S)\frac{d}{dt}\left[V_L(\psi_{LS} - \psi_{LU}) + V_W \psi_{LU}\right] = -\rho_P Q_T - \rho_{IL} Q_{LEAK} + \rho_B Q_W F_B \quad (A.14)$$

and

$$\frac{d}{dt}(\rho_P V_P w_P) + \rho_{IL}(1-\phi_S) w_{IL}\frac{d}{dt}\left[V_L(\psi_{LS} - \psi_{LU}) + V_W \psi_{LU}\right] = -\rho_P Q_T w_P - \rho_{IL} Q_{LEAK} w_{IL} + \rho_H Q_W \quad (A.15)$$

As specified in Section A2.1, the interstitial liquid density was assumed constant and the pool liquid density is allowed to vary. Solving Eqs. (A.14) and (A.15) for Q_{LEAK} gives the general leak rate detection expressions

$$Q_{LEAK} = \frac{1}{\rho_{IL}}\left\{-\frac{d}{dt}(\rho_P V_P) - \rho_P Q_T + \rho_B Q_W F_B\right\} - (1-\phi_S)\frac{d}{dt}\left[V_L(\psi_{LS} - \psi_{LU}) + V_W \psi_{LU}\right] \quad (A.16)$$

for the liquid and

$$Q_{LEAK} = \frac{1}{\rho_{IL} w_{IL}}\left\{-\frac{d}{dt}(\rho_P V_P w_P) - \rho_P Q_T w_P + \rho_H Q_W\right\} - (1-\phi_S)\frac{d}{dt}\left[V_L(\psi_{LS} - \psi_{LU}) + V_W \psi_{LU}\right] \quad (A.17)$$

from the water contained in the liquid.

A2.7 LEAK VOLUME EQUATIONS

Eqs. (A.16) and (A.17) define the leak rate at any instant in time. An expression for the total leak volume over some time period can also be derived by integrating Eqs. (A.16) and (A.17) from initial time, t_0, to final time, t_1. It is assumed that integrals of products can be reasonably represented by products of averages and that flow totalizers automatically integrate the flow rate to provide a measurement of the volume. Hence

$$\int_{t_0}^{t_1} Q_T dt = V_T$$

$$\int_{t_0}^{t_1} Q_W dt = V_{QW} \quad (A.18)$$

$$\int_{t_0}^{t_1} Q_{LEAK} dt = V_{LEAK}$$

With Eq. (A.18), Eqs. (A.16) and (A.17) can be integrated to provide expressions for the total leak volume:

$$\begin{aligned} V_{LEAK} = \frac{1}{\rho_{IL}} \{ & -\rho_{P1} V_{P1} + \rho_{P0} V_{P0} - \rho_{P1} V_T + \rho_B V_{QW} F_B \\ & -(1-\phi_S)\{(\psi_{LS} - \psi_{LU})[V_{L1} - V_{L0}] + \psi_{LU}[V_{W1} - V_{W0}]\} \end{aligned} \tag{A.19}$$

for the "liquid mass balance" and

$$\begin{aligned} V_{LEAKW} = \frac{1}{\rho_{IL} w_{IL}} \{ & -\rho_{P1} V_{P1} w_{P1} + \rho_{P0} V_{P0} w_{P0} - \rho_{P1} V_T w_{P1} + \rho_H V_{QW} \\ & -(1-\phi_S)\{(\psi_{LS} - \psi_{LU})[V_{L1} - V_{L0}] + \psi_{LU}[V_{W1} - V_{W0}]\} \end{aligned} \tag{A.20}$$

for the "water mass balance".

A2.8 LEAK DETECTION FROM TOTAL WASTE MASS BALANCE

With Eqs. (A.1) and (A.5), the rate of change of the total solid and liquid mass inventory for the three regions of the tank may be developed in a similar fashion as above to be

$$\begin{aligned} & \frac{d}{dt}\{\rho_S \phi_S V_W + \rho_{IL}(1-\phi_S)[(\psi_{LS} - \psi_{LU})V_L + \psi_{LU} V_W] + \rho_P V_P\} \\ & = -\rho_P Q_P - \rho_{IL} Q_{LEAK} + \rho_H Q_W \end{aligned} \tag{A.21}$$

from which the leak volume can be determined as

$$\begin{aligned} V_{LEAKT} = \frac{1}{\rho_{IL}} \{ & -\rho_{P1} V_{P1} + \rho_{P0} V_{P0} - \rho_S \phi_S (V_{W1} - V_{W0}) - \rho_{P1} V_T + \rho_H V_{QW} \\ & -(1-\phi_S)\{(\psi_{LS} - \psi_{LU})(V_{L1} - V_{L0}) + \psi_{LU}(V_{W1} - V_{W0})\} \end{aligned} \tag{A.22}$$

Equation (A.22) is referred to as the "total mass balance" model.

A3.0 INPUT PARAMETERS AND UNCERTAINTY ANALYSIS

In-tank and process instrumentation are required to determine the leak volume via the mass balance equations. In Section A3.1, parameter data sources are summarized. The mass balance leak detection models are applied to tank S-112. Parameter values specific to S-112 and the evaluation results are presented in Section A3.2. The parameters that contribute most significantly to the uncertainty analysis results are identified in Section A3.3.

A3.1 MODEL INPUT PARAMETERS

To determine the leak volumes, each of the quantities in Eqs. (A.19), (A.20), and (A.22) must be determined. The actual and potential sources of data for each term in the equations are listed in Table A.2 below.

Table A.2. Data Sources for Leak Detection Parameters

Parameter	Source
ρ_{IL}	Core sample analysis, data reconciliation
ψ_{LU}	"
ψ_{LS}	"
ϕ_S	"
ρ_B	ESP runs, dissolution tests, data reconciliation
F_B	"
F_T	"
w_{IL}	"
w_P	"
ρ_P	Saltwell dip tubes, grab samples, Densimeter
ρ_H	Handbook
Q_T, V_T	Flow meter, flow totalizer, allowing for in-line dilution
Q_W, V_{QW}	Flow meter, flow totalizer
V_W	Enraf level gauge early in retrieval, video
V_L	Neutron logs early in retrieval, unknown later, porous media flow theory
V_P	Saltwell dip tubes, Enraf level gauge later in retrieval, video, pump stop-start estimates

The majority of these parameters have significant uncertainties. The uncertainty may be due to a combination of factors including measurement uncertainty, model accuracy, process instrumentation uncertainty, and spatial and temporal variability. A deterministic calculation with all parameters set to bounding values has no physical or statistical basis. Instead, we must account for all the parameter uncertainties and establish the overall probability distribution for the model's predictions. To accomplish this, a large number of model simulations are run with input parameter sets selected from their respective distributions. The collection of output values from all the model simulations then forms the desired overall probability distribution.

A Monte Carlo simulation approach was used. This approach can be employed to estimate the uncertainty of modeling results when the input parameters have uncertainty distributions. For each evaluation, 10,000 simulation runs were conducted. Simulating a large number of runs allows all important physical effects included in the model to influence the predicted behavior. The result is a set of 10,000 model outputs, each with its own predicted result, that constitutes a probability distribution over those predicted results. This allows us to predict the probability of a given result given the input probability distributions.

A3.2 TANK S-112 UNCERTAINTY ANALYSIS

Tank S-112 was evaluated as it is the first tank scheduled for retrieval by saltcake dissolution. This tank also lacks a free liquid surface (see Figure A.1) and its waste configuration is representative of a typical SST that has been saltwell pumped. The uncertainty in the leak volumes (Eqs. [A.19], [A.20], and [A.22]) was evaluated sequentially through the retrieval process when 10, 20, 40, 60, and 80 % of the original waste volume was retrieved.

The best estimate parameter uncertainty ranges and distributions used in this analysis as determined from the available measurements and analyses listed in Table A.2 are presented in Tables A.3, A.4, and A.5. The subscripts 0 through 5 denote the initial and sequential tank conditions (1 is 10 % retrieved, 2 is 20 % retrieved, 3 is 40 % retrieved, etc.) respectively. Where the subscript j appears it denotes conditions 1-5. Assumptions and analyses used to determine specific parameter values and uncertainties are discussed below.

The solid volume fraction, volume fraction of the pore space in the saturated region that is occupied by liquid, and the volume of brine produced per unit volume of water added are determined concurrently within the Monte Carlo simulation. The solid volume fraction is calculated from the solid density, bulk degassed waste density, and interstitial liquid and bulk water mass fractions as

$$\phi_S = \left(1 - \frac{w_T}{w_{IL}}\right)\frac{\rho_T}{\rho_S} \qquad \text{(A.23)}$$

Table A.3. Input Distributions for Liquid Mass Balance, V_{LEAK} [Eq. (A.19)] (2 Sheets)

Variable	(units)	Median	Maximum	Minimum	Distribution
ρ_{P0}	(kg/m^3)	1455			normal, SD=30, truncated to 2SD
ρ_{Pi}	(kg/m^3)	1380	1390	1370	normal
ρ_{IL}	(kg/m^3)	1455			normal, SD=30, truncated to 2SD, same half of distribution as ρ_T
ρ_S	(kg/m^3)	2250	2300	2200	uniform
ρ_H	(kg/m^3)	1000			point value
□	(m^3/kg)	-0.0010229	-0.00117	-0.000975	skewed normal
w_T		0.128			normal, SD=0.05, truncated –1SD, +2SD
ρ_T	(kg/m^3)	1700	1900	1500	uniform, same half of distribution as ρ_{IL}
ψ_{LU}		0.08	0.04	0.12	normal
α		0.045	0.09	0	normal
V_{QW1}	(m^3)	339	342	336	uniform
V_{T1}	(m^3)	426.4			point value
V_{QW2}	(m^3)	697	704	690	uniform
V_{T2}	(m^3)	883.3			point value
V_{QW3}	(m^3)	1358	1372	1344	uniform
V_{T3}	(m^3)	1733.5			point value
V_{QW4}	(m^3)	2003	2023	1983	uniform
V_{T4}	(m^3)	2560.3			point value
V_{QW5}	(m^3)	2715	2742	2688	uniform
V_{T5}	(m^3)	3492.8			point value
V_{P0}	(m^3)	1.125	2.1	0.15	uniform
V_{P1}	(m^3)	0.54	6	0.05	skewed normal
V_{P2}	(m^3)	7.1	22.6	0.24	skewed normal
V_{P3}	(m^3)	28.1	62	2.9	skewed normal
V_{P4}	(m^3)	51	63.1	6.5	skewed normal
V_{P5}	(m^3)	88.1	101.3	15	skewed normal
V_{L0}	(m^3)	1252	1304	1200	uniform
V_{L1}	(m^3)	1209	1293	1098	skewed normal
V_{L2}	(m^3)	1125	1286	957	normal
V_{L3}	(m^3)	931	1193	663	normal

Table A.3. Input Distributions for Liquid Mass Balance, V_{LEAK} [Eq. (A.19)] (2 Sheets)

Variable	(units)	Median	Maximum	Minimum	Distribution
V_{L4}	(m^3)	740	1117	655	skewed normal
V_{L5}	(m^3)	446	1020	387	skewed normal
V_{W0}	(m^3)	2335	2522	2150	normal
V_{W1}	(m^3)	2105	2406	1800	normal
V_{W2}	(m^3)	1872	2469	1476	skewed normal
V_{W3}	(m^3)	1404	2166	835	skewed normal
V_{W4}	(m^3)	973	1905	835	skewed normal
V_{W5}	(m^3)	468	1196	400	skewed normal

Table A.4. Input Distributions for Water Mass Balance, V_{LEAKW} [Eq. (A.20)] (2 Sheets)

Variable	(units)	Median	Maximum	Minimum	Distribution
ρ_{P0}	(kg/m^3)	1455			normal, SD=30, truncated to 2SD
ρ_{Pi}	(kg/m^3)	1380	1390	1370	normal
ρ_{IL}	(kg/m^3)	1455			normal, SD=30, truncated to 2SD, same half of distribution as ρ_T
ρ_S	(kg/m^3)	2250	2300	2200	uniform
ρ_H	(kg/m^3)	1000			point value
□	(m^3/kg)	-0.0010229	-0.00117	-0.000975	skewed normal
w_T		0.128			normal, SD=0.05, truncated –1SD, +2SD
ρ_T	(kg/m^3)	1700	1900	1500	uniform, same half of distribution as ρ_{IL}
ψ_{LU}		0.08	0.04	0.12	normal
α		0.045	0.09	0	normal
V_{QW1}	(m^3)	339	342	336	uniform
V_{T1}	(m^3)	423.3			point value
V_{QW2}	(m^3)	697	704	690	uniform
V_{T2}	(m^3)	875.2			point value
V_{QW3}	(m^3)	1358	1372	1344	uniform
V_{T3}	(m^3)	1714.4			point value
V_{QW4}	(m^3)	2003	2023	1983	uniform
V_{T4}	(m^3)	2530.6			point value
V_{QW5}	(m^3)	2715	2742	2688	uniform
V_{T5}	(m^3)	3447.3			point value
V_{P0}	(m^3)	1.125	2.1	0.15	uniform
V_{P1}	(m^3)	0.54	6	0.05	skewed normal
V_{P2}	(m^3)	7.1	22.6	0.24	skewed normal
V_{P3}	(m^3)	28.1	62	2.9	skewed normal
V_{P4}	(m^3)	51	63.1	6.5	skewed normal
V_{P5}	(m^3)	88.1	101.3	15	skewed normal
V_{L0}	(m^3)	1252	1304	1200	uniform
V_{L1}	(m^3)	1209	1293	1098	skewed normal
V_{L2}	(m^3)	1125	1286	957	normal
V_{L3}	(m^3)	931	1193	663	normal

Table A.4. Input Distributions for Water Mass Balance, V_{LEAKW} [Eq. (A.20)] (2 Sheets)

Variable	(units)	Median	Maximum	Minimum	Distribution
V_{L4}	(m^3)	740	1117	655	skewed normal
V_{L5}	(m^3)	446	1020	387	skewed normal
V_{W0}	(m^3)	2335	2522	2150	normal
V_{W1}	(m^3)	2105	2406	1800	normal
V_{W2}	(m^3)	1872	2469	1476	skewed normal
V_{W3}	(m^3)	1404	2166	835	skewed normal

Table A.5. Input Distributions for Total Mass Balance, V_{LEAKT} [Eq. (A.22)] (2 Sheets)

Variable	(units)	Median	Maximum	Minimum	Distribution
ρ_{P0}	(kg/m^3)	1455			normal, SD=30, truncated to 2SD
ρ_{Pi}	(kg/m^3)	1380	1390	1370	normal
ρ_{IL}	(kg/m^3)	1455			normal, SD=30, truncated to 2SD, same half of distribution as ρ_T
ρ_S	(kg/m^3)	2250	2300	2200	uniform
ρ_H	(kg/m^3)	1000			point value
□	(m^3/kg)	-0.0010229	-0.00117	-0.000975	skewed normal
w_T		0.128			normal, SD=0.05, truncated –1SD, +2SD
ρ_T	(kg/m^3)	1700	1900	1500	uniform, same half of distribution as ρ_{IL}
ψ_{LU}		0.08	0.04	0.12	normal
α		0.045	0.09	0	normal
V_{QW1}	(m^3)	339	342	336	uniform
V_{T1}	(m^3)	485.7			point value
V_{QW2}	(m^3)	697	704	690	uniform
V_{T2}	(m^3)	995.9			point value
V_{QW3}	(m^3)	1358	1372	1344	uniform
V_{T3}	(m^3)	1980.0			point value
V_{QW4}	(m^3)	2003	2023	1983	uniform
V_{T4}	(m^3)	2913.5			point value
V_{QW5}	(m^3)	2715	2742	2688	uniform
V_{T5}	(m^3)	3991.0			point value
V_{P0}	(m^3)	1.125	2.1	0.15	uniform
V_{P1}	(m^3)	0.54	6	0.05	skewed normal
V_{P2}	(m^3)	7.1	22.6	0.24	skewed normal
V_{P3}	(m^3)	28.1	62	2.9	skewed normal
V_{P4}	(m^3)	51	63.1	6.5	skewed normal
V_{P5}	(m^3)	88.1	101.3	15	skewed normal
V_{L0}	(m^3)	1252	1304	1200	uniform
V_{L1}	(m^3)	1209	1293	1098	skewed normal
V_{L2}	(m^3)	1125	1286	957	normal
V_{L3}	(m^3)	931	1193	663	normal

Table A.5. Input Distributions for Total Mass Balance, V_{LEAKT} [Eq. (A.22)] (2 Sheets)

Variable	(units)	Median	Maximum	Minimum	Distribution
V_{L4}	(m^3)	740	1117	655	skewed normal
V_{L5}	(m^3)	446	1020	387	skewed normal
V_{W0}	(m^3)	2335	2522	2150	normal
V_{W1}	(m^3)	2105	2406	1800	normal
V_{W2}	(m^3)	1872	2469	1476	skewed normal
V_{W3}	(m^3)	1404	2166	835	skewed normal

The volume fraction of the pore space in the saturated region that is occupied by liquid is a function of the solid volume fraction and gas volume fraction in the saturated region or

$$\psi_{LS} = 1 - \frac{\alpha}{1-\phi_S} \qquad (A.24)$$

and the volume of brine produced per unit volume of water added is given by

$$F_B = \frac{\rho_H}{\rho_B w_B} \qquad (A.25)$$

It is assumed that the brine density is equivalent to the pool density. The mass fraction of water in the liquid is determined from the liquid density from TWINS[1] S-112 core sample data as shown in Figure A.2. A linear function of the form

$$w_H = m \cdot \rho_L + (1 - 1000 \cdot m) \quad (A.26)$$

where w_H is the mass fraction of water in the liquid and ρ_L is the liquid density was fit to the TWINS data. The slope m was assigned a skewed-normal distribution between -1.17E-3 and –9.75E-4 m^3/kg as depicted by the dashed lines in Figure A.2 and is used to represent the uncertainty of the functional relation. ESP simulation results for S-112 are also shown on the plot for comparison, and indicate that, for the purposes of our current evaluation, a linear fit is an acceptable representation.

[1] TWINS: Tank Waste Information System database.

Figure A.2. S-112 Liquid Density as a Function of the Mass Fraction of Water in the Liquid

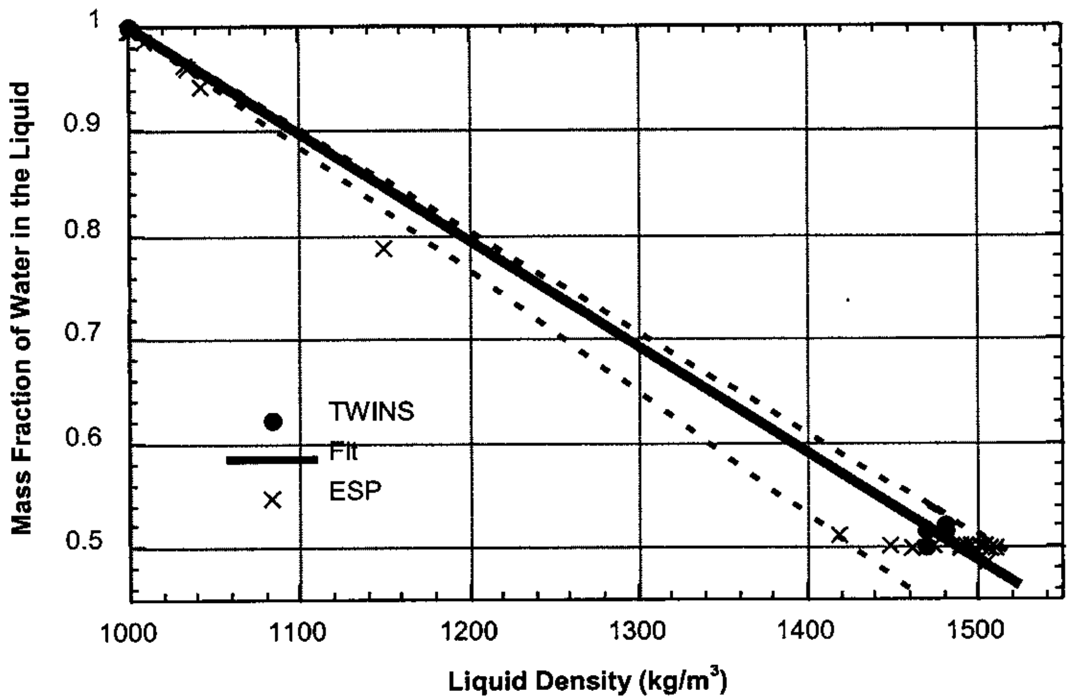

Initial waste volumes are estimated using the available level measurements. Subsequent volume uncertainties are predicted based on the three-region waste configuration. A simplified schematic of the potential effects of center-out saltcake dissolution on this waste configuration is illustrated in Figure A.3. For the initial conditions, the uncertainty in the total non-pool waste volume is primarily a function of the uncertainty in the waste depth. As the retrieval progresses and the waste acquires the configuration depicted in retrieval state "1", uncertainty in the non-pool waste volume increases due to the uncertainty of the retrieved volume. In our simplified configuration, the total waste depth (and waste depth uncertainty) remains the same. However, the uncertainty in the retrieved volume is quite large, increasing the overall uncertainty. As the waste configuration reaches retrieval state "2", the volume affected by the waste depth is reduced, and the overall non-pool waste volume uncertainty reduces accordingly. Note also that as the retrieval progresses, the volume of insolubles at the bottom of the pool increases, adding to the uncertainty of the non-pool volume. These predicted changes in the non-pool waste volume maximum (i.e. all inputs set to bounding values) uncertainty as the retrieval progresses are shown in Figure A.4.

Figure A.3. Simplified Schematic of Waste Configuration During Center-Out Saltcake Dissolution

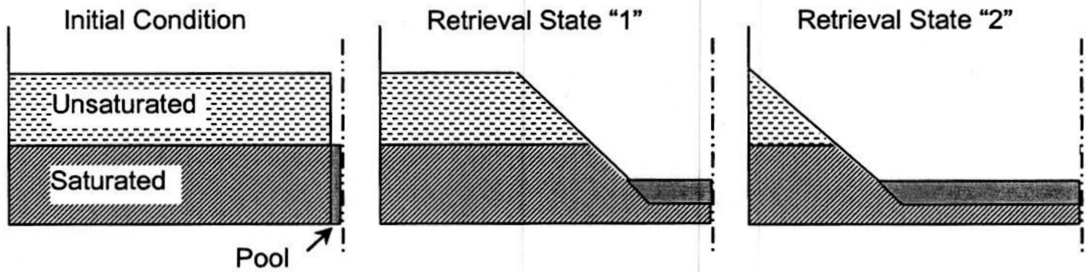

Figure A.4. Predicted Maximum Waste Volume Uncertainty Range as a Function of the Volume of Original Waste Retrieved

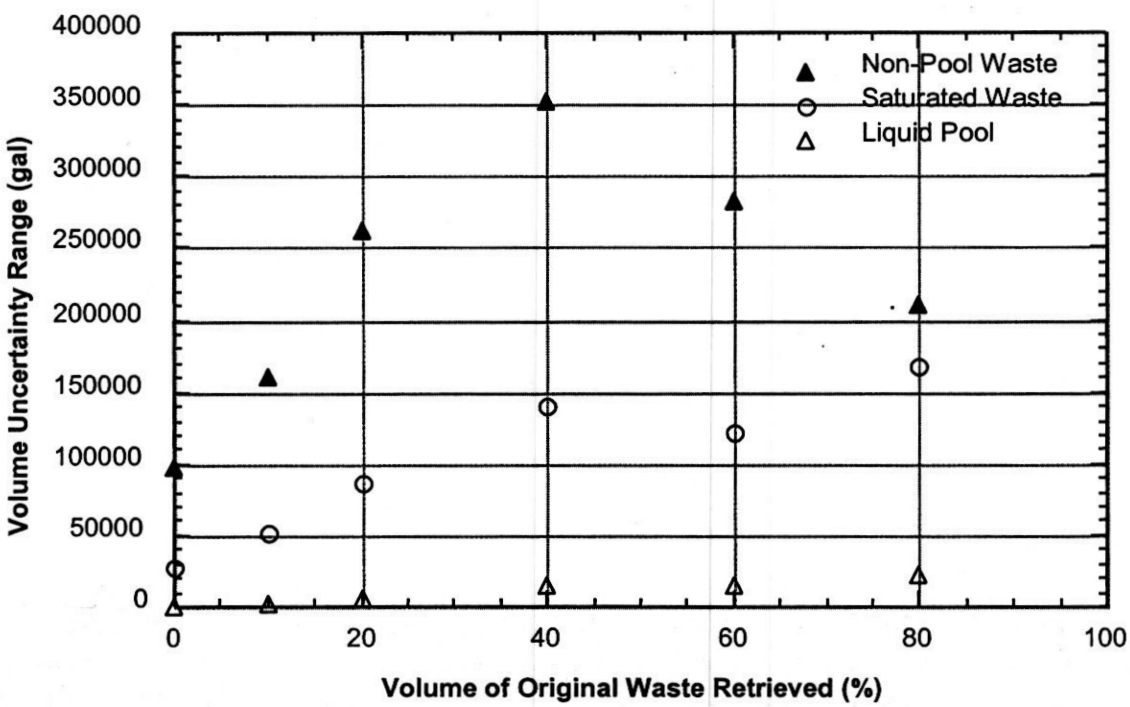

We have assumed that the initial level of interstitial liquid (which dictates the initial saturated region volume) remains constant throughout the retrieval process. As shown in Figure A.4, the maximum uncertainty of the saturated region volume follows the same trend as the non-pool volume until it is dominated by the uncertainty in the insolubles at the bottom of the pool, at which point it again increases. The maximum uncertainty in the pool volume mimics this behavior, Figure A.4.

It is of interest to note the range of the uncertainty for the initial total non-gaseous waste volume, liquid volume, and water volume. The initial non-gaseous waste volume can be computed from Eq. (A.22) as

$$V_{NG0} = V_{P0} + V_{L0}[\phi_S + (1-\phi_S)\psi_{LS}] + (V_{W0} - V_{L0})[\phi_S + (1-\phi_S)\psi_{LU}] \quad (A.27)$$

The initial liquid volume is then simply

$$V_{L0} = V_{P0} + V_{L0}(1-\phi_S)\psi_{LS} + (V_{W0} - V_{L0})(1-\phi_S)\psi_{LU} \quad (A.28)$$

The volume fraction of water in the liquid in waste region i can be computed directly from the mass fraction of water in the liquid by

$$\phi_{Hi} = w_i \frac{\rho_{Li}}{\rho_H} \quad (A.29)$$

With Eqs. (A.28) and (A.29), the initial water volume may be computed as

$$V_{H0} = V_{P0}\phi_{HP0} + [V_{L0}(1-\phi_S)\psi_{LS} + (V_{W0} - V_{L0})(1-\phi_S)\psi_{LU}]\phi_{HIL} \quad (A.30)$$

The 95% confidence interval (CI) range of the uncertainty for the initial total non-gaseous waste volume, liquid volume, and water volume as dictated by the best estimate parameter distributions presented in Tables A.3, A.4, and A.5 are listed in Table A.6. The 95% CI range is computed from the difference in the upper and lower bounds (denoted by UB and LB, respectively) of the 95% CI.

Table A.6. Initial Waste Volume Uncertainty Ranges

Initial Waste Volume	95% CI Range (gallons)
Total Non-gaseous Waste	72,100
Total Liquid	87,800
Total Water	71,200
Total Dissolved Solids	23,600

The uncertainty range in the total dissolved solids is also included in Table A.3. The liquid volume is necessarily the sum of the water and dissolved solids (as they exist in the liquid state) volumes. Note that the total initial liquid uncertainty range is not the sum of the uncertainty in the water and dissolved solids. This is caused by two effects. First, the uncertainty range is, in effect, another means of presenting the standard deviation. (Note that the uncertainty range is presented instead of the standard deviation to provide the 95% CI, as the relation between the quantiles [percentiles] and the distribution's standard deviation is a function of the shape of the distribution.) From $a^2+b^2=c^2$, we can see that $a+b \neq c$. Therefore, we do not expect the sum of the standard deviations (or, representatively, the uncertainty range from the quantiles) to be equal to the standard deviation of the result. Second, the volumes of water and dissolved solids in a given volume of liquid are not independent, therefore also precluding the possibility of the sum of the variances being equal to the variance of the result. The uncertainty ranges of the initial conditions from Table A.6 are not directly additive to the final results, and are also altered by the effect of the integration (see Eqs. [A.19], [A.20], and [A.22]).

For each model, the transfer volumes were set such that, when all other parameters in the simulation are equal to their median values, the leak volumes are zero. *The results therefore directly show the magnitude of the uncertainty and not specific leak volumes.* The UB and LB of the 95% CI and the resulting 95% CI range from the Monte Carlo analysis are summarized in Table A.7. These best estimate results indicate the uncertainty range for a leak volume determined sequentially through the retrieval process as specified above. If a leak volume is determined via the liquid mass balance when 10% of the original waste has been retrieved, we have 95% confidence that the true leak volume will be between the determined volume minus 8,400 gallons and the determined volume plus 9,600 gallons, resulting in a total uncertainty in the 95% CI of 18,000 gallons.

Table A.7. Best Estimate Uncertainty in Leak Detection

Equation	Original Waste Retrieved (%)	LB 95% CI (gallons)	UB 95% CI (gallons)	95% CI Range (gallons)
Liquid Mass Balance V_{LEAK} [Eq. (A.19)]	10	-8,400	9,600	18,000
	20	-12,600	15,900	28,500
	40	-21,700	27,200	48,900
	60	-28,000	34,100	62,100
	80	-37,000	45,400	82,400
Water Mass balance V_{LEAKW} [Eq. (A.20)]	10	-8,300	9,700	18,000
	20	-13,200	16,500	29,700
	40	-23,600	28,600	52,200
	60	-30,700	35,700	66,400
	80	-42,300	48,600	90,800
Total Mass Balance V_{LEAKT} [Eq. (A.22)]	10	-43,300	47,000	90,300
	20	-69,900	67,900	137,800
	40	-105,300	97,900	203,200
	60	-120,700	77,900	198,600
	80	-82,900	78,100	161,000

The 95% CI uncertainty range results are presented graphically in Figure A.5. The lowest leak volume uncertainty with the best estimate input parameters is achieved via a mass balance on the total liquid in the tank (liquid mass balance, V_{LEAK} of Eq. [A.19]). The effect of the uncertainty in the non-pool volume (Figure A.4) is clearly evident in the total mass balance uncertainty. The significance of the input parameters on the leak volume uncertainties is investigated below.

Figure A.5. 95% CI Uncertainty Range for Leak Volume as a Function of the Volume of Original Waste Retrieved

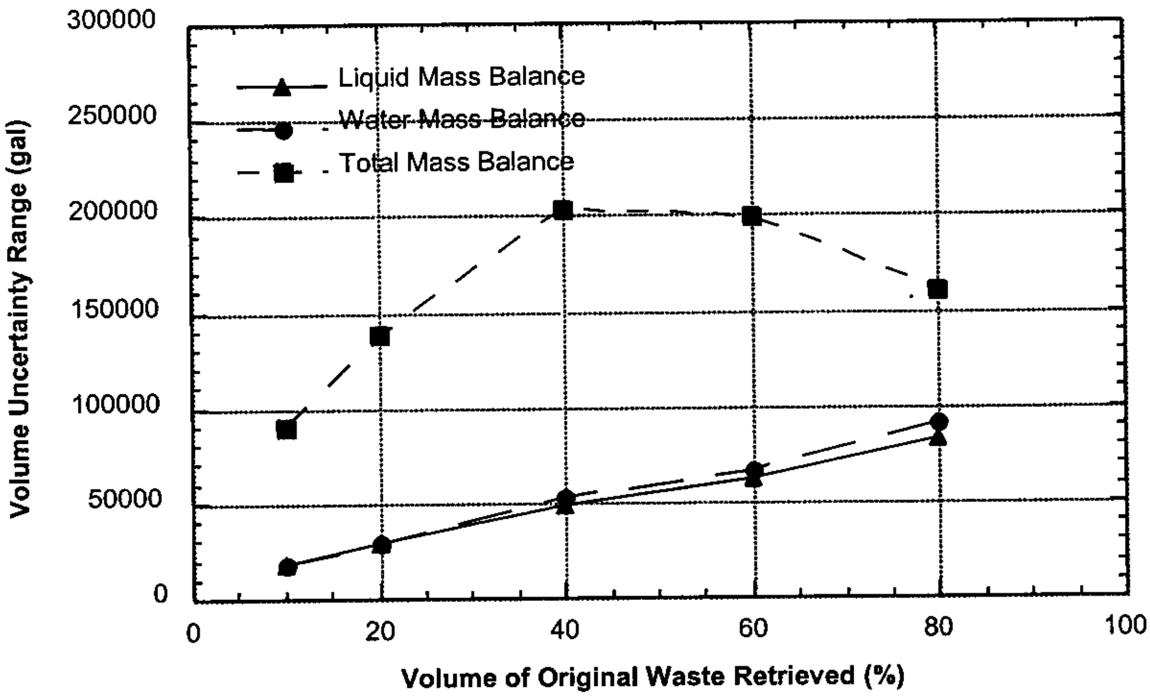

A3.3 SIGNIFICANT PARAMETER IDENTIFICATION

An analysis was conducted to determine which variables have the most impact on the output results. These results provide insight into the leak volume uncertainty ranges as well as providing a means to identify the most effective means to reduce the leak volume uncertainty.

Stepwise forward regression was used to determine which explanatory variables (the input parameters) best predict or describe the response variable (leak volume). Using stepwise regression provides the advantage of being able to determine which variable is most predictive of the response by observing which variable is chosen first for the "best" model. Using the stepwise forward regression method assumes there is no co-linearity among the explanatory variables. If known relationships exist between variables where one variable could easily describe the other then only one of those two variables was made available for choosing in the stepwise forward regression procedure. The procedure is accomplished by successively fitting models containing increasing numbers of explanatory variables and observing criteria that make up the "best" model. Three criteria are used: the R-squared value, the Mallow's Cp value, and the sequential sums of squares. A good model has a very high R-squared value along with a Cp value approaching p, the number of parameters in the model. The sequential sums of squares should be minimized.

The initial step in a stepwise forward regression is to fit the best model that contains only one variable plus the intercept. The stepwise forward regression results for the total mass balance model (V_{LEAKT} of Eq. [A.22]) with 10% of the original waste volume retrieved are presented in

Table A.8. The first explanatory variable chosen was the initial non-pool waste volume (V_{W0}). The model V_{LEAKT} = intercept + V_{W0} provides an R-squared value of 0.2527 with Cp equal to 7.88E5. No other single parameter model from the set of variables would make a "better" model. This reveals that the distribution of V_{W0} has the most significant impact on V_{LEAKT}, or V_{W0} is most correlated with V_{LEAKT}. Obviously, this is not the best model in itself, as the R-squared value is not unity, Cp >> p, and the sums of the squares is not minimized.

Table A.8. Stepwise Regression Analysis Results for the Total Mass Balance at 10% of the Original Waste Volume Retrieved

Parameter	Sequential Sums of Squares	R-squared	Cp	p
V_{W0}	19322982	0.2527	788224	2
V_{W1}	50649756	0.9152	80625	3
w_T	2430553	0.9470	46671	4
ρ_T	895774.7	0.9587	34159	5
V_{L0}	1189751	0.9742	17539	6
V_{L1}	1155958	0.9893	1391.9	7
ρ_{P0}	37108.21	0.9898	875.46	8
V_{QW1}	14663.08	0.9900	672.61	9
ρ_{P1}	13862.25	0.9902	480.95	10
ψ_{LU}	11831.38	0.9904	317.66	11
m	10550.57	0.9905	172.26	12
α	5336.914	0.9906	99.705	13
V_{P0}	2975.537	0.9906	60.135	14
V_{P1}	2081.806	0.9906	33.051	15
ρ_S	1363.671	0.9907	16	16

The next most important variable is the non-pool waste volume during the retrieval (V_{W1}), which, when combined with V_{W0}, increases the R-squared value to 0.9152, and reduces the Cp value to 8.06E4. The solid volume fraction also has a significant impact on the results (see w_T and ρ_T: Eq. [A.23]). The procedure continues until all the variables that significantly impact the results (probability of significance < 0.25) are used. Notice that the Cp approaches p when all the significant variables (including the intercept) are included in the model, R-squared is approaching unity, and the sequential sums of squares is minimized. As would be expected, having all the significant variables in the model provide the "best" model according to all criteria.

The stepwise regression analysis results for the total mass balance at 20%,40%, 60%, and 80% retrieval are presented in Tables A.9 through A.12. The variance in the significance rankings (lowest significance ranking provides best single parameter model, next higher significance ranking provides best two-parameter combination model, etc.) of the input parameters throughout the retrieval process for the total mass balance are shown in Figure A.6. As expected (see Figures A.4 and A.5), the non-pool volume initially and during retrieval (V_{W0} and V_{Wj} respectively; j denotes sequential retrieval conditions) are significant parameters (i.e. significance ranks are low), and their significance changes during the retrieval process as the relative region volumes are altered. Other observations may be made such as the increasing significance of the liquid pool volume whose uncertainty increases by an order of magnitude during the retrieval (Tables A.3 through A.5 and Figure A.4).

Table A.9. Stepwise Regression Analysis Results for the Total Mass Balance (V_{LEAKT}) at 20% of the Original Waste Volume Retrieved

Parameter	Sequential Sums of Squares	R-squared	Cp	p
V_{W2}	1.3562e8	0.7734	234163	2
w_T	7642952	0.8170	187196	3
V_{W0}	22029192	0.9426	51818	4
ρ_T	3328650	0.9616	31364	5
V_{L0}	1212960	0.9685	23912	6
V_{L2}	3264002	0.9872	3855.4	7
V_{P2}	273351.9	0.9887	2177.5	8
ρ_{P0}	99895.42	0.9893	1565.6	9
V_{QW2}	73896.48	0.9897	1113.5	10
ρ_{P1}	52919.31	0.9900	790.3	11
M	41607.65	0.9902	536.6	12
α	39944.04	0.9905	293.13	13
ψ_{LU}	30945.44	0.9906	104.95	14
ρ_S	11481.08	0.9907	36.398	15
V_{P0}	3644.596	0.9907	16	16

Table A.10. Stepwise Regression Analysis Results for the Total Mass Balance (V_{LEAKT}) at 40% of the Original Waste Volume Retrieved

Parameter	Sequential Sums of Squares	R-squared	Cp	p
V_{W3}	3.1164e8	0.8036	207212	2
w_T	28352247	0.8767	126379	3
ρ_T	11099167	0.9053	94736	4
V_{L3}	6364526	0.9217	76593	5
V_{W0}	22597710	0.9800	12167	6
V_{P3}	1738247	0.9844	7212.7	7
V_{L0}	1141509	0.9874	3960.2	8
ρ_{P0}	311194.4	0.9882	3075	9
V_{QW3}	303176.2	0.9890	2212.6	10
ρ_{P1}	219874.6	0.9895	1587.7	11
α	209108.3	0.9901	993.51	12
M	151964.1	0.9905	562.25	13
ψ_{LU}	109916.2	0.9908	250.87	14
ρ_S	83605.83	0.9910	14.504	15
V_{W3}	3.1164e8	0.8036	207212	2

Table A.11. Stepwise Regression Analysis Results for the Total Mass Balance (V_{LEAKT}) at 60% of the Original Waste Volume Retrieved

Parameter	Sequential Sums of Squares	R-squared	Cp	p
w_T	54880426	0.1595	930224	2
V_{W4}	2.2821e8	0.8228	188188	3
ρ_{P0}	8244460	0.8468	161382	4
ρ_T	15185830	0.8909	112006	5
V_{L4}	7352385	0.9123	88101	6
V_{W0}	22309203	0.9772	15563	7
V_{P4}	1435397	0.9813	10897	8
V_{L0}	1105296	0.9845	7305.5	9
V_{QW4}	565352	0.9862	5469.2	10
α	550941.3	0.9878	3679.8	11
ρ_{P1}	422938.6	0.9890	2306.6	12
M	313188.5	0.9899	1290.2	13
ψ_{LU}	220231.2	0.9906	576.09	14
ρ_S	172310.1	0.9911	17.807	15
V_{P0}	1170.66	0.9911	16	16

Table A.12. Stepwise Regression Analysis Results for the Total Mass Balance (V_{LEAKT}) at 80% of the Original Waste Volume Retrieved

Parameter	Sequential Sums of Squares	R-squared	Cp	p
w_T	1.0148e8	0.4038	754439	2
ρ_T	42391935	0.5725	538127	3
V_{W0}	22154641	0.6607	425080	4
V_{W5}	66560768	0.9256	85441	5
V_{L5}	6528177	0.9516	52131	6
V_{P5}	3399547	0.9651	34786	7
α	1387441	0.9706	27709	8
V_{QW5}	1170945	0.9753	21736	9
ρ_{P0}	964208	0.9791	16817	10
ρ_{P1}	828234.4	0.9824	12593	11
V_{L0}	1111157	0.9868	6925.3	12
M	566141	0.9891	4038.4	13
ρ_S	396617.6	0.9907	2016.6	14
ψ_{LU}	390151.6	0.9922	27.757	15
V_{P0}	2696.102	0.9922	16	16

Figure A.6. Significance Ranking of Parameters as a Function of the Volume of Original Waste Retrieved: Total Mass Balance

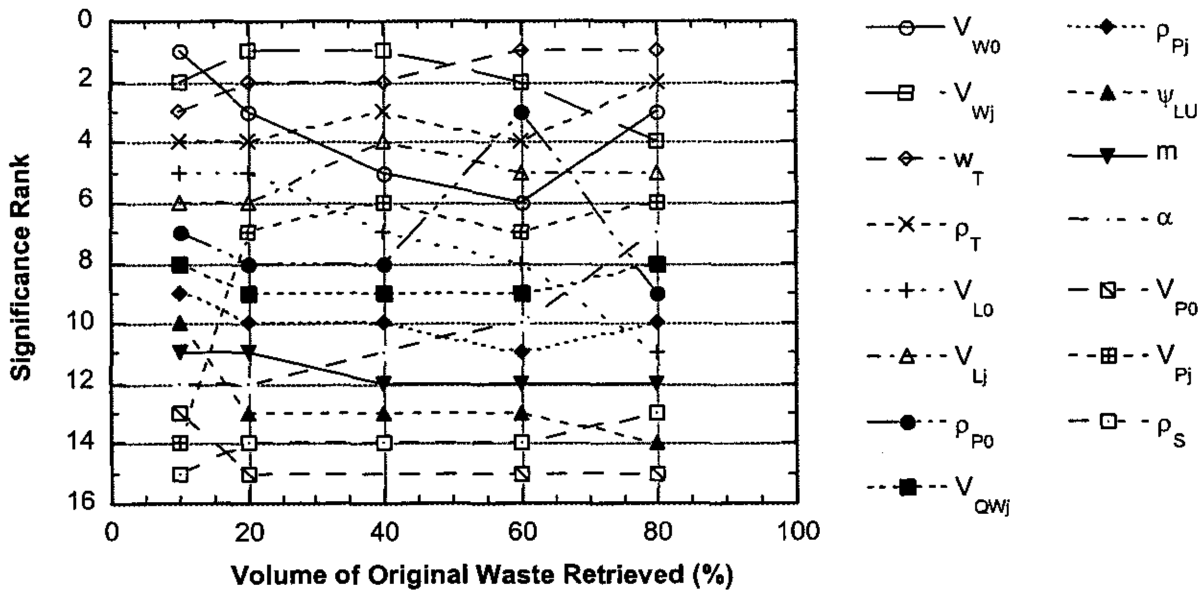

Insight into the relative significance rank may be achieved by examination of the R-squared values in conjunction with Figure A.6. As discussed above in reference to Table A.8, the R-squared value for the model using the initial non-pool waste volume (most significant rank) and an intercept is 0.2527. With the sequential non-pool waste volume, the next most significant variable (Figure A.6), added to the model, R-squared improves to 0.9152. Subsequent parameter additions provide less of an effect on R-squared, with the improvement after the initial pool density almost negligible. Therefore, the first seven most significant variables have more impact on the results than the remaining variables. Note, however, that the significance rank is based on the combination of the Mallow's Cp value and the sequential sums of squares as well as the R-squared value, and that the R-squared values are for the combination model (i.e. the difference in the R-squared values is attributable to the addition of a parameter to the model and cannot be ascribed to an individual parameter).

Stepwise regression analysis results for the liquid mass balance (V_{LEAK}) and the water mass balance (V_{LEAKW}) are provided in Tables A.13 through A.22. The variance in the significance rankings of the input parameters are similar between these two models, Figures A.7 and A.8. In each case, the mass fractions of water in the interstitial liquid and pool liquid (as indicated by m, see Eq. [A.26]), are significant parameters. The significance ranking of the non-pool and saturated waste volumes decreases while the significance of the parameters determining the liquid volume in these regions increases (see Eqs. [A.23] and [A.24]). As discussed above, the relative significance rank of the parameters may be investigated by considering the R-squared values (Tables A.8 through A.22).

Table A.13. Stepwise Regression Analysis Results for the Liquid Mass Balance (V_{LEAK}) at 10% of the Original Waste Volume Retrieved

Parameter	Sequential Sums of Squares	R-squared	Cp	p
V_{L0}	1192600	0.3900	271065	2
m	303728.4	0.4894	225297	3
V_{L1}	1188800	0.8781	46155	4
w_T	86854.14	0.9066	33069	5
V_{QW1}	39451.85	0.9195	27126	6
V_{W1}	79440.28	0.9454	15157	7
V_{W0}	28224.1	0.9547	10905	8
ρ_T	35202.28	0.9662	5602.7	9
ρ_{P1}	13633.76	0.9706	3550.2	10
ψ_{LU}	11795.57	0.9745	1774.7	11
ρ_{P0}	3982.545	0.9758	1176.6	12
V_{P0}	3954.97	0.9771	582.59	13
α	2097.127	0.9778	268.57	14
V_{L1}	1646.366	0.9783	22.471	15
ρ_S	65.97873	0.9783	14.529	16

Table A.14. Stepwise Regression Analysis Results for the Liquid Mass Balance (V_{LEAK}) at 20% of the Original Waste Volume Retrieved

Parameter	Sequential Sums of Squares	R-squared	Cp	p
m	1325614	0.1756	460568	2
V_{L0}	1161252	0.3294	372761	3
V_{L2}	3265064	0.7620	125870	4
w_T	628544.9	0.8452	78344	5
V_{QW2}	197164.6	0.8714	63437	6
ρ_T	140965.4	0.8900	52780	7
V_{P2}	262330.6	0.9248	32945	8
V_{W2}	220050.5	0.9539	16308	9
ρ_{P1}	57686.96	0.9616	11948	10
ψ_{LU}	37161.77	0.9665	9140	11
ρ_{P0}	34439.93	0.9711	6537.7	12
α	37418.33	0.9760	3710.3	13
V_{W0}	35359.34	0.9807	1038.6	14
ρ_S	10549.27	0.9821	242.86	15
V_{P0}	3026.6	0.9825	16	16

Table A.15. Stepwise Regression Analysis Results for the Liquid Mass Balance (V_{LEAK}) at 40% of the Original Waste Volume Retrieved

Parameter	Sequential Sums of Squares	R-squared	Cp	p
m	4893284	0.2190	591901	2
w_T	3682327	0.3838	464898	3
V_{P3}	1871540	0.4675	400350	4
V_{L3}	7374867	0.7976	145992	5
ρ_T	863476.2	0.8362	116212	6
V_{QW3}	808781	0.8724	88319	7
V_{L0}	1183781	0.9254	47492	8
α	223176.5	0.9354	39797	9
ρ_{P0}	209965.7	0.9448	32557	10
ρ_{P1}	202810.6	0.9539	25564	11
V_{W3}	515324.2	0.9769	7792.2	12
ρ_S	69688.73	0.9801	5390.7	13
ψ_{LU}	118846.7	0.9854	1293.6	14
V_{W0}	34064.51	0.9869	120.72	15
V_{P0}	3094.2	0.9870	16	16

Table A.16. Stepwise Regression Analysis Results for the Liquid Mass Balance (V_{LEAK}) at 60% of the Original Waste Volume Retrieved

Parameter	Sequential Sums of Squares	R-squared	Cp	p
m	10769857	0.3082	661467	2
w_T	8014278	0.5376	438839	3
V_{L4}	7258658	0.7453	237201	4
ρ_T	1917390	0.8002	183940	5
V_{QW4}	1682482	0.8484	137204	6
V_{P4}	1502051	0.8913	95480	7
α	507728.5	0.9059	81378	8
ρ_{P0}	477471	0.9195	68116	9
ρ_{P1}	445606.7	0.9323	55739	10
V_{L0}	1222001	0.9673	21795	11
ρ_S	162635.4	0.9719	17279	12
ψ_{LU}	221878.4	0.9783	11118	13
V_{W4}	359654.7	0.9886	1128.6	14
V_{W0}	37273.58	0.9896	95.201	15
V_{P0}	2923.083	0.9897	16	16

Table A.17. Stepwise Regression Analysis Results for the Liquid Mass Balance (V_{LEAK}) at 80% of the Original Waste Volume Retrieved

Parameter	Sequential Sums of Squares	R-squared	Cp	p
m	20533804	0.3191	782734	2
w_T	19944855	0.6290	421884	3
ρ_T	4534120	0.6995	339852	4
V_{QW5}	3375754	0.7520	278779	5
V_{L5}	6322905	0.8502	164384	6
α	1347037	0.8712	140014	7
ρ_{P0}	1115400	0.8885	119836	8
V_{P5}	3667039	0.9455	53492	9
ρ_{P1}	827653.7	0.9583	38520	10
ρ_S	388277.8	0.9644	31497	11
ψ_{LU}	402460.9	0.9706	24217	12
V_{L0}	1190530	0.9891	2679.8	13
V_{W5}	106129.6	0.9908	761.63	14
V_{W0}	37472.11	0.9914	85.671	15
V_{P0}	3961.372	0.9914	16	16

Table A.18. Stepwise Regression Analysis Results for the Water Mass Balance (V_{LEAKW}) at 10% of the Original Waste Volume Retrieved

Parameter	Sequential Sums of Squares	R-squared	Cp	p
V_{L0}	1172794	0.3709	276615	2
m	392188.8	0.4949	220114	3
V_{L1}	1172131	0.8656	51247	4
w_T	92973.3	0.8950	37854	5
ρ_T	52830.05	0.9117	30245	6
V_{QW1}	49367.08	0.9273	23135	7
V_{W1}	81996.57	0.9532	11323	8
ρ_{P1}	21130.32	0.9599	8281.1	9
V_{W0}	33839.3	0.9706	3407.9	10
ψ_{LU}	11769.98	0.9743	1714.2	11
α	4082.077	0.9756	1128.1	12
V_{P1}	3002.808	0.9766	697.46	13
V_{P0}	2860.676	0.9775	287.32	14
ρ_S	1873.131	0.9781	19.459	15
ρ_{P0}	37.89298	0.9781	16	16

Table A.19. Stepwise Regression Analysis Results for the Water Mass Balance (V_{LEAKW}) at 20% of the Original Waste Volume Retrieved

Parameter	Sequential Sums of Squares	R-squared	Cp	p
m	1542101	0.1882	465141	2
V_{L0}	1261265	0.3422	375037	3
V_{L2}	3194378	0.7321	146828	4
w_T	635027.6	0.8096	101463	5
ρ_T	364679.7	0.8541	75411	6
V_{QW2}	263816.4	0.8863	56566	7
V_{P2}	363741	0.9307	30582	8
ρ_{P1}	89212.34	0.9416	24210	9
V_{W2}	217035.2	0.9681	8707.1	10
ψ_{LU}	36755.08	0.9726	6083.2	11
α	36637.08	0.9770	3467.8	12
V_{W0}	32856.75	0.9810	1122.5	13
ρ_S	12112.32	0.9825	259.17	14
V_{P0}	2885.163	0.9829	55.051	15
ρ_{P0}	574.6167	0.9829	16	16

Table A.20. Stepwise Regression Analysis Results for the Water Mass Balance (V_{LEAKW}) at 40% of the Original Waste Volume Retrieved

Parameter	Sequential Sums of Squares	R-squared	Cp	p
m	5973551	0.2346	621200	2
w_T	3997726	0.3917	491697	3
ρ_T	2133887	0.4755	422572	4
V_{P3}	2286479	0.5653	348504	5
V_{L3}	7128670	0.8453	117574	6
V_{QW3}	1098028	0.8885	82005	7
ρ_{P1}	387354.4	0.9037	69459	8
V_{L0}	1188907	0.9504	30947	9
ρ_S	229349.4	0.9594	23519	10
V_{W3}	496440.4	0.9789	7438.9	11
ψ_{LU}	117008.2	0.9835	3650.4	12
ρ_S	67101.6	0.9861	1478.7	13
V_{W0}	36301.4	0.9875	304.69	14
ρ_{P0}	5472.139	0.9878	129.42	15
V_{P0}	3562.883	0.9879	16	16

Table A.21. Stepwise Regression Analysis Results for the Water Mass Balance (V_{LEAKW}) at 60% of the Original Waste Volume Retrieved

Parameter	Sequential Sums of Squares	R-squared	Cp	p
m	13081374	0.3130	681664	2
w_T	8703243	0.5213	471981	3
ρ_{P0}	2671871	0.5852	407611	4
V_{L4}	7264357	0.7591	232595	5
ρ_T	2123075	0.8099	181447	6
V_{QW4}	2175278	0.8619	129040	7
ρ_{P1}	830186	0.8818	109041	8
V_{P4}	1960650	0.9287	61806	9
α	573693.7	0.9424	47986	10
V_{L0}	1191396	0.9709	19284	11
ψ_{LU}	227119	0.9764	13814	12
ρ_S	159850.8	0.9802	9964.8	13
V_{W4}	376950.4	0.9892	885.1	14
V_{W0}	33436.38	0.9900	81.53	15
V_{P0}	2802.911	0.9901	16	16

Table A.22. Stepwise Regression Analysis Results for the Water Mass Balance (V_{LEAKW}) at 80% of the Original Waste Volume Retrieved

Parameter	Sequential Sums of Squares	R-squared	Cp	p
m	23464345	0.3082	874062	2
w_T	20549690	0.5781	529119	3
ρ_{P0}	6743407	0.6667	415926	4
ρ_T	5196326	0.7350	328703	5
V_{QW5}	3668162	0.7831	267132	6
V_{P5}	2514075	0.8162	224933	7
V_{L5}	8452202	0.9272	83057	8
ρ_{P1}	1530752	0.9473	57364	9
α	1353543	0.9651	34645	10
ψ_{LU}	359585.3	0.9698	28611	11
ρ_S	356189.7	0.9745	22634	12
V_{L0}	1197463	0.9902	2535.8	13
V_{W5}	113238.5	0.9917	637	14
V_{W0}	33316.95	0.9921	79.743	15
V_{P0}	3916.551	0.9922	16	16

Figure A.7. Significance Ranking of Parameters as a Function of the Volume of Original Waste Retrieved: Liquid Mass Balance

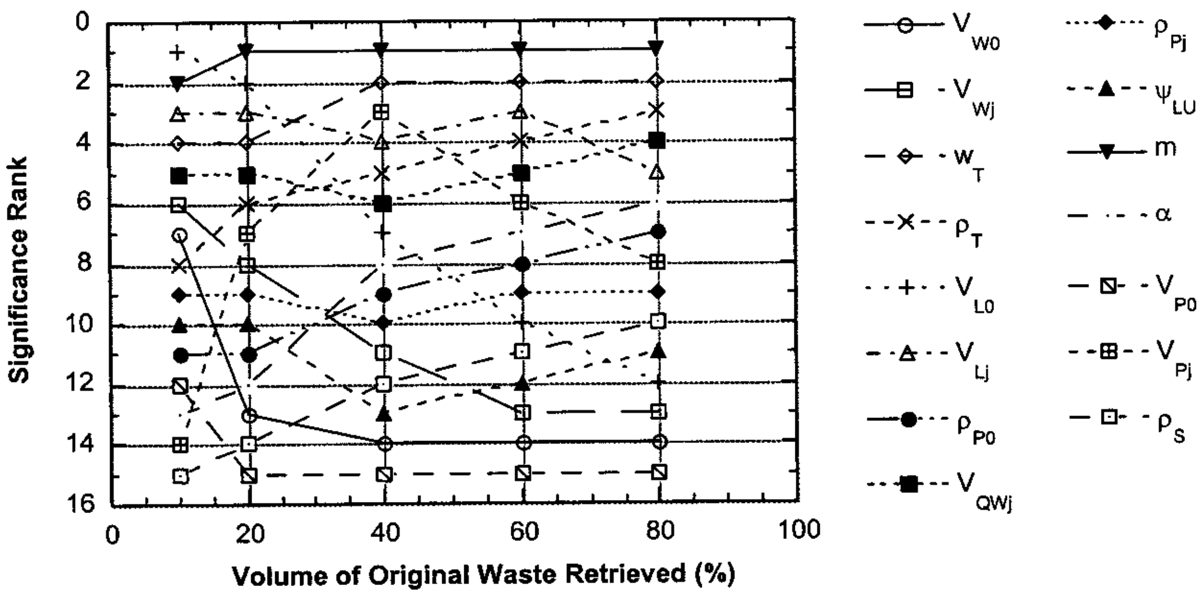

Figure A.8. Significance Ranking of Parameters as a Function of the Volume of Original Waste Retrieved: Water Mass Balance

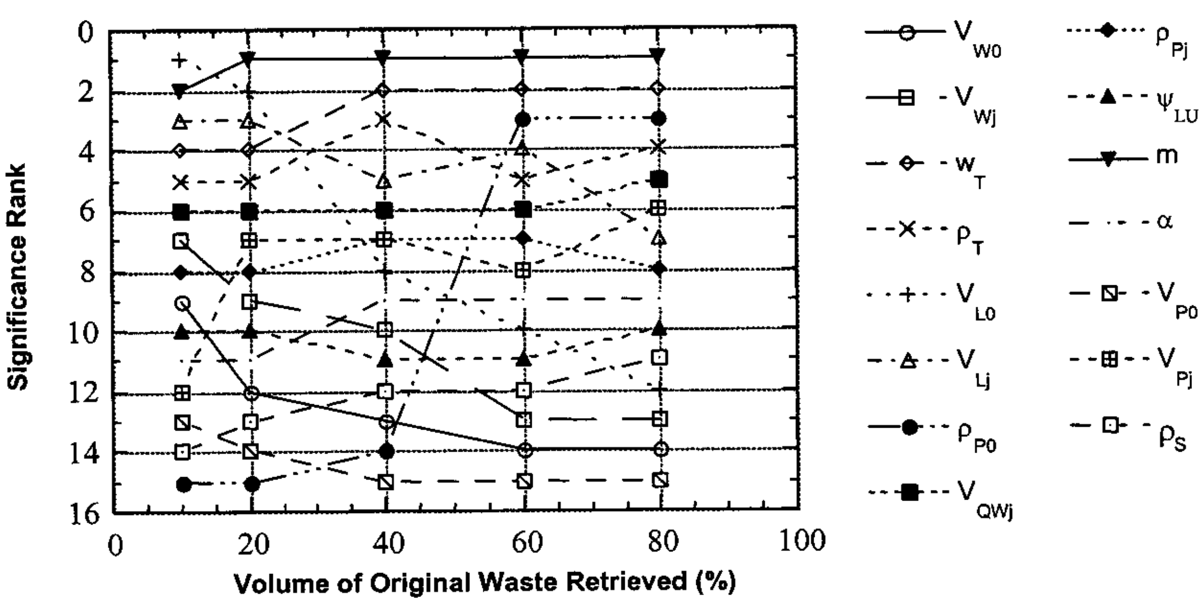

As illustrated in Figures A.6, A.7, and A.8, the uncertainty in the waste region volumes (pool, non-pool, and saturated waste) affects the uncertainty in the leak volume. The leak volume determined by the total mass balance is most significantly impacted by the uncertainty in the non-pool waste volume. Therefore, if the uncertainty in this parameter is reduced, the leak volume uncertainty will be reduced as well. The tank volume measurement system (TVMS) is capable of measuring the waste surface features to within approximately ± 1%. We have investigated the effect of using the TVMS during the retrieval process by reducing the uncertainty in the waste region volumes to those presented in Table A.23 (see Tables A.3 through A.5 for comparison without the TVMS). Note that there are still significant uncertainties in the waste volumes due to uncertainty in the interstitial liquid level and the depth and volume of the liquid pool (or, inversely, the insoluble solids depth and volume at the bottom of the pool).

Table A.23. Waste Region Volume Uncertainty Distributions with the TVMS

Variable	(units)	Median	Maximum	Minimum	Distribution
V_{P0}	(m^3)	1.125	1.136	1.114	Normal
V_{P1}	(m^3)	0.54	0.78	0.19	skewed normal
V_{P2}	(m^3)	7.1	8.07	2.4	skewed normal
V_{P3}	(m^3)	28.1	30.42	9.35	skewed normal
V_{P4}	(m^3)	51	52.59	16.9	skewed normal
V_{P5}	(m^3)	88.1	89.91	29.4	skewed normal
V_{L0}	(m^3)	1252	1304	1200	uniform
V_{L1}	(m^3)	1209	1291	1157	skewed normal
V_{L2}	(m^3)	1125	1216	1074	skewed normal
V_{L3}	(m^3)	931	1091	883	skewed normal
V_{L4}	(m^3)	740	1021	710	skewed normal
V_{L5}	(m^3)	446	991	433	skewed normal
V_{W0}	(m^3)	2335	2358	2312	normal
V_{W1}	(m^3)	2105	2329	2075	skewed normal
V_{W2}	(m^3)	1872	2110	1836	skewed normal
V_{W3}	(m^3)	1404	1724	955	skewed normal
V_{W4}	(m^3)	973	1424	955	skewed normal
V_{W5}	(m^3)	468	1039	459	skewed normal

The 95% CI uncertainty range for the leak volume results with the TVMS are presented in Table A.24. The lowest leak volume uncertainty with the best estimate input parameters is again achieved via a mass balance on the total liquid in the tank (liquid mass balance, V_{LEAK} of Eq. [A.19]). At 80% of the original waste volume retrieved, the improvement with the TVMS is approximately 12% for the total mass balance uncertainty range, and approximately 4% for the liquid and water mass balances as compared to the results in Table A.7. The 95% CI leak volume uncertainty ranges with and without the TVMS are compared graphically in Figure A.9. The effect of the uncertainty in the non-pool volume still significantly effects the total mass balance uncertainty range. The apparent "dip" in uncertainty is caused by the insolubles at the bottom of the pool as discussed in Section A3.2 in reference to Figure A.4. This is confirmed by a stepwise forward regression analysis, which showed that R-squared values approached 0.9 only after the non-pool waste volume at the sequential retrieval volumes was included in the model (i.e. the uncertainty in the waste volume has a significant impact on the results).

Table A.24. Best Estimate Uncertainty in Leak Detection with the TVMS

Equation	Original Waste Retrieved (%)	LB 95% CI (gallons)	UB 95% CI (gallons)	95% CI Range (gallons)
Liquid Mass Balance V_{LEAK} [Eq. (A.19)]	10	-7,100	8,600	15,700
	20	-9,300	12,400	21,700
	40	-16,700	22,500	39,200
	60	-23,900	31,200	55,000
	80	-35,500	43,400	78,800
Water Mass balance V_{LEAKW} [Eq. (A.20)]	10	-7,000	8,500	15,500
	20	-10,000	13,100	23,100
	40	-18,600	23,500	42,100
	60	-27,200	33,700	61,000
	80	-40,400	46,700	87,100
Total Mass Balance V_{LEAKT} [Eq. (A.22)]	10	-24,900	16,600	41,500
	20	-29,700	24,700	54,400
	40	-65,000	74,100	139,100
	60	-58,300	52,700	111,000
	80	-72,800	69,100	141,900

Figure A.9. 95% CI Uncertainty Range for Leak Volume with the TVMS as a Function of the Volume of Original Waste Retrieved

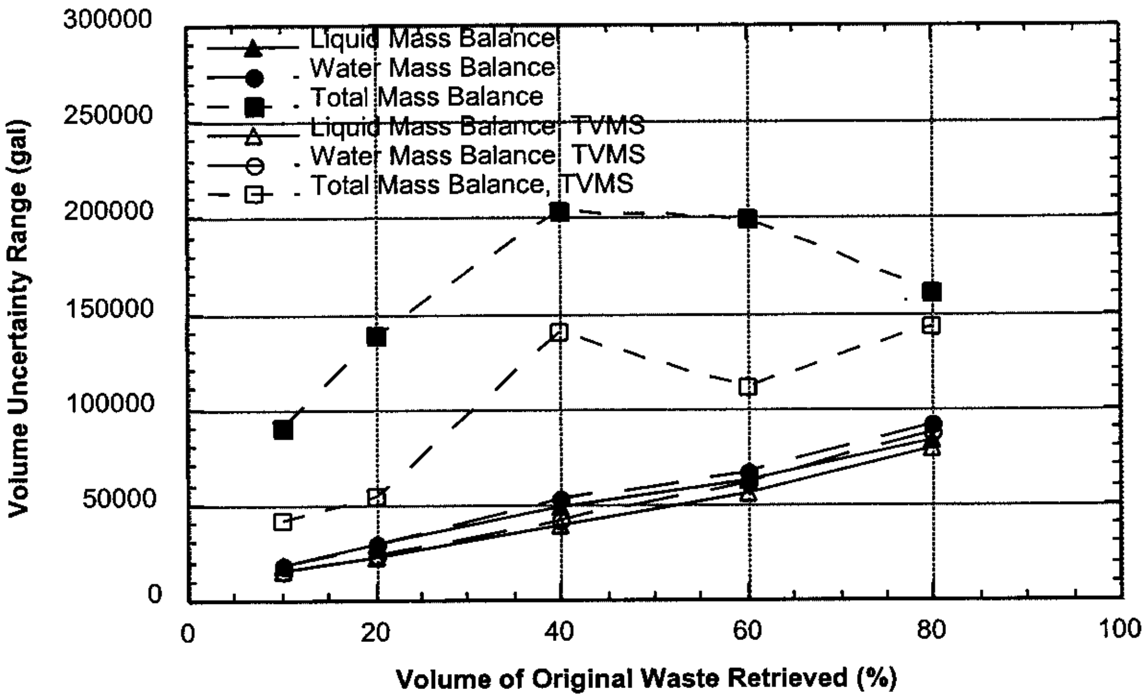

A4.0 CONCLUSIONS

Mass balance equations have been developed to determine the leak volume during retrieval of SSTs. These equations were exercised via a Monte Carlo simulation on the retrieval of Tank S-112. For this investigation, the magnitude of the uncertainty (and not specific leak volumes) was evaluated. The model parameters that have the most significant impact on the uncertainty are identified using a stepwise forward regression analysis, and the effect of the inclusion of the tank volume measurement system (TVMS) is evaluated.

The 95% CI leak volume best estimate uncertainty range in S-112 for each of the models is summarized in Table A.25. The results with the TVMS are also presented. The lowest leak volume uncertainty range as compared to the other presented mass balance equations with the best estimation of the uncertainties of the input parameters is achieved via the mass balance on the total liquid in the tank.

Table A.25. 95% CI Best Estimate Uncertainty Range in Leak Detection for Tank S-112

Equation	95% CI Range (gallons)				
	Original Waste Retrieved (%)				
	10	20	40	60	80
Liquid Mass Balance	18,000	28,500	48,900	62,100	82,400
Water Mass Balance	18,000	29,700	52,200	66,400	90,800
Total Mass Balance	90,300	137,800	203,200	198,600	161,000
Liquid Mass Balance, TVMS	15,700	21,700	39,200	55,000	78,800
Water Mass Balance, TVMS	15,500	23,100	42,100	61,000	87,100
Total Mass Balance, TVMS	41,500	54,400	139,100	111,000	141,900

Although we have shown that the uncertainties associated with the leak volume are quite large (> 80,000 gallons at 80% waste retrieval), they are relatively small compared to the total transfer volume. The "best" best estimate 95% CI uncertainty range for the liquid mass balance at 80% of the original waste volume retrieved is approximately 9% of the transfer volume. At 80% of the original waste volume retrieved, the improvement with the TVMS is approximately 12% for the total mass balance uncertainty range, and approximately 4% for the liquid and water mass balances. The leak volume uncertainty range may be further improved by including additional measurements and/or modeling to reduce the uncertainty of the most significant (as determined by the stepwise forward regression analysis) input parameters.

A5.0 REFERENCES

Adams, M. R., 1999, *River Protection Project Process Engineering Desk Instruction and Guidance Manual*, HNF-SD-WM-PROC-021, Rev. 3, Lockheed Martin Hanford Corp., Richland, Washington.

Crass, D. W., 2001, *Single-Shell Tank S-112 Full Scale Saltcake Waste Retrieval Technology Demonstration Functions and Requirements*, RPP-7825, CH2MHILL Hanford Group, Inc., Richland, Washington.

Cuta, J. M., K. G. Carothers, D. W. Damschen, W. L. Kuhn, J. A. Lechelt, K. Sathyanayarana, and L. A. Stauffer, 2000, *Review of Waste Retrieval Sluicing System Operations and Data for Tanks 241-C-106 and 241-AY-102*, PNNL-13319, Pacific Northwest National Laboratory, Richland, Washington.

Estey, S. D., J. L. Huckaby, L. A. Mahoney, C. W. Stewart, and B. E. Wells, 2001, *Process Control Plan for Single-Shell Tank Saltcake Dissolution Proof-of-Concept*, RPP-7715, Rev. 2, CH2MHILL Hanford Group, Inc., Richland, Washington.

Onishi, Y., B. E. Wells, S. A. Hartley, and C. W. Enderlin, 2001, *Material Balance Assessment for Double-Shell Tank Waste Pipeline Transfer*, PNNL-13485, Pacific Northwest National Laboratory, Richland, Washington.

Stewart, C. W., F. F. Erian, P. A. Meyer, K. P. Recknagle, W. B. Gregory, Z. I. Antoniak, and D. M. Pfund, 1997, *Monitoring Gas Retention and Slurry Transport During the Transfer of Waste from Tank 241-C-106 to Tank 241-AY-102*, PNNL-11627, Pacific Northwest National Laboratory, Richland, Washington.

APPENDIX B
S-112 DRYWELL LOGGING PERFORMANCE ESTIMATE – EX-TANK LEAK DETECTION: PERFORMING DRY WELL MOISTURE MEASUREMENTS IN SUPPORT OF TANK WASTE RETRIEVAL

This page intentionally left blank.

CONTENTS

ATTACHMENTS

This page intentionally left blank.

APPENDIX B
S-112 DRYWELL LOGGING PERFORMANCE ESTIMATE – EX-TANK LEAK DETECTION: PERFORMING DRY WELL MOISTURE MEASUREMENTS IN SUPPORT OF TANK WASTE RETRIEVAL

B1.0 INTRODUCTION

Drywell logging will be used for monitoring fluid losses that may occur during retrieval of Single Shell Tanks. Low water retrieval methods selected for waste retrieval to minimize leak potential do not lend themselves to free surface leak evaluation. While Gamma logging is the baseline for long-term Vadose Zone monitoring, some conditions of waste and soil may inhibit the migration of gamma emitters to the drywells. Neutron Moisture monitoring will be as sensitive as the original Ruthenium detection methods and with the addition of hand-held units that can quickly monitor elevations of interest a more timely evaluation can be made. This Appendix describes the process for the use of hand held neutron moisture probes, specifically for the first four SST's identified for retrieval. Technical Addenda describe models for leak volumes detected and moisture travel rates though the soil. The stochastic results presented in this section are the fraction of cases that are above or below a particular value. These results should not be interpreted as confidence intervals.

B2.0 HISTORY

Drywells consist of drilled, steel-cased wells that extend to depths ranging from 75 ft to 150 ft that do not tap the regional groundwater flow system. The majority of these wells were installed in the 1960s and 1970s as an early leak-detection system. At that time the wells were monitored using gamma detectors; short-lived, mobile gamma emitting radionuclides such as ruthenium-106 made up a significant part of the inventory stored in the tanks. Monitoring was conducted on a schedule that ranged from weekly to annual. If differences in gamma photon intensity, above a threshold value, were detected it was evidence of a potential leak. In two farms, 241-A and 241-SX, these vertical drywells were supplemented by horizontal drywells that extended beneath the tanks. An assessment of the detection capability, based on gamma emitting constituents, of the vertical drywells can be found in Isaacson (1982).

B3.0 PROPOSED APPROACH

Drywells surrounding Single-Shell Tanks (SSTs) will be used for monitoring of fluid losses that may take place during retrieval operations. The primary constituent to be monitored is to be water. Water has been selected over other potential waste constituents for the following reasons:

- Water will be added to the tanks during the planned retrieval demonstrations
- Gamma emitting radionuclides that remain in the tanks have decayed to the point where cesium-137 is the primary nuclide remaining; cesium-137 in dilute tank waste is only

slightly mobile and its retardation could be sufficient to keep it from reaching the available monitoring structures in a timely fashion.

- Neutron moisture gauges are readily available and can be deployed by retrieval personnel.
- Data from the neutron moisture gauge can be readily analyzed to determine if changes have taken place.
- Neutron moisture gauges are fully capable of detecting moisture content changes on the order of 2 to 15%. (The likely range of moisture increase that would result from a water loss during retrieval.)

Some difficulties are associated with using moisture as the monitored constituent, these include:

- There is no direct means of differentiating between waste that has been lost and clean water that has been lost.
- Precipitation events such as rainfall or snowmelt have the possibility of influencing measurements and their interpretation.
- Anthropomorphic additions of water, exclusive of retrieval sources can influence the measurements and their interpretation.

This methodology is designed to make the maximum use of the positive elements of moisture monitoring while minimizing or mitigating the impacts of the negative attributes. Each SST is unique in the number and distribution of drywells used in monitoring.

B3.1 TANK U-107

Seven (7) monitoring wells, ranging in depth from 105 to 125 ft below ground surface are in relatively close proximity to tank 241-U-107. These drywells are all constructed of 6-inch diameter welded steel casing. Four of the wells are situated within 10 ft of U-107, these wells are all located along the northern half of the tank. The remaining drywells are used primarily to monitor tank U-110 to the south (2) and tank U-108 to the west (1). Two additional wells are proposed to provide a continuing basis of comparison away from the activity around U-107.

B3.2 TANK S-102

Eight (8) monitoring wells, ranging in depth from 100 to 150 ft below ground surface are in close proximity to than 241-S-102. These drywells are all constructed of 6-inch diameter welded steel casing.

B3.3 TANK S-112

Eight (8) monitoring wells, ranging in depth from 100 to 145 ft below ground surface are relatively close to tank 241-S-112. Five of the wells are nominally within 10 ft of the tank.

Three wells, 40-09-06 near tank S-109 and wells 40-11-09 and 40-11-08 near tank S-111, will provide additional monitoring coverage.

B3.4 TANK C-106

Eight (8) monitoring wells, ranging in depth from 100 to 145 ft below ground surface are in relatively close proximity to 241-C-106. Six of the wells are nominally within 10 ft of the tank. One well, 30-05-02, is used to monitor tank C-105 but is close enough to C-106 to provide coverage in the southwest quadrant. The other well 30-00-01 provides additional coverage in the down "dip" direction.

B4.0 ANTICIPATED EFFICIENCY

Efficiency of the moisture monitoring approach to leak detection using existing monitoring wells depends on the proximity of the leak to the monitoring well(s). Because the neutron moisture monitoring system is capable of interrogating the surrounding soils only out to about 2 ft, the moisture front must move to the well in order to be detected. Movement of water through the soils under unsaturated conditions is generally controlled by movement within or along fine-grained horizons. Thus, under unsaturated conditions, movement within the vadose zone has a propensity to be lateral along depositional surfaces. The further the source of the leak is from the monitoring well, the larger the amount of liquid loss that must take place before detection is possible. Coincident with the amount of water that must be lost is the rate at which it is lost. A high rate of loss can result in greater vertical transport as locally saturated zones develop. A slow rate of loss will likely maximize the lateral movement, but extend the time for the water to reach a detection point.

- **Best Case**: The best case involves a low leak rate (0-1.5 gph – less than 50 gal/day) the leak source being separated by the shortest distance to the drywell. The closest drywells are about 10-ft from the edge of a tank. The most favorable condition under which a water loss would be detected involves water moving from the base of the tank along the construction-compacted surface to the drywell. Analyses presented in the Technical Appendix indicate the mean time of travel for a moisture plume to reach an optimally placed drywell is 12 days.

- **Worst Case**: The worst case involves a high rate (5-100 gph – 100 to 2500 gal/day) leak source at the center of the tank, below the construction-compacted surface. Drywell distribution results in a nominal 45-ft separation of the source and detector. Under this scenario, water distribution is controlled by the subsurface geologic environment. That environment differs greatly between the 200-East Area and the 200-West Area.

Analyses presented in the Technical Appendix indicate the mean time of travel for a moisture plume based on a low leak rate to reach an optimally placed drywell is on the order of 710 days. A high-rate leak (mean rate of about 10 gph) could saturate the soil and drain straight down without spreading out to the drywells.

B5.0 CAUTIONS

Additions of water to the vadose zone surrounding any tank should be avoided to the maximum extent possible. This includes losses from water supply piping servicing the retrieval operation.

When water is added to the ground, the timing, location, and amount (either measured or estimated) must be recorded so that it can be taken into account during data analysis and interpretation. This need is in no way intended to preclude the emergency use of water to decontaminate and protect site personnel.

Rain that falls on the tank farm should be monitored for timing and amount. Likewise in the event of snow on the ground, temperature should be recorded to account for infiltrating water from that source.

B6.0 INITIAL BASELINE

Drywells will be measured using a calibrated neutron moisture gage over their entire depths. Measurements are to be taken at 0.25-foot intervals over the entire depth. Measurements are to consist of a standard 16-second count. Prior to start and at the completion of each day's effort, a verification run is to be made for internal calibration of the system.

The data derived through the baseline acquisition will be assessed to provide information on the initial moisture distribution around the targeted tank. The data will be reviewed along with the existing gamma distribution data to aid in determining the likely distribution of fine-grained sediments beneath the tank. These fine grained sediments are expected to be recognized by both increased potassium-40 and increased moisture content. This initial analysis will be used to define specific zones to be monitored by retrieval personnel during ongoing retrieval operations.

The baseline analysis will be reviewed to identify specific zones that can be regularly (daily frequency) monitored to identify moisture content changes during retrieval activities. The expected intervals are approximately 20-ft thick starting at about 5-ft above the base of the tank farm excavation and extending to 15-ft below that surface. These projected intervals have been identified based on the construction history of the various farms and the nature of moisture movement within the vadose zone. Tank farm excavation bases were subject to extensive compaction during construction, resulting in a low permeability horizon along which moisture moves laterally. The undisturbed sediments beneath the farms in the 200-West Area have a southwesterly depositional "dip" which has shown a tendency to cause waste migration in that direction. In the 200-East Area, movement of moisture and contaminants has a preferential direction of movement to the east.

B7.0 RETRIEVAL MONITORING

Monitoring during retrieval is based on several assumptions:

- Addition of water during retrieval will be carried out continuously once initiated

- Personnel will be available to take moisture measurements
- Measurements can be collected in less than 2-hours if conducted without interruption
- Data will be made available for analysis at a predetermined time each day.
- Rebaselining, using a fully calibrated tool, will be done monthly or at approximately that frequency depending on personnel availability.

Every effort will be made to avoid the possibility of reporting false positive changes in moisture content that could impact the continuation of retrieval. An equally intensive effort will be made to assure that false negative analyses are avoided.

Vadose Zone Project staff have come to a consensus that the impact of a false positive will be no less impacting that that of a true positive. To that end, it is important to monitor the effect of precipitation events and the effects of any inadvertent water addition in the tank farm. Monitoring of the upper 10-ft of the drywells is to be implemented following a water addition event, monitoring of this interval will continue until such time as the analysis shows no further recognizable downward movement. Some drywells are grouted near the surface to reduce moisture intrusion. The water of hydration in grout will impact the ability to read the movement of water is adjacent regions. Fortunately, the presence of grout in these structures is a rarity.

In the event of an unexplained increase in moisture content during retrieval, a determination of the cause of the increase is needed. Several methods are potentially applicable:

- An analysis using either the Radiation Assessment System or Spectral Gamma Logging System could be used to determine if any changes in gamma emitting radionuclide concentration has take place. The low levels of potential contamination would indicate that the SGLS system might best be applied.
- Relogging of the suspect drywell(s) to ascertain if logging error could be the cause, this would be accompanied by an official recalibration of the tool.
- Cessation of water additions to the tank (retrieval would continue), followed by regular monitoring of the interval(s) showing increased moisture. Analysis of the Vadose Zone Field Site in the 200 East Area indicates a relatively rapid (days) return to background conditions following a recharge event. If a clean water line is the source of the water, water content should return to normal shortly after the water is turned off.
- Drilling and sampling of the impacted zone could be used to directly determine the nature of the water and or contaminants present.

Further actions are at the discretion of the individual retrieval project.

B8.0 DATA ANALYSIS AND TURN-AROUND

Timely turn-around of data collected and analyzed under this effort is essential to its usefulness. The rate of water movement through the vadose zone is sufficiently slow that collection of data suites on a daily basis is appropriate. If data are collected at the beginning of the day shift and electronically transmitted to the analyst, turn around of the analysis within 4-hours should be do-able. A 4-hr turn around would allow sufficient time to remeasure the wells before the end of the day shift. Analysis of the retaken data could then be made and appropriate action taken.

B9.0 REFERENCE

Isaacson, R. E., 1982, *Supporting Information for the Scientific Basis for Establishing Dry Well Monitoring Frequencies*, RHO-RE-EV-4 P, Rockwell Hanford Operations, Richland, Washington.

ATTACHMENT B1
ADDENDUM A – LEAK VOLUME DETECTABILITY AND MOISTURE TRAVEL TIME FROM UNDERGROUND TANK LEAKS TO NEARBY DRYWELLS

This page intentionally left blank.

ATTACHMENT B1
ADDENDUM A – LEAK VOLUME DETECTABILITY AND MOISTURE TRAVEL TIME FROM UNDERGROUND TANK LEAKS TO NEARBY DRYWELLS

SUMMARY

The models used by Rockwell Hanford in the 1980's for use of the drywells for leak detection based on the soluble fission product, Ruthenium are revisited to predict leak volume detection probability and underground moisture travel times. Two leak volume models are considered. One using a linear probability of tank leak is limited to slow leaks (less than 1,5 gph) predicts expansion of the plume based on capillary action of the soil as the primary driver. The second, using a lognormal cumulative probability, includes leak rates up to 100 gpm adds the effect of gravity in draining the liquid through the soil.

The method used here is an adaptation of a simple geometric model presented in RHO-RE-EV-4 P (Isaacson 1982). In this model, the liquid that has leaked is distributed in an ellipsoidal volume of soil centered at the leak. This is illustrated in Figure B1.1 below.

Figure B1.1. Geometric Model for the Leak Plume

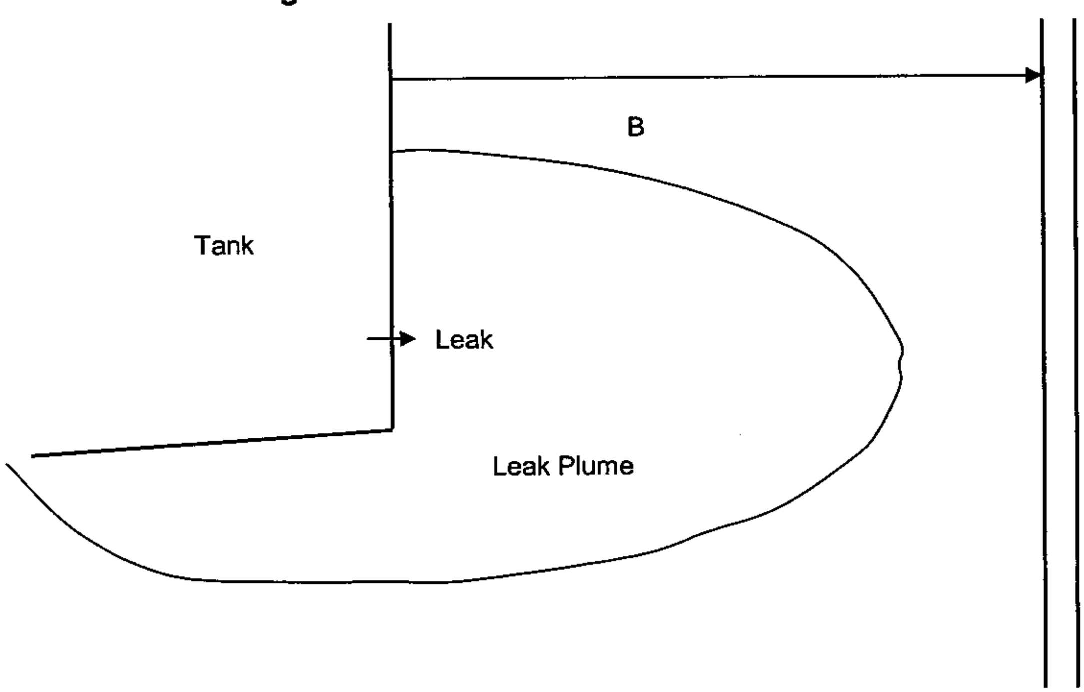

The travel time from the leak to the drywell is proportional to the volume of soil contaminated times the increase in moisture content divided by the tank leak rate. The greater the distance from the leak to the drywell, the longer the plume takes to arrive.

The increase in soil moisture content is assumed to range from 2% to 15%, and the plume anisotropy factor is assumed to range from 5 to 50. Two assumptions were made for the tank leak rate. The first is a simple model that excludes very high leak rates and ranges from 0.030 gal/h to 1.44 gal/h. The second includes the very high leak rates using a lognormal function. For the 10-foot separation between the leak and the drywell, the average travel times for the simple and lognormal cases are 12 days and 20 days. For the 45-foot separation between the leak and the drywell, the average travel times for the simple and lognormal cases are 710 days and 1,200 days.

CALCULATIONAL METHOD

The volume of waste that leaks from the tank, the volume of soil contaminated, and the increase in soil moisture due to the leak are given in the equations below.

$$V_L = Q\,t$$

$$V_S = \frac{f\,4\pi\,b^3}{3g}$$

$$\Delta\theta = \frac{V_L}{V_S} = \frac{3g\,Q\,t}{f\,4\pi\,b^3}$$

where,

V_L = The volume of liquid waste that leaves the tank through the leak, in ft^3.

Q = The average flow rate from the tank into the soil, in ft^3/d. Also known as the tank leak rate.

t = The duration of the leak, in days.

V_S = The volume of the contaminated soil plume, in ft^3.

f = The fraction of the ellipsoid volume that is soil. The remaining volume (1-f) belongs to the tank. The soil volume fraction (f) ranges from 0.5 to 1.0.

b = The horizontal spread of the plume, in ft. The plume is assumed to spread equally in all horizontal directions, unless prevented by the tank.

g = The ratio of horizontal spread to the vertical spread of the plume. The volume of the ellipsoid (ignoring the tank) is $4\pi b^3/(3g)$. The plume anisotropy can be as large as 50 due to soil compacting during tank construction.

$\Delta\theta$ = The increase in soil moisture content due to the leak. This is the difference between the average moisture content in the plume and the moisture content in the surrounding soil. The increase in soil moisture content is assumed to range from 2% to 15%.

The travel time to the drywell can be estimated by setting b=B, the distance between the leak and the drywell, and solving for leak duration. The equation for total volume leaked is calculated similarly. The resulting formulas are shown below.

$$t = \frac{f\,4\pi B^3\,\Delta\theta}{3\,g\,Q} \quad \text{and} \quad V_L = \frac{f\,4\pi B^3\,\Delta\theta}{3\,g}$$

Each of the parameters on the right sides of the above equations have a range of possible values. Two distances (B) are of interest, 10 feet and 45 feet. The 10-foot distance represents a leak on the edge of the tank, near the bottom, as shown in Figure B1.1. For this case the soil volume fraction (f) was assumed to be 0.75 because the spheroid is about 25% tank and 75% soil while the tank is leaking. The 45-foot distance represents a leak from the bottom of the tank near the center. For this case the soil volume fraction was assumed to be 0.50 because the majority of the plume growth occurs with the tank occupying the upper half of the plume volume.

The moisture travel times (t) for these two cases are shown in Table B1.1 to Table B1.4 for various combinations of input values. The increase in moisture content ($\Delta\theta$) has values from 2% to 15%. The anisotropy factor (g) has values from 5 to 50. Finally, the tank leak rate (Q) has values from 0.1 gal/h to 20 gal/h. Other values may be readily calculated using the formula for travel time shown above.

Table B1.1. Travel Times (days) with the Anisotropy Factor Set to 50

10-foot Distance (f=0.75)	Increase in Moisture Content			
Leak Rate	**2%**	**5%**	**10%**	**15%**
20 gal/h (64 ft^3/d)	0.0196	0.0490	0.0979	0.147
10 gal/h (32 ft^3/d)	0.0392	0.0979	0.196	0.294
5 gal/h (16 ft^3/d)	0.078	0.196	0.392	0.59
2 gal/h (6.4 ft^3/d)	0.196	0.490	0.979	1.47
1 gal/h (3.2 ft^3/d)	0.392	0.979	1.958	2.94
0.3 gal/h (0.96 ft^3/d)	1.31	3.26	6.53	9.79
0.1 gal/h (0.32 ft^3/d)	3.92	9.79	19.6	29.4
45-foot Distance (f=0.5)	**Increase in Moisture Content**			
Leak Rate	**2%**	**5%**	**10%**	**15%**
20 gal/h (64 ft^3/d)	1.19	2.97	5.95	8.92
10 gal/h (32 ft^3/d)	2.38	5.95	11.9	17.8
5 gal/h (16 ft^3/d)	4.76	11.9	23.8	35.7
2 gal/h (6.4 ft^3/d)	11.9	29.7	59.5	89.2
1 gal/h (3.2 ft^3/d)	23.8	59.5	119	178
0.3 gal/h (0.96 ft^3/d)	79.3	198	397	595
0.1 gal/h (0.32 ft^3/d)	238	595	1,190	1,785

Table B1.2. Travel Times (days) with the Anisotropy Factor Set to 20

10-foot Distance (f=0.75)	Increase in Moisture Content			
Leak Rate	**2%**	**5%**	**10%**	**15%**
20 gal/h (64 ft^3/d)	0.0490	0.122	0.245	0.367
10 gal/h (32 ft^3/d)	0.0979	0.245	0.490	0.734
5 gal/h (16 ft^3/d)	0.196	0.490	0.979	1.47
2 gal/h (6.4 ft^3/d)	0.490	1.22	2.45	3.67
1 gal/h (3.2 ft^3/d)	0.979	2.45	4.90	7.34
0.3 gal/h (0.96 ft^3/d)	3.26	8.16	16.3	24.5
0.1 gal/h (0.32 ft^3/d)	9.79	24.5	49.0	73.4
45-foot Distance (f=0.5)	**Increase in Moisture Content**			
Leak Rate	**2%**	**5%**	**10%**	**15%**
20 gal/h (64 ft^3/d)	2.97	7.44	14.9	22.3
10 gal/h (32 ft^3/d)	5.95	14.9	29.7	44.6
5 gal/h (16 ft^3/d)	11.9	29.7	59.5	89.2
2 gal/h (6.4 ft^3/d)	29.7	74.4	149	223
1 gal/h (3.2 ft^3/d)	59.5	149	297	446
0.3 gal/h (0.96 ft^3/d)	198	496	991	1,487
0.1 gal/h (0.32 ft^3/d)	595	1,487	2,974	4,461

Table B1.3. Travel Times (days) with the Anisotropy Factor Set to 10

10-foot Distance (f=0.75)	Increase in Moisture Content			
Leak Rate	**2%**	**5%**	**10%**	**15%**
20 gal/h (64 ft^3/d)	0.0979	0.245	0.490	0.734
10 gal/h (32 ft^3/d)	0.196	0.490	0.979	1.47
5 gal/h (16 ft^3/d)	0.392	0.979	1.96	2.94
2 gal/h (6.4 ft^3/d)	0.979	2.45	4.90	7.34
1 gal/h (3.2 ft^3/d)	1.96	4.90	9.79	14.7
0.3 gal/h (0.96 ft^3/d)	6.53	16.3	32.6	49.0
0.1 gal/h (0.32 ft^3/d)	19.6	49.0	97.9	147
45-foot Distance (f=0.5)	**Increase in Moisture Content**			
Leak Rate	**2%**	**5%**	**10%**	**15%**
20 gal/h (64 ft^3/d)	5.95	14.9	29.7	44.6
10 gal/h (32 ft^3/d)	11.9	29.7	59.5	89.2
5 gal/h (16 ft^3/d)	23.8	59.5	119	178
2 gal/h (6.4 ft^3/d)	59.5	149	297	446
1 gal/h (3.2 ft^3/d)	119	297	595	892
0.3 gal/h (0.96 ft^3/d)	397	991	1,983	2,974
0.1 gal/h (0.32 ft^3/d)	1,190	2,974	5,949	8,923

Table B1.4. Travel Times (days) with the Anisotropy Factor Set to 5

10-foot Distance (f=0.75)	Increase in Moisture Content			
Leak Rate	**2%**	**5%**	**10%**	**15%**
20 gal/h (64 ft^3/d)	0.196	0.490	0.979	1.47
10 gal/h (32 ft^3/d)	0.392	0.979	1.96	2.94
5 gal/h (16 ft^3/d)	0.783	1.96	3.92	5.88
2 gal/h (6.4 ft^3/d)	1.96	4.90	9.79	14.7
1 gal/h (3.2 ft^3/d)	3.92	9.79	19.6	29.4
0.3 gal/h (0.96 ft^3/d)	13.1	32.6	65.3	97.9
0.1 gal/h (0.32 ft^3/d)	39.2	97.9	196	294
45-foot Distance (f=0.5)	**Increase in Moisture Content**			
Leak Rate	**2%**	**5%**	**10%**	**15%**
20 gal/h (64 ft^3/d)	11.9	29.7	59.5	89.2
10 gal/h (32 ft^3/d)	23.8	59.5	119	178
5 gal/h (16 ft^3/d)	47.6	119	238	357
2 gal/h (6.4 ft^3/d)	119	297	595	892
1 gal/h (3.2 ft^3/d)	238	595	1,190	1,785
0.3 gal/h (0.96 ft^3/d)	793	1,983	3,966	5,949
0.1 gal/h (0.32 ft^3/d)	2,379	5,949	11,897	17,846

To obtain an overall picture of the likely range of travel times, the Crystal Ball™ software was used to calculate a distribution of travel times. The Crystal Ball software performs a Monte Carlo calculation in which a value for each parameter is randomly selected and a travel time is calculated. This process is repeated many times to construct a probability distribution for the travel time.

The soil fraction (f) and distance (B) are fixed at the values mentioned earlier. The soil fraction is 0.75 for the 10-foot distance and 0.5 for the 45-foot distance.

The increase in moisture content ($\Delta\theta$) is assumed to range from 2% to 15%. This range is based on general knowledge of moisture contents of Hanford formation soils and waste plumes. The increased moisture content is assumed to have a uniform probability distribution between the low and high values. In other words, the increase in moisture content can take on any value between 2% and 15% with equal probability. The mean value for a uniform probability distribution is the average of the low and high values for the range. In this case, the mean value is 8.5%.

™ Crystal Ball is a registered trademark of Decisioneering, Inc.

The anisotropy factor (g) is assumed to range from 5 to 50. This range is based on observed anisotropies in compacted soil. It is assumed to have a uniform probability distribution, which is to say that the parameter can take on any value between 5 and 50 with equal probability. The mean value for a uniform probability distribution is the average of the low and high values for the range. In this case, the mean value is 27.5.

Two distributions were used to represent tank leak rates (Q). Both are based on 13 measured values reported in RHO-RE-EV-4 P Appendix K. The first is a uniform distribution representing a subset of the data. It is referred to as the simple model for tank leak rates. The second distribution represents all the values plus a few more using a lognormal distribution. It is referred to as the lognormal model.

The uniform distribution was used to represent the 11 lowest values listed. The two highest values are described in the RHO-RE-EV-4 P as being atypical and were therefore not used. This omission also tends to shift the distribution toward lower tank leak rates and higher travel times, because travel time is inversely related to leak rate.

The uniform distribution that was used to represent tank leak rates ranges from 0.0005 gpm to 0.024 gpm. The mean value is 0.0120 gpm. The cumulative distribution assumed for tank leak rate is shown in Figure B1.2. A cumulative probability distribution shows the fraction of leak rates that are below a particular value. For a uniform distribution, the cumulative distribution is a straight line, as shown in Figure B1.2. Also shown in this figure are the data values from Appendix K of RHO-RE-EV-4 P. The 11 data values were sorted and plotted using a cumulative probability of 0.5/11=0.0455 for the first point and 1/11=0.0909 for each value after that. This approach preserves the mean value (0.111 gpm) of the distribution. Figure B1.2 shows that the data values are adequately represented using this uniform distribution.

Figure B1.2. Uniform Cumulative Probability Distribution for Tank Leak Rate

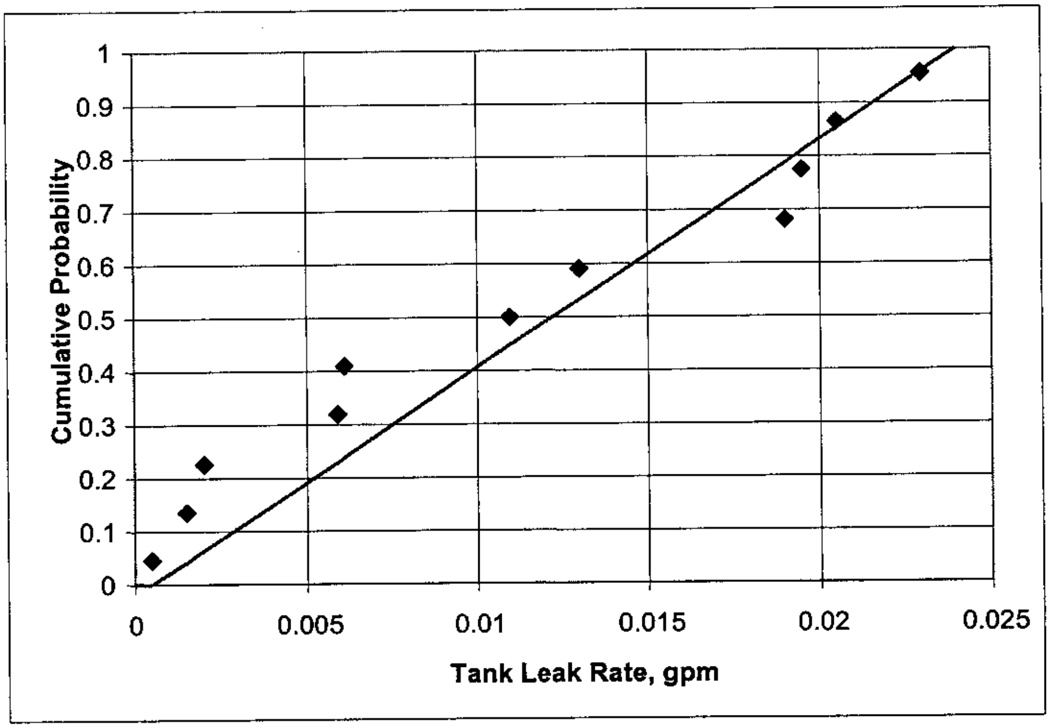

The lognormal distribution was used to represent all 13 of the data values as well as a few extra. The values are listed in Table B1.5. The lognormal distribution has a geometric mean value of 1.4 gal/h and a geometric standard deviation of 7.109. These parameters give a lognormal function that has the same mean value (9.58 gal/h) as the data it represents. The lognormal cumulative probability distribution is plotted in Figure B1.3 along with the data values from RHO-RE-EV-4 P (diamonds). The three extra points are shown as squares. The 16 data values were sorted and plotted using a cumulative probability of 0.5/16=0.0313 for the first point and 1/16=0.0625 for each value after that. This approach preserves the mean value (9.58 gal/h) of the distribution.

Table B1.5. Lognormal Distribution to Represent the Tank Leak Rate

Tank Identification	Tank Leak Rate (gal/h)	Cumulative Probability	
		Data	Lognormal
B-201	0.03	0.0313	2.503E-02
T-108	0.09	0.0938	8.087E-02
T-111	0.12	0.1563	1.052E-01
T-103	0.354	0.2188	2.416E-01
TX-107	0.366	0.2813	2.470E-01
B-107	0.66	0.3438	3.507E-01
TY-101	0.78	0.4063	3.828E-01
C-101	1.14	0.4688	4.583E-01
B-110	1.17	0.5313	4.635E-01
U-112	1.23	0.5938	4.737E-01
U-110	1.38	0.6563	4.971E-01
Added	2	0.7188	5.722E-01
Added	10	0.7813	8.419E-01
SX-110	12	0.8438	8.633E-01
Added	20	0.9063	9.124E-01
T-106	102	0.9688	9.856E-01

The lines with an identified tank are from RHO-RE-EV-4 P Appendix K. The lines labeled as "Added" have been inserted based on proposed testing.

The arithmetic mean of both the data and the lognormal distributions is 9.5825 gal/h.

The lognormal distribution has a geometric mean of 1.4 gal/h and a geometric standard deviation of 7.109.

Figure B1.3. Lognormal Cumulative Probability Distribution for Tank Leak Rate

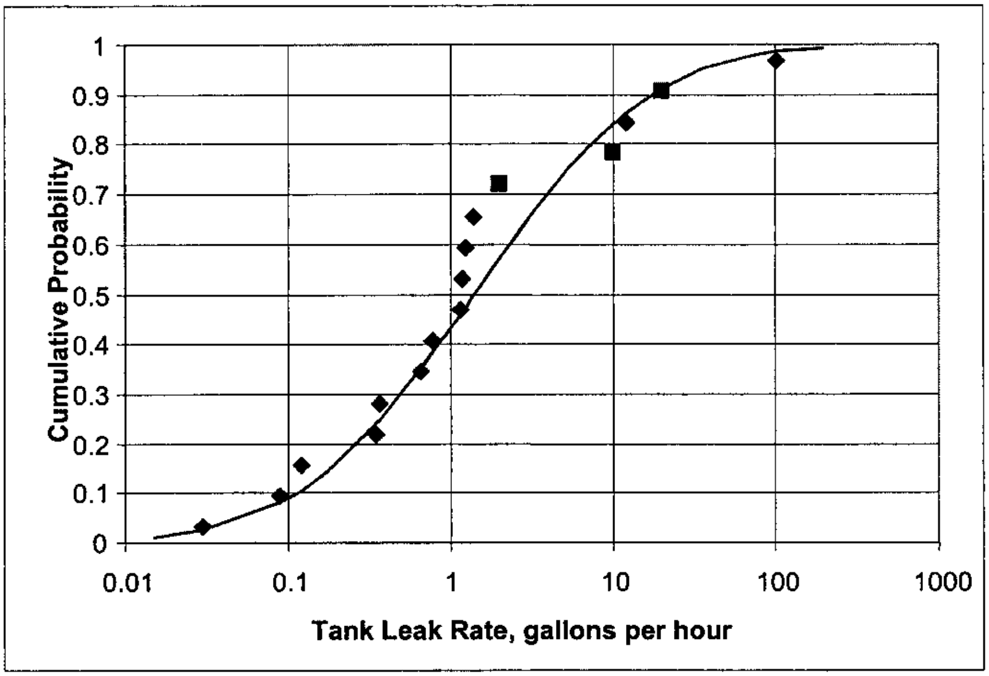

STOCHASTIC RESULTS – SIMPLE MODEL

Using the simple model for tank leak rate that excludes the higher values, the travel time distribution for the 10-foot distance is shown in Figure B1.4. The travel time distribution for the 45-foot distance has the same shape, but a longer time scale.

Figure B1.4. Moisture Travel Times for the 10-foot Distance, Simple Leak Rate Model

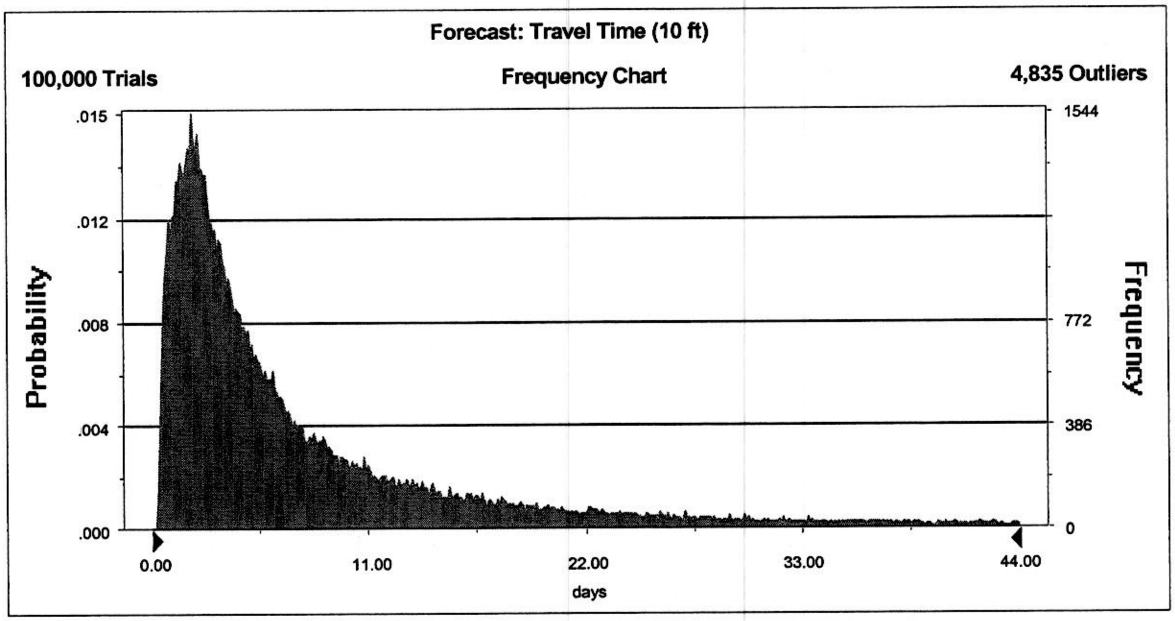

The graphical presentation of a calculated quantity is referred to as a "Forecast" in Crystal Ball. Figure B1.4 shows the Crystal Ball forecast for the travel time from leaks that are 10 feet from the drywell. The horizontal scale is days, while the vertical scale is probability per bin. The figures show that 100,000 trials were run. This means that the process of randomly selecting values for leak rate, moisture increase, and anisotropy factor followed by the calculation of travel time was carried out 100,000 times. The graph is constructed by dividing the time scale into equal-sized bins and counting the number of travel times in each bin. The probability per bin is the number of results in each bin divided by the total number of trials.

The number of "Outliers" listed in the upper right corner of each figure indicates the number of calculated travel times that are greater than the largest shown in the horizontal scale. The upper end of the time scale was selected so that the number of outliers is about 5% of the total number of trials.

The summary statistics for travel time and total volume leaked are shown in Table B1.6. The mean values for travel times are 12 days for the 10-foot distance and 2.0 years for the 45-foot distance. The corresponding mean values for volume leaked are 100 gallons and 6,200 gallons. Also listed in the table are the 5th and 95th percentile values. Approximately 90% of the results fall between these two extremes.

Table B1.6. Summary Statistical Results for the Simple Leak Rate Model

Parameter	10-foot Distance (f = 0.75)	45-foot Distance (f = 0.50)
Mean Travel Time	12 d	710 d (2.0 y)
Median Travel Time	4.8 d	290 d (0.80 y)
5th Percentile Time	1.0 d	59 d
95th Percentile Time	43 d	2,600 d (7.1 y)
Mean Volume Leaked	100 gal	6,200 gal
Median Volume Leaked	73 gal	4,400 gal
5th Percentile Volume	20 gal	1,200 gal
95th Percentile Volume	300 gal	18,000 gal

The simple model for the leak flow rate uses a uniform distribution that ranges from 0.03 gal/hour to 1.44 gal/hour.

The mean value is the sum of the times or volumes divided by the number of trials.

The median value is the time or volume is the 50th percentile in the cumulative distribution, i.e., half the results lie below the median value.

The 5th percentile and 95th percentiles show the range of times or volumes that encompass 90% of the calculated results.

The Crystal Ball forecast for total volume leaked using a drywell at 10 feet is shown in Figure B1.5. Because the volume leaked is the product of the leak rate and the travel time, the distribution shown is the result of one uniform distribution (increase in moisture content) divided by another uniform distribution (anisotropy factor). The forecast for the 45-foot distance has the same shape, but a larger volume scale.

Figure B1.5. Total Volume Leaked for the 10-foot Distance, Simple Leak Rate Model

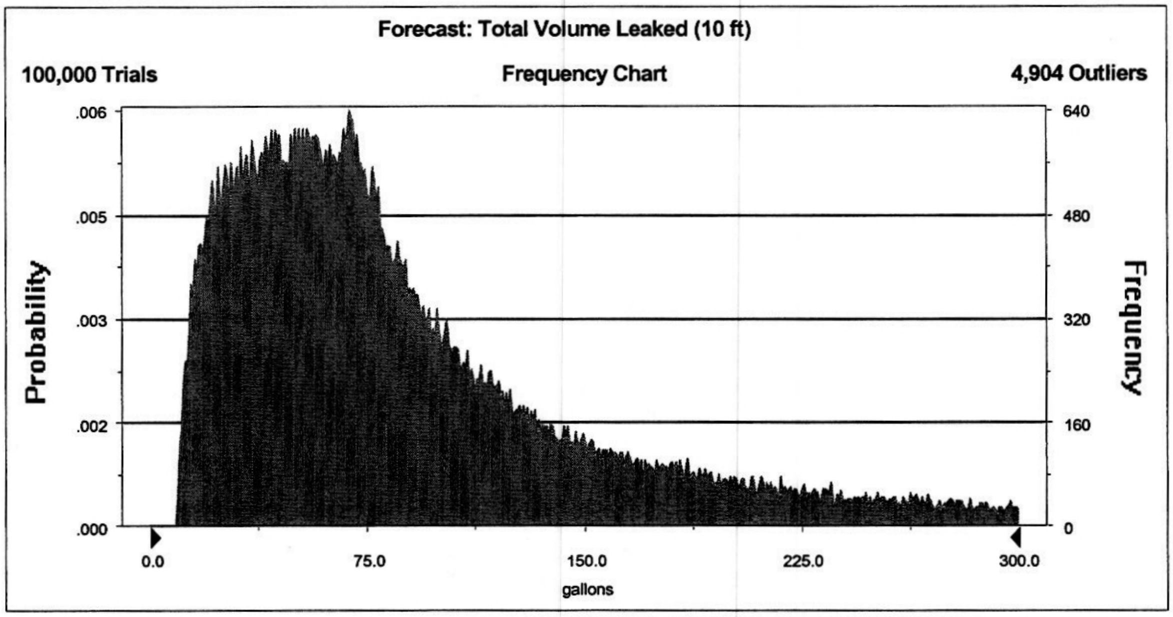

In the simple model, the lower bound chosen for the tank leak rate is important because small leak rates mean large travel times. In Table B1.6, the lower bound is 0.03 gal/h. Additional cases were run using 0.006 gal/h and 0.0006 gal/h for comparison. The Crystal Ball results are shown in Table B1.7. The lower leak rates lead to much larger travel times, but there are very few points (1,670 in the range 0.03 to 0.006 gal/h, and 2,040 in the range 0.03 to 0.0006 gal/h) at these lower values. The very large travel times affect the calculated mean value primarily.

Table B1.7. Stochastic Results with Different Lower Bounds for Leak Rate

Parameter	Lower Bound for Tank Leak Rate		
	0.03 gal/h	0.006 gal/h	0.0006 gal/h
10-foot Separation Between Leak and Drywell			
Mean Travel Time	12 d	16 d	23 d
Median Travel Time	4.8 d	5.0 d	5.0 d
5th Percentile Time	1.0 d	1.0 d	1.0 d
95th Percentile Time	43 d	55 d	59 d
Mean Volume Leaked	100 gal	100 gal	100 gal
Median Volume Leaked	73 gal	73 gal	73 gal
5th Percentile Volume	20 gal	20 gal	20 gal
95th Percentile Volume	300 gal	300 gal	300 gal

45-foot Separation Between Leak and Drywell			
Mean Travel Time	710 d (2.0 y)	990 d (2.7 y)	1,400 d (3.9 y)
Median Travel Time	290 d (0.80 y)	300 d (0.82 y)	300 d (0.83 y)
5th Percentile Time	59 d	59 d	60 d
95th Percentile Time	2,600 d (7.1 y)	3,400 d (9.2 y)	3,600 d (9.8 y)
Mean Volume Leaked	6,200 gal	6,200 gal	6,200 gal
Median Volume Leaked	4,400 gal	4,400 gal	4,400 gal
5th Percentile Volume	1,200 gal	1,200 gal	1,200 gal
95th Percentile Volume	18,000 gal	18,000 gal	18,000 gal

The simple model for tank leak rates was used with different lower bounds for the uniform distribution. The upper bound is 1.44 gal/h in every case.

The mean value is the sum of the times or volumes divided by the number of trials.

The median value is the time or volume is the 50th percentile in the cumulative distribution, i.e., half the results lie below the median value.

The 5th percentile and 95th percentiles show the range of times or volumes that encompass 90% of the calculated results.

The total volumes leaked are the same because the same variables contribute to the final distribution in each case.

STOCHASTIC RESULTS – LOGNORMAL MODEL

Using the lognormal representation of tank leak rate that includes the extra values, the travel time distribution for the 10-foot distance is shown in Figure B1.6. The travel time distribution for the 45-foot distance has the same shape, but a longer time scale.

Figure B1.6. Moisture Travel Times for the 10-foot Distance, Lognormal Leak Rate Model

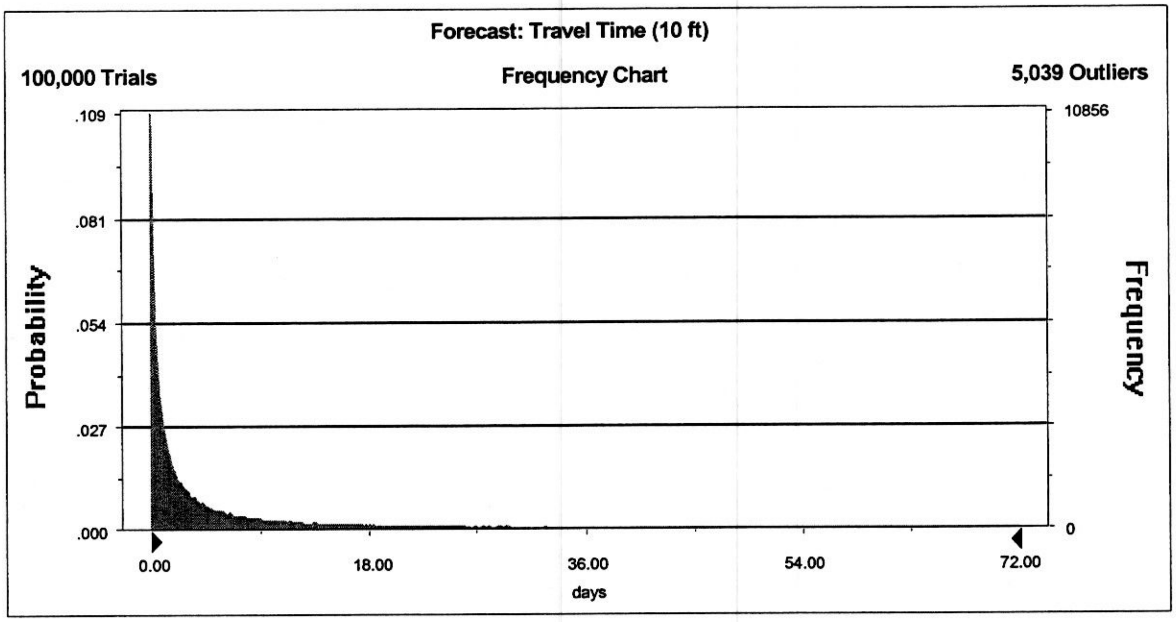

The number of "Outliers" listed in the upper right corner of each figure indicates the number of calculated travel times that are greater than the largest shown in the horizontal scale. The upper end of the time scale was selected so that the number of outliers is about 5% of the total number of trials.

The summary statistics for travel time and total volume leaked are shown in Table B1.8. The mean values for travel times are 20 days for the 10-foot distance and 3.3 years for the 45-foot distance. The corresponding mean values for volume leaked are 100 gallons and 6,200 gallons. Also listed in the table are the 5th and 95th percentile values. Approximately 90% of the results fall between these two extremes. The volume results are the same as the simple model because the volume leaked is calculated from the same distributions. Compared to the simple model, the lognormal model includes lower leak rates as well as larger leak rates. Thus, the stochastic results for travel time may be either larger or smaller than shown in Table B1.6.

Table B1.8. Summary Statistical Results for the Lognormal Leak Rate Model

Parameter	10-foot Distance (f = 0.75)	45-foot Distance (f = 0.50)
Mean Travel Time	20 d	1,200 d (3.3 y)
Median Travel Time	2.2 d	130 d
5th Percentile Time	0.07 d	4.1 d
95th Percentile Time	72 d	4,400 d (12 y)
Mean Volume Leaked	100 gal	6,200 gal
Median Volume Leaked	73 gal	4,400 gal
5th Percentile Volume	20 gal	1,200 gal
95th Percentile Volume	300 gal	18,000 gal

The lognormal leak-rate model has a geometric mean of 1.4 gal/hour and a geometric standard deviation of 7.109. The distribution mean is 9.58 gal/hour.

The mean value is the sum of the times or volumes divided by the number of trials.

The median value is the time or volume is the 50th percentile in the cumulative distribution, i.e., half the results lie below the median value.

The 5th percentile and 95th percentiles show the range of times or volumes that encompass 90% of the calculated results.

The Crystal Ball forecast for total volume leaked using a drywell at 10 feet is shown in Figure B1.7. Because the total volume leaked is based on the same input distributions as the simple model, the result is essentially the same as shown in Figure B1.5.

Figure B1.7. Total Volume Leaked for the 10-foot Distance, Lognormal Leak Rate Model

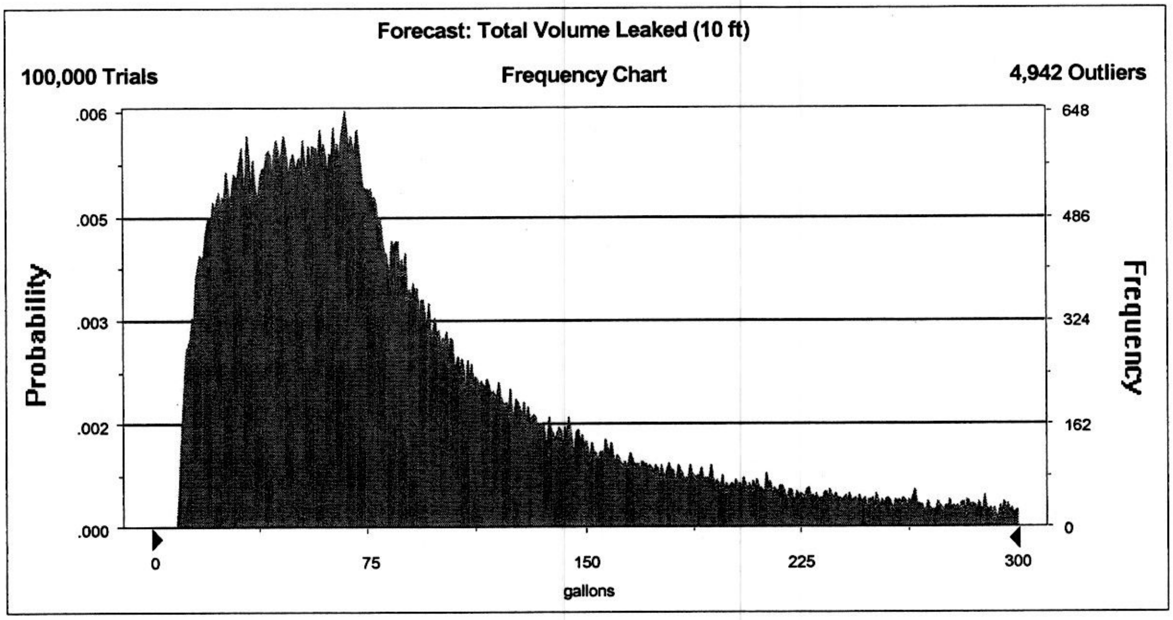

REFERENCE

Isaacson, R. E., 1982, *Supporting Information for the Scientific Basis for Establishing Dry Well Monitoring Frequencies*, RHO-RE-EV-4 P, Rockwell Hanford Company, Richland, Washington.

This page intentionally left blank.

ATTACHMENT B2
ADDENDUM B – RECALCULATION OF THE TIME FOR RU-106 PHOTON COUNT RATES TO INCREASE AND BY ANALOGY FOR MOISTURE LEVELS TO INCREASE

This page intentionally left blank.

ATTACHMENT B2
ADDENDUM B – RECALCULATION OF THE TIME FOR RU-106 PHOTON COUNT RATES TO INCREASE AND BY ANALOGY FOR MOISTURE LEVELS TO INCREASE

SUMMARY

Because the Ru-106 has such a short half-life, it has for all practical purposes disappeared from the tank waste. A more current method for finding leak plumes uses neutron radiation to sense the increase in moisture content. The simple formalism presented in RHO-RE-EV-4 P can be applied to neutron radiation provided that the neutron detector response to moisture changes associated with an advancing plume can be represented in an equation.

The method used to estimate the time for the Ru-106 photon count rate to go from the alert level to the action level is an adaptation of a simple geometric model presented in RHO-RE-EV-4 P (Isaacson 1982). In this model, the plume spreads as an ellipsoid. This is illustrated in Figure 1 of the main text. The size of the ellipsoid depends on the increased moisture content of the plume and the total volume that has leaked. Using the notation from the main report, the formulas listed below can be stated.

$$V_L = Q\,t$$

$$V_S = \frac{f\,4\pi\,b^3}{3\,g} \quad \text{and} \quad C_S = C_W\,\Delta\theta$$

$$\Delta\theta = \frac{V_L}{V_S} = \frac{3\,g\,Q\,t}{f\,4\pi\,b^3}$$

where,

V_L = The volume of liquid waste that leaves the tank through the leak, in ft^3.

Q = The average flow rate from the tank into the soil. Also known as the tank leak rate, in ft^3 per day.

t = The duration of the leak, in days.

V_S = The volume of the contaminated soil plume, in ft^3.

f = The fraction of the ellipsoid volume that is soil. The remaining volume (1-f) belongs to the tank. The soil volume fraction (f) ranges from 0.5 to 1.0.

b = The horizontal spread of the plume, in feet. The plume is assumed to spread equally in all horizontal directions, unless prevented by the tank.

g = The ratio of horizontal spread to the vertical spread of the plume. The volume of the ellipsoid (ignoring the tank) is $4\pi b^3/(3g)$. The plume anisotropy can be as large as 50 due to soil compacting during tank construction.

C_S = The concentration of Ru-106 in the soil, in Ci/L.

C_W = The concentration of Ru-106 in the waste liquid, in Ci/L.

$\Delta\theta$ = The increase in soil moisture content due to the leak. This is the difference between the average moisture content in the plume and the moisture content in the surrounding soil. The increase in soil moisture content is assumed to range from 2% to 15%.

Note that the radioactive progeny nuclides (e.g. Rh-106 and Ba-137m) have not been shown explicitly. It is assumed that they are present in secular equilibrium with the parent nuclide.

As the plume grows closer to the drywell, the instrument located in the drywell measures an increasing count rate. In RHO-RE-EV-4 P the alert level is 20 cps and the action level is 160 cps. The instrument count rate is related to the exposure rate in the center of the drywell with the formula derived in RHO-RE-EV-4 P Appendix K. This formula is shown below. The curve is derived from calibration with Ra-226 and Cs-137 sources. These radionuclides have photon spectra that are similar to Ru-106.

$$N = K\, D^{\gamma}$$

where,

N = The instrument count rate, in cps.

K = A constant unique to the type of detector and radionuclide. For the scintillation probe measuring Cs-137 and Ra-226, $K = 1.816 \times 10^6$ cps.

D = The exposure rate from Cs-137, Ra-226, or similar radionuclides measured at the center of the well, in R/h.

γ = A constant unique to the type of detector and radionuclide. For the scintillation probe measuring Cs-137 and Ra-226, $\gamma = 0.918$.

The exposure rate from a given concentration in the soil was estimated in Appendix J of RHO-RE-EV-4 P using the ISOSHLD software (BNWL-236). The formula for the attenuation of spherical radiation sources in soil has been rederived using the most recent version of ISO-PC, Version 2.2. This relationship is shown below. It was determined using a polynomial least squares fit to the logarithms of the exposure rates.

$$\mathrm{Ln}\left(\frac{D}{C_S}\right) = \alpha_0 + \alpha_1\, d + \alpha_2\, d^2 + \alpha_3\, d^3$$

where,

D = The exposure rate from Ru-106, in R/h.

C_S = The concentration of Ru-106 in the soil, in Ci/L

d = The thickness of uncontaminated soil between the plume and the drywell, in cm.

α_K = The constants determined by least squares fitting of the ISO-PC dose rates. α_0= 4.0491, α_1= -0.16013, α_2= 5.5754E-04, α_3= -1.3927E-06

The exposure rates from ISO-PC are shown in Table B2.1. These were used to derive the formula for dose rate as a function of shield thickness. The exposure rates computed from the formula are compared with the ISO-PC results in Table B2.1. In all cases, the exposure rates from the formula are within 4% of the ISO-PC results.

Given that the distance between the leak and the drywell is B, the shielding soil thickness (d) is B-b, where b is the plume radius.

Table B2.1. Exposure Rates Computed by ISO-PC Version 2.2

Soil Thickness (cm)	Exposure Rates (R/h)		Percent Difference
	ISO-PC	Formula	
0	5.962E+01	5.735E+01	-3.8%
1	4.995E+01	4.889E+01	-2.1%
2	4.211E+01	4.172E+01	-0.9%
5	2.576E+01	2.611E+01	1.3%
10	1.192E+01	1.221E+01	2.4%
15	5.722E+00	5.859E+00	2.4%
20	2.822E+00	2.882E+00	2.1%
30	7.358E-01	7.478E-01	1.6%
40	2.091E-01	2.116E-01	1.2%
50	6.442E-02	6.472E-02	0.5%
60	2.135E-02	2.123E-02	-0.6%
70	7.529E-03	7.404E-03	-1.7%
80	2.790E-03	2.723E-03	-2.4%
90	1.074E-03	1.047E-03	-2.5%
100	4.258E-04	4.175E-04	-1.9%
110	1.726E-04	1.712E-04	-0.8%
120	7.108E-05	7.159E-05	0.7%
130	2.964E-05	3.028E-05	2.1%
140	1.247E-05	1.284E-05	3.0%
150	5.276E-06	5.416E-06	2.7%
160	2.241E-06	2.253E-06	0.5%
170	9.537E-07	9.168E-07	-3.9%

The spherical geometry with slab shields was used. The distance between the center of the sphere and the detector is fixed at 305 cm.

The contaminated soil is a sphere with varying radius. The contaminated soil has a water density of 0.09 g/cc and a sand density of 1.83 g/cc. The concentration of Ru-106 in the contaminated soil is 1 Ci per liter of soil.

The uncontaminated soil has a water density of 0.07 g/cc and a sand density of 1.83 g/cc. This gives an increase in moisture content of 2%. Note that another case was tried using a water density of 0.22 g/cc in the contaminated soil. The exposure rates were 7.8% lower, a difference that is insignificant. The thickness of the uncontaminated soil is shown in the first column of numbers.

A layer of steel 0.25 inch thick was used to represent the drywell casing. This also has little effect against the Ru-106 photons. The drywell casing is assumed to have an outside diameter of 10 cm.

The ISO-PC exposure rates used Version 2.2, a recent update.

The exposure rates calculated from the formula are shown for comparison. The formula is shown in the text.

The final relationships needed to compute count rate in the detector in the drywell as a function of time after the leak begins are (1) the horizontal radius of the plume as a function of time, and (2) the concentration of Ru-106 in the soil as a function of time. The first relationship is obtained from the definition of increase in soil moisture ($\Delta\theta$) shown in the first set of equations. The concentration of Ru-106 as a function of time is assumed to be the initial waste concentration times the increase in soil moisture and a decay factor to account for the radioactive decay of the Ru-106. This relationship is also shown below.

$$b^3 = \frac{3\,g\,Q\,t}{4\,\pi\,f\,\Delta\theta} \quad \text{and} \quad C_S = C_{WO}\,\Delta\theta\,e^{-\lambda t}$$

where,

Q = The average flow rate from the tank into the soil. Also known as the tank leak rate, in ft^3 per day.

t = The duration of the leak, in days.

f = The fraction of the ellipsoid volume that is soil. The remaining volume (1-f) belongs to the tank. The soil volume fraction (f) ranges from 0.5 to 1.0.

b = The horizontal spread of the plume, in feet. The plume is assumed to spread equally in all horizontal directions, unless prevented by the tank.

g = The ratio of horizontal spread to the vertical spread of the plume. The volume of the ellipsoid (ignoring the tank) is $4\pi b^3/(3g)$. The plume anisotropy can be as large as 50 due to soil compacting during tank construction.

$\Delta\theta$ = The increase in soil moisture content due to the leak. This is the difference between the average moisture content in the plume and the moisture content in the surrounding soil. The increase in soil moisture content is assumed to range from 2% to 15%.

C_S = The concentration of Ru-106 in the soil as a function of time, in Ci/L.

C_{WO} = The initial (t=0) concentration of Ru-106 in the waste liquid, in Ci/L.

λ = The radioactive decay constant for Ru-106, 0.001884 per day. This is calculated from the decay half-life of 368 days.

Given values for the leak rate (Q), the initial waste concentration (C_{WO}), the decay constant (λ), the soil fraction (f), the anisotropy factor (g), and increase in soil moisture ($\Delta\theta$), and the distance between the leak and the drywell (B), the count rate in drywell as a function of time can be calculated. The combined formula is shown below.

$$N = K\left[C_{W0}\,\Delta\theta\,\mathrm{Exp}\left(\alpha_0 + \alpha_1\,d + \alpha_2\,d^2 + \alpha_3\,d^3 - \lambda\,t\right)\right]^{\gamma}$$

$$d = B - b \quad \text{and} \quad b = \left(\frac{3\,g\,Q\,t}{4\pi\,f\,\Delta\theta}\right)^{1/3}$$

For comparison with the formula derived and used in RHO-RE-EV-4 P, the same input values were assumed, except that the soil fraction was added. The input values are shown in Table B2.2 together with the computed times to reach specific count rates.

Table B2.2. Assumed Values and Computed Results

Parameter	Value Assumed
Leak Rate (Q)	0.03 gpm (5.77 ft^3/d)
Initial Waste Concentration (C_{w0})	4.0 x 10^{-4} Ci/L
Radioactive Decay Constant (λ)	0.001884 per day
Soil Fraction (f)	0.6
Anisotropy factor (g)	1 for 200 East; 2 for 200 West
Increase in Soil Moisture ($\Delta\theta$)	0.08
Distance from the Leak to the Drywell (B)	10 ft
Time to Reach 20 cps in Drywell	21.8 d (200 East); 10.9 d (200 West)
Time to Reach 160 cps in Drywell	26.6 d (200 East); 13.3 d (200 West)

The evaluation of incremental times for the count rate to increase from 20 cps to 160 cps were computed and graphed in RHO-RE-EV-4 P. Several values were read from the graph and compared with the time differences computed using the above formalism. These are shown graphically in Figure B2.1.

Figure B2.1. Incremental Time for Count Rates to Increase from 20 cps to 160 cps

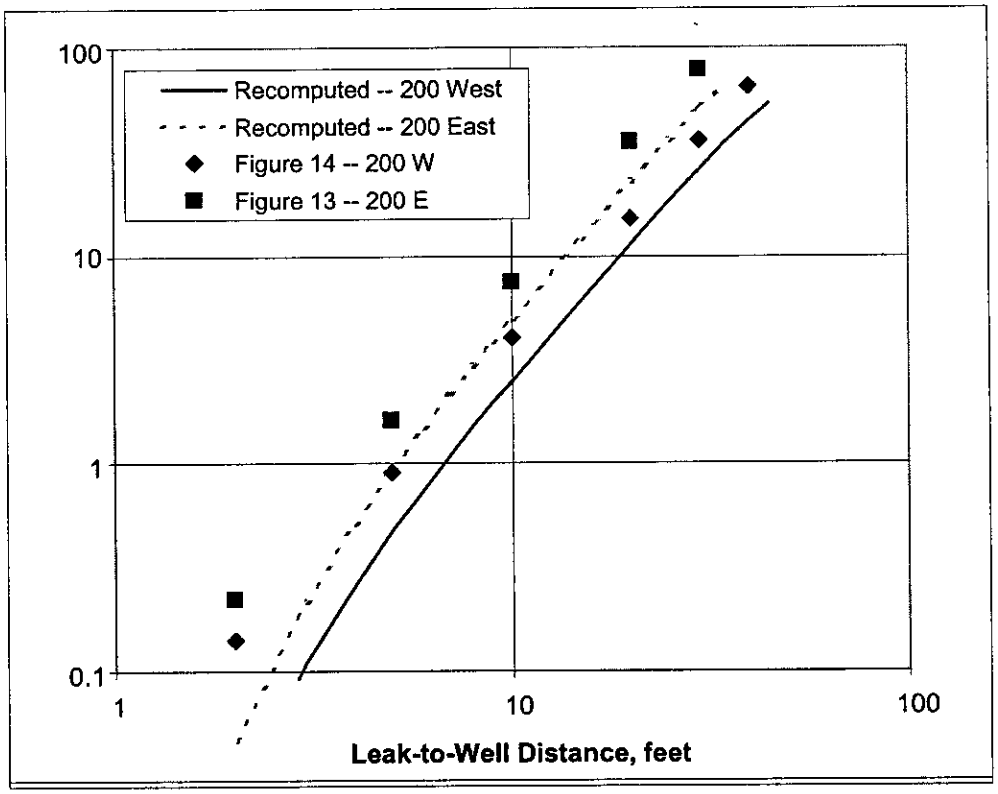

In Figure B2.1, values from RHO-RE-EV-4 P are shown as individual points, while the recalculated values are shown as solid or broken lines. The factor of two change in the anisotropy factor leads to the same effect, but the recalculated values are generally smaller. Note that the recomputed values end at 38 ft for 200 East and 49 ft for 200 West. At these distances, the waste has decayed to the point that a count rate of 160 cps is not possible. The formalism used in RHO-RE-EV-4 P did not recognize this limit.

Because the Ru-106 has such a short half-life, it has for all practical purposes disappeared from the tank waste. A more current method for finding leak plumes uses neutron radiation to sense the increase in moisture content. The simple formalism presented in RHO-RE-EV-4 P can be applied to neutron radiation provided that the neutron detector response to moisture changes associated with an advancing plume can be represented in an equation.

The distinction between 200 East and 200 West Areas is only relevant for the comparison with RHO-RE-EV-4P. The construction methods used in both East and West Areas will leave the soils surrounding the tanks in a similar condition.

This page intentionally left blank.

ATTACHMENT B3
ADDENDUM C – TRAVEL TIMES AND DETECTABLE LEAK VOLUMES WHERE THE LEAK-TO-DRYWELL DISTANCE VARIES

This page intentionally left blank.

ATTACHMENT B3
ADDENDUM C – TRAVEL TIMES AND DETECTABLE LEAK VOLUMES WHERE THE LEAK-TO-DRYWELL DISTANCE VARIES

SUMMARY

The main text shows stochastic results for two leak-to-drywell distances, 10 ft and 45 ft. In this appendix, the leak-to-drywell distance (B) is allowed to vary over the bottom and side surfaces of the tank. It will be assumed that a leak could occur anywhere on the sides or bottom of the underground tank. It is further assumed that the sides are more likely locations for the leak. A probability distribution is constructed for B and the distribution of travel times is calculated. Three cases are considered. The first has only one drywell for the tank. The second has two drywells on opposite sides of the tank. The third case has three drywells evenly spread around the tank. As might be expected, as the number of drywells increases, the mean travel time decreases.

GENERAL FEATURES

The mathematical models use the symbols defined in Figure B3.1 and the equations that follow.

From the law of cosines,

$$\cos \Phi_R = \frac{2R^2 + 2RB + B^2 - r^2}{2r(R+B)}$$

where,

B = The distance between the drywell centerline and the outside of the tank. This is assumed to be 10 feet.

r = The distance between the drywell centerline and an arc of locations on the tank bottom and side walls.

R = The radius of the tank, 38 feet.

Φ_R = The angle between the line joining the tank centerline and the drywell centerline (length of this line is R+B) and the location on the tank wall that is a distance r from the drywell centerline. Φ_R ranges from 0 to π radians as the distance from the drywell (r) increases from B to B+2R.

Figure B3.1. Sketch of Tank and Symbols

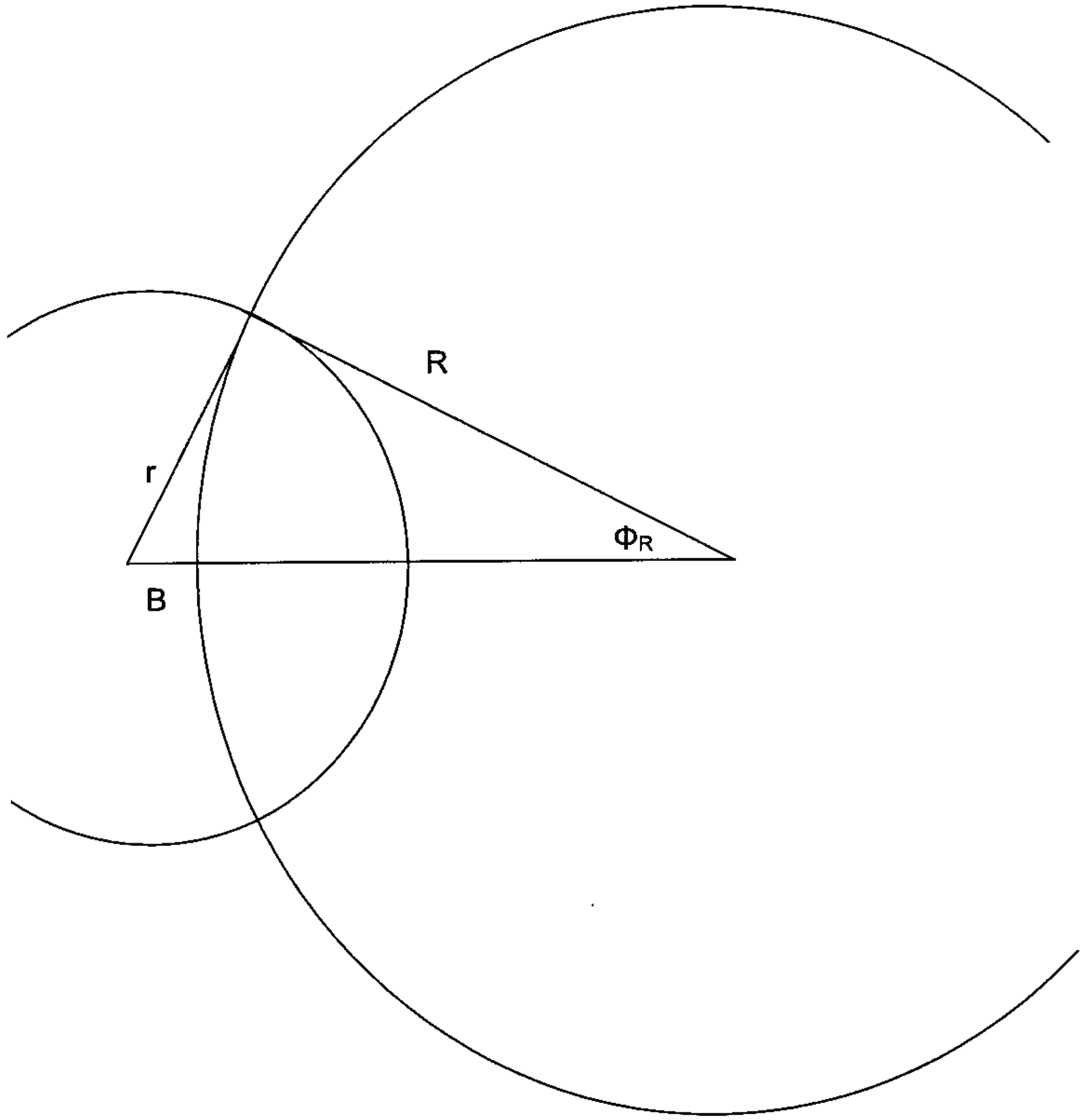

It will be assumed that the sidewall of the tank is more likely to leak than the bottom. With this assumption, the sidewall area distribution as a function of distance from the drywell (r) determines the shape. The bottom of the tank has a comparable surface area, but is assumed to have a lower probability per unit area of developing a leak.

In general, this area is given by ($2\Phi_R R$) times the height of the sidewall. To calculate a cumulative probability distribution, this must be divided by the total sidewall area, namely, ($2\pi R$) times the height of the sidewall. Thus, the cumulative probability is given by (Φ_R / π).

The stochastic calculations carried out in Crystal Ball use the same uniform probability distributions for leak rate (Q), anisotropy factor (g), and increase in moisture content ($\Delta\theta$) that were described in the main text. The soil fraction (f) is assumed to be a uniform distribution ranging from 0.5 to 0.75 because all the leaks are from the sidewall of the tank. Leaks near the bottom have the larger soil fractions. The distance from the leak to the drywell (B) has a distribution that depends on the number of drywells near the tank. The distributions for one, two, or three drywells are derived in the sections that follow. The stochastic results for these three cases are summarized in Table B3.1. As the number of drywells increases, the moisture travel time and volume leaked decrease.

Table B3.1. Summary of Stochastic Results

Parameter	One	Two	Three
Mean Travel Time	2,670 d	650 d	234 d
Median Travel Time	716 d	144 d	54 d
5th Percentile Time	6.6 d	3.4 d	2.5 d
95th Percentile Time	10,500 d	2,590 d	924 d
Mean Volume Leaked	23,100 gal	5,620 gal	2,030 gal
Median Volume Leaked	11,200 gal	2,160 gal	795 gal
5th Percentile Volume	105 gal	59 gal	46 gal
95th Percentile Volume	87,700 gal	22,400 gal	7,980 gal

The mean value is the sum of the times or volumes divided by the number of trials.

The median value is the time or volume is the 50th percentile in the cumulative distribution, i.e., half the results lie below the median value.

The 5th percentile and 95th percentiles show the range of times or volumes that encompass 90% of the calculated results.

The final probability distributions for travel time and volume leaked have long tails toward large values. These distributions are shown in the sections that follow. Such distributions have upper bound (95th percentile) values that are very sensitive to the percentage selected. Typically, reducing the bound from 95% to 94% (a 1% difference) reduces the moisture travel time by 9%.

ONE DRYWELL

With a single drywell, the cumulative probability distribution is calculated using (Φ_R / π). Values are selected for r ranging from B to (B+2R). The incremental probability is the difference between selected values for r. The probability distribution used for the stochastic analysis is shown in Table B3.2 and Figure B3.2.

Figure B3.2. Sidewall Leak Probability per Foot of Distance from One Drywell

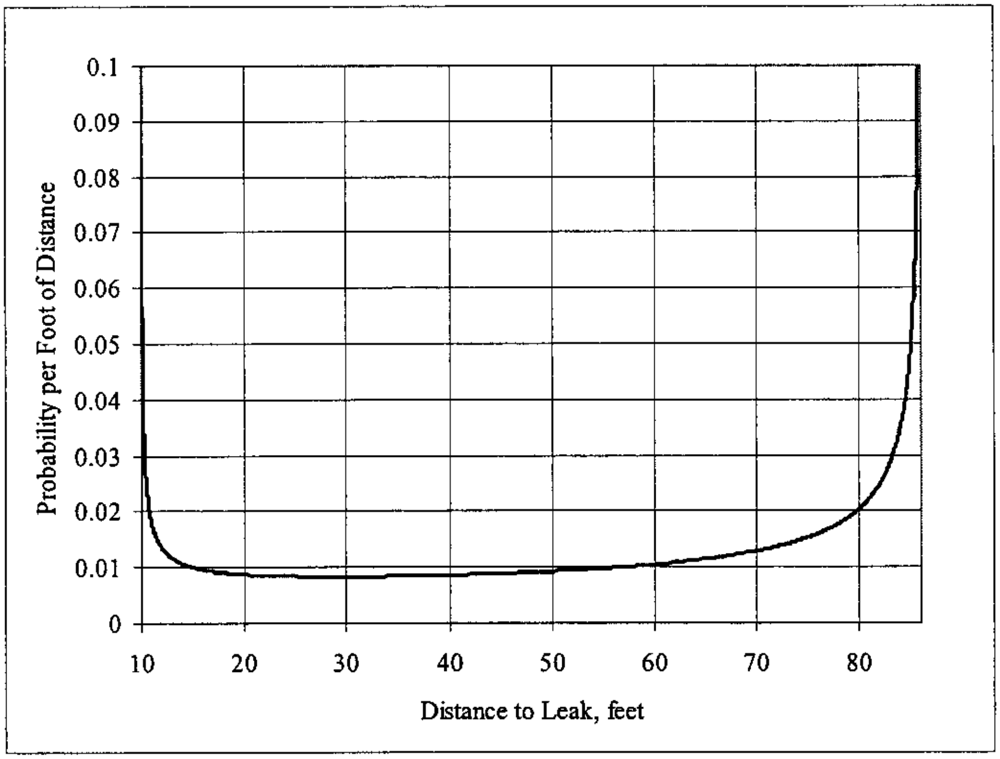

The probabilities shown in Table B3.2 were computed as the difference between the cumulative probabilities at the distances shown in the table. The distances are not evenly spaced, but were chosen to give probabilities that are nearly equal.

The probability curve shown in Figure B3.2 is the probability per foot of distance from the drywell (r). This normalization gives the differential function shown in the figure. Note that the curve uses much finer distance increments than are shown in the table.

The stochastic results for moisture travel time are shown graphically in Figure B3.3. Note the long tail at large travel times. The maximum time shown is 8 years, and about 20% of the trials give travel times greater than this.

Table B3.2. Probability Distribution for a Single Drywell

Distance Range, ft		Probability	Distance Range, ft		Probability
Low	High		Low	High	
10	10.4	0.0213	60.4	62.3	0.0203
10.4	11.4	0.0195	62.3	64.2	0.0210
11.4	12.9	0.0200	64.2	66	0.0206
12.9	14.7	0.0197	66	67.7	0.0202
14.7	16.8	0.0205	67.7	69.4	0.0211
16.8	19	0.0201	69.4	71	0.0207
19	21.3	0.0202	71	72.5	0.0203
21.3	23.7	0.0206	72.5	73.9	0.0199
23.7	26.1	0.0203	73.9	75.3	0.0210
26.1	28.6	0.0210	75.3	76.6	0.0207
28.6	31.1	0.0209	76.6	77.8	0.0203
31.1	33.6	0.0210	77.8	78.9	0.0199
33.6	36.1	0.0211	78.9	80	0.0215
36.1	38.5	0.0205	80	81	0.0212
38.5	40.9	0.0207	81	81.9	0.0209
40.9	43.2	0.0201	81.9	82.7	0.0206
43.2	45.5	0.0204	82.7	83.4	0.0201
45.5	47.8	0.0208	83.4	84	0.0195
47.8	50	0.0202	84	84.6	0.0227
50	52.2	0.0206	84.6	85.1	0.0230
52.2	54.3	0.0202	85.1	85.5	0.0237
54.3	56.4	0.0207	85.5	85.8	0.0254
56.4	58.4	0.0202	85.8	86	0.0437
58.4	60.4	0.0208			

The distance range is measured from the drywell, which is 10 feet from the outside of the tank. Note that the distances (r) are not evenly distributed, but have been chosen to give probabilities that are approximately equal.

The sum of the probabilities is 1.0000.

Figure B3.3. Stochastic Result for Travel Time with One Drywell

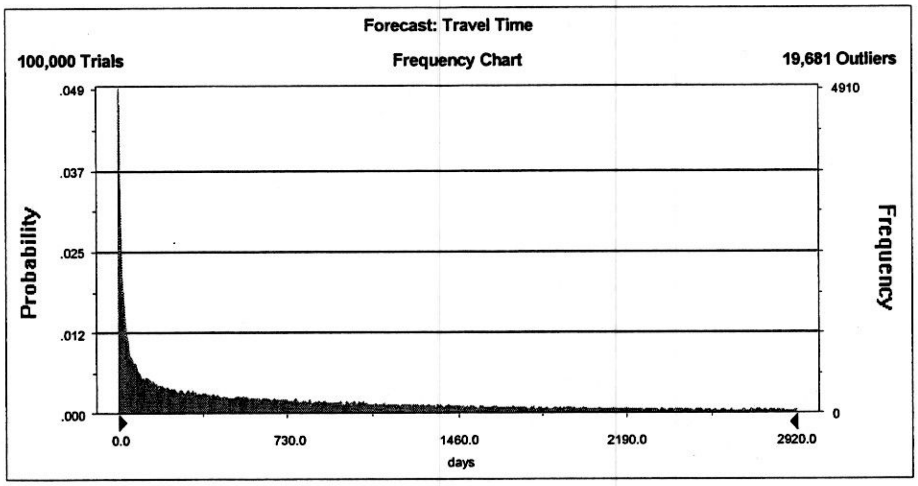

Numerical results are listed in Table B3.3. The 95th percentile time is 15 times greater than the 50th percentile time. The distribution of total volumes leaked has a shape similar to the moisture travel time, although the tail is not quite as long. The 95th percentile volume is 8 times greater than the 50th percentile volume.

Table B3.3. Summary Statistical Results for One Drywell

Parameter	Moisture Travel Time	Volume Leaked
Mean	2,670 d (7.3 y)	23,100 gal
Median	716 d (2.0 y)	11,200 gal
5th Percentile	6.6 d	105 gal
95th Percentile	10,500 d (29 y)	87,700 gal

The mean value is the sum of the times or volumes divided by the number of trials.

The median value is the time or volume is the 50th percentile in the cumulative distribution, i.e., half the results lie below the median value.

The 5th percentile and 95th percentiles show the range of times or volumes that encompass 90% of the calculated results.

TWO DRYWELLS

With two drywells, the tank is divided in half with a line that is equidistant from the two drywells. If the angle between the drywells is Φ_W, then the dividing line makes an angle $\Phi_M = 0.5\ \Phi_W$ with the line joining one of the drywells with the tank centerline. The cumulative probability is given by the formula shown below.

$$\text{Cumulative Probability} = \frac{\text{MIN}(\Phi_M, \Phi_R) + \text{MIN}(\pi - \Phi_M, \Phi_R)}{\pi}$$

where,

MIN = A function that returns the smaller of the two values.

Φ_M = The angle between the line joining the tank centerline and the drywell centerline and the line that is equidistant from the two drywells. Φ_M can be at most $\pi/2$ radians.

Φ_R = The angle between the line joining the tank centerline and the drywell centerline and the location on the tank wall that is a distance r from the drywell centerline. Φ_R ranges from 0 to π radians as the distance from the drywell (r) increases from B to B+2R.

As before, the probability distribution is calculated by taking the difference between the cumulative probabilities at successive distances (r).

The specific case examined has the two drywells π radians (180 degrees) apart. The dividing line is therefore at $\pi/2$ radians (90 degrees). The probability distribution is shown in Table B3.4.

The probability curve shown in Figure B3.4 is the probability per foot of distance from the drywell (r). This normalization gives the differential function shown in the figure. Note that the curve uses much finer distance increments than are shown in the table.

Figure B3.4. Sidewall Leak Probability per Foot of Distance from Two Drywells

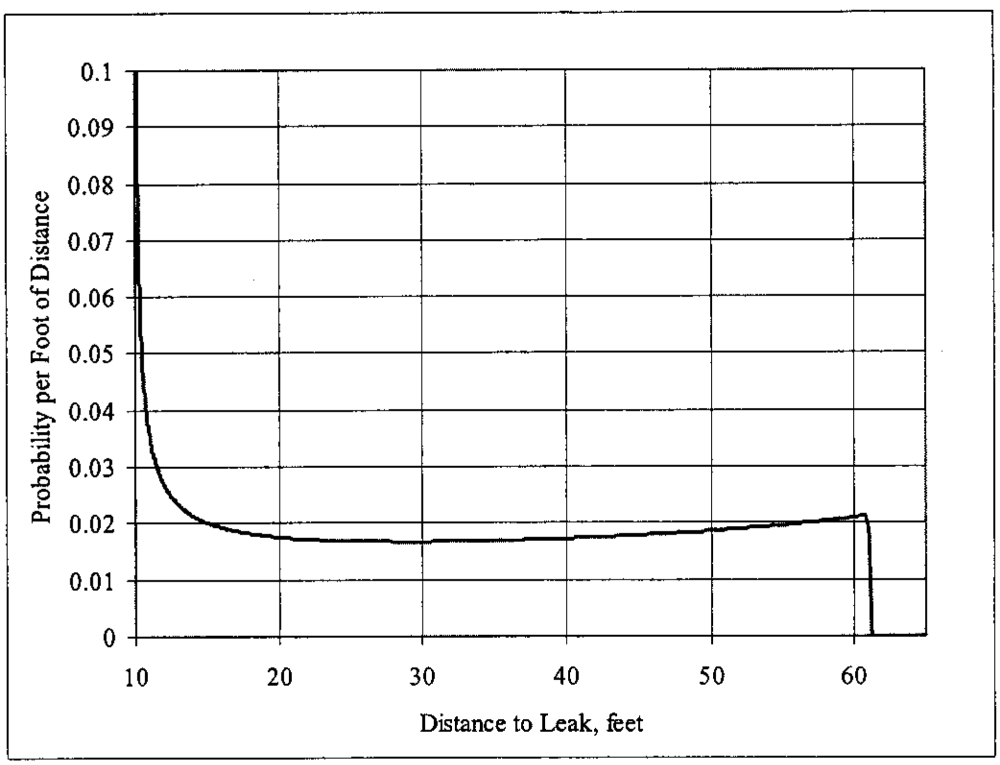

Table B3.4. Probability Distribution for Two Drywells

Distance Range, ft		Probability	Distance Range, ft		Probability
Low	High		Low	High	
10	10.1	0.0211	34.2	35.5	0.0220
10.1	10.4	0.0215	35.5	36.8	0.0221
10.4	10.9	0.0221	36.8	38.1	0.0222
10.9	11.5	0.0200	38.1	39.4	0.0223
11.5	12.3	0.0222	39.4	40.7	0.0225
12.3	13.2	0.0218	40.7	42	0.0226
13.2	14.2	0.0220	42	43.3	0.0228
14.2	15.3	0.0225	43.3	44.5	0.0212
15.3	16.4	0.0214	44.5	45.7	0.0214
16.4	17.6	0.0224	45.7	46.9	0.0216
17.6	18.8	0.0218	46.9	48.1	0.0218
18.8	20	0.0213	48.1	49.3	0.0220
20	21.2	0.0209	49.3	50.5	0.0223
21.2	22.5	0.0224	50.5	51.7	0.0225
22.5	23.8	0.0222	51.7	52.9	0.0228
23.8	25.1	0.0220	52.9	54	0.0212
25.1	26.4	0.0219	54	55.1	0.0214
26.4	27.7	0.0218	55.1	56.2	0.0217
27.7	29	0.0218	56.2	57.3	0.0220
29	30.3	0.0218	57.3	58.4	0.0223
30.3	31.6	0.0218	58.4	59.5	0.0227
31.6	32.9	0.0218	59.5	60.5	0.0210
32.9	34.2	0.0219	60.5	61.3	0.0153

The distance range is measured from the drywell, which is 10 feet from the outside of the tank. Note that the distances (r) are not evenly distributed, but have been chosen to give probabilities that are approximately equal.

The sum of the probabilities is 1.0000.

The stochastic results for moisture travel time are shown graphically in Figure B3.5. Note the long tail at large travel times. The maximum time shown is 4 years, and about 10% of the trials give travel times greater than this.

Figure B3.5. Stochastic Result for Travel Time with Two Drywells

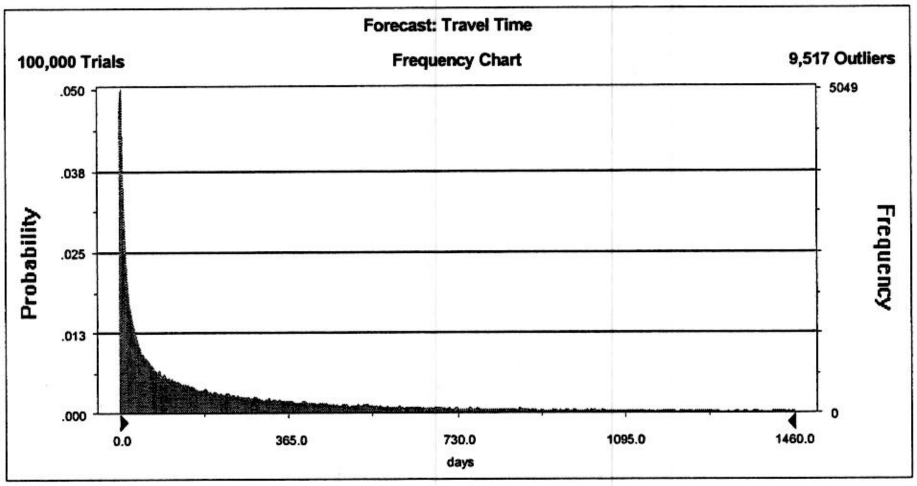

Numerical results are listed in Table B3.5. The 95th percentile time is 18 times greater than the 50th percentile time. The volume distribution has a shape similar to the moisture travel time, although the tail is not quite as long. The 95th percentile time is 10 times greater than the 50th percentile time.

Table B3.5. Summary Statistical Results for Two Drywells

Parameter	Moisture Travel Time	Volume Leaked
Mean	650 d	5,620 gal
Median	144 d	2,160 gal
5th Percentile	3.4 d	59 gal
95th Percentile	2,590 d	22,400 gal

The mean value is the sum of the times or volumes divided by the number of trials.

The median value is the time or volume is the 50th percentile in the cumulative distribution, i.e., half the results lie below the median value.

The 5th percentile and 95th percentiles show the range of times or volumes that encompass 90% of the calculated results.

THREE DRYWELLS

With three drywells, the tank is divided into three parts with three radial lines that are equidistant from pairs of drywells. Selecting one of the drywells, there is a second drywell to the left and a third to the right of the one selected. If the angle between the selected drywell and the one to the left is Φ_{W1}, then the dividing line between them is at an angle $\Phi_{M1} = 0.5\ \Phi_{W1}$. Similarly, if the angle between the selected drywell and the one to the right is Φ_{W2}, then the dividing line between them is at an angle $\Phi_{M2} = 0.5\ \Phi_{W2}$. The cumulative probability is given by the formula shown below.

$$\text{Cumulative Probability} = \frac{\text{MIN}(\Phi_{M1}, \Phi_R) + \text{MIN}(\Phi_{M2}, \Phi_R)}{\pi}$$

where,

MIN = A function that returns the smaller of the two values.

Φ_{M1} = The angle between the line joining the tank centerline and the drywell centerline and the line that is equidistant with the drywell on the left. Φ_{M1} can be at most $\pi/2$ radians.

Φ_{M2} = The angle between the line joining the tank centerline and the drywell centerline and the line that is equidistant with the drywell on the right. Φ_{M2} can be at most $\pi/2$ radians.

Φ_R = The angle between the line joining the tank centerline and the drywell centerline and the location on the tank wall that is a distance r from the drywell centerline. Φ_R ranges from 0 to π radians as the distance from the drywell (r) increases from B to B+2R.

As before, the probability distribution is calculated by taking the difference between the cumulative probabilities at successive distances (r).

The specific case examined has the three drywells $2\pi/3$ radians (120 degrees) apart. The dividing line is therefore at $\pi/3$ radians (60 degrees). The probability distribution is shown in Table B3.6.

The probability curve shown in Figure B3.6 is the probability per foot of distance from the selected drywell. This normalization gives the differential function shown in the figure. Note that the curve uses much finer distance increments than are shown in the table.

The stochastic results for moisture travel time are shown graphically in Figure B3.7. Note the long tail at large travel times. The maximum time shown is 2 years, and about 7% of the trials give travel times greater than this.

Numerical results are listed in Table B3.7. The 95th percentile time is 17 times greater than the 50th percentile time. The volume distribution has a shape similar to the moisture travel time, although the tail is not quite as long. The 95th percentile time is 10 times greater than the 50th percentile time.

Table B3.6. Probability Distribution for Three Drywells

Distance Range, ft		Probability	Distance Range, ft		Probability
Low	High		Low	High	
10	10.1	0.0317	25.3	26.2	0.0227
10.1	10.3	0.0235	26.2	27.1	0.0227
10.3	10.6	0.0234	27.1	28	0.0226
10.6	11	0.0239	28	28.9	0.0226
11	11.5	0.0246	28.9	29.8	0.0226
11.5	12	0.0214	29.8	30.7	0.0226
12	12.6	0.0232	30.7	31.6	0.0226
12.6	13.3	0.0248	31.6	32.5	0.0227
13.3	14	0.0232	32.5	33.4	0.0227
14	14.7	0.0220	33.4	34.3	0.0228
14.7	15.5	0.0241	34.3	35.2	0.0228
15.5	16.3	0.0233	35.2	36.1	0.0229
16.3	17.2	0.0254	36.1	37	0.0230
17.2	18.1	0.0248	37	37.9	0.0230
18.1	19	0.0243	37.9	38.8	0.0231
19	19.9	0.0239	38.8	39.7	0.0232
19.9	20.8	0.0236	39.7	40.6	0.0233
20.8	21.7	0.0234	40.6	41.5	0.0235
21.7	22.6	0.0232	41.5	42.4	0.0236
22.6	23.5	0.0230	42.4	43.2	0.0211
23.5	24.4	0.0229	43.2	43.9	0.0176
24.4	25.3	0.0228			

The distance range is measured from the drywell, which is 10 feet from the outside of the tank. Note that the distances (r) are not evenly distributed, but have been chosen to give probabilities that are approximately equal.

The sum of the probabilities is 1.0000.

Figure B3.6. Sidewall Leak Probability per Foot of Distance from Three Drywells

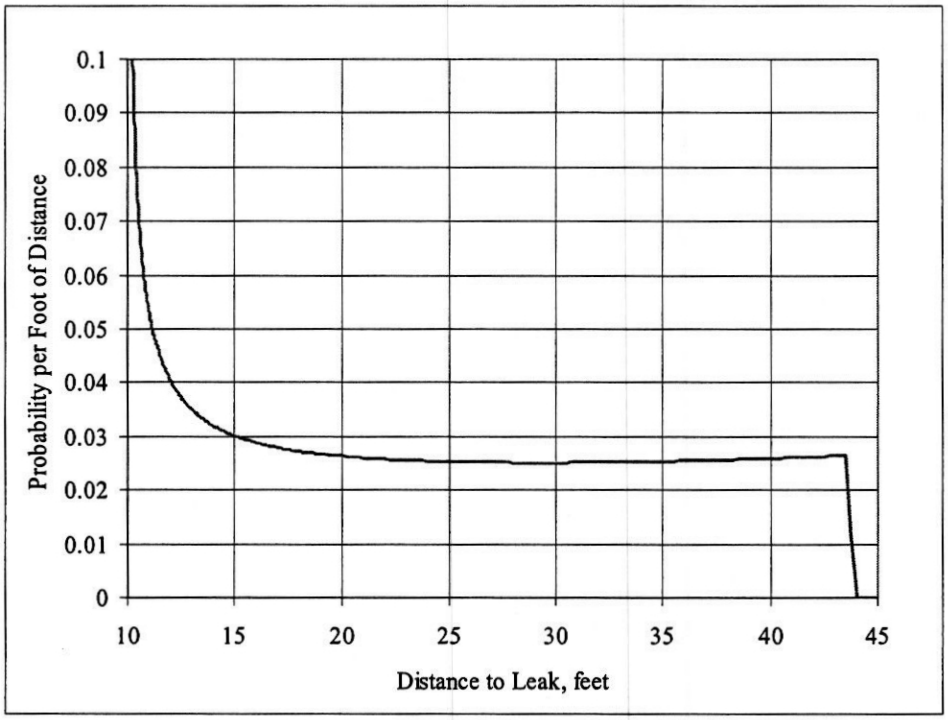

Figure B3.7. Stochastic Result for Travel Time with Three Drywells

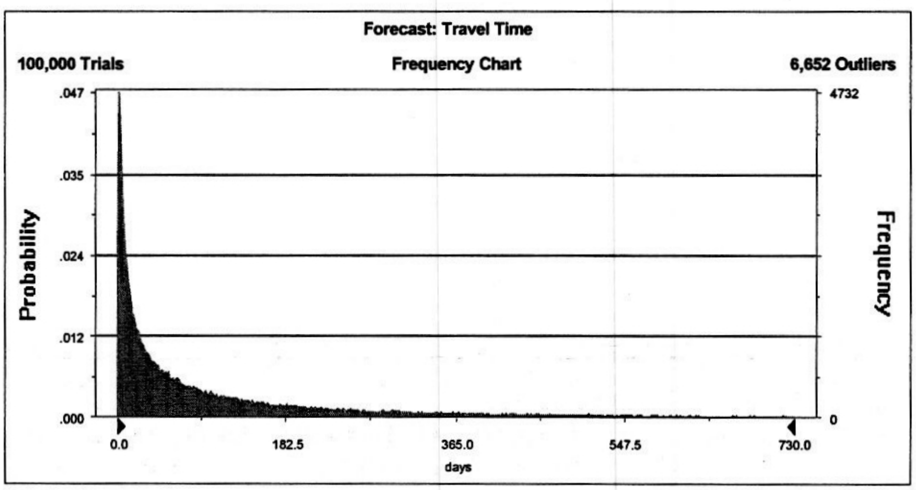

Table B3.7. Summary Statistical Results for Three Drywells

Parameter	Moisture Travel Time	Volume Leaked
Mean	234 d	2,030 gal
Median	54 d	795 gal
5th Percentile	2.5 d	46 gal
95th Percentile	924 d	7,980 gal

The mean value is the sum of the times or volumes divided by the number of trials.

The median value is the time or volume is the 50th percentile in the cumulative distribution, i.e., half the results lie below the median value.

The 5th percentile and 95th percentiles show the range of times or volumes that encompass 90% of the calculated results.

This page intentionally left blank.